Continuum Mech. Thermodyn. (2023) 35:347–391
https://doi.org/10.1007/s00161-022-01180-x

ORIGINAL ARTICLE

Noël Challamel · Y. P. Zhang · C. M. Wang · Giuseppe Ruta · Francesco dell'Isola

Discrete and continuous models of linear elasticity: history and connections

Received: 4 March 2022 / Accepted: 14 December 2022 / Published online: 13 January 2023

Abstract This paper tracks the development of lattice models that aim to describe linear elasticity of solids and the field equations of which converge asymptotically toward those of isotropic continua, thus showing the connection between discrete and continuum. In 1759, Lagrange used lattice strings/rod dynamics to show the link between the mixed differential-difference equation of a one-dimensional (1D) lattice and the partial differential equation of the associated continuum. A consistent three-dimensional (3D) generalization of this model was given much later: Poincaré and Voigt reconciled the molecular and the continuum approaches at the end of the nineteenth century, but only in 1912 Born and von Kármán presented the mixed differential-difference equations of discrete isotropic elasticity. Their model is a 3D generalization of Lagrange's 1D lattice and considers longitudinal, diagonal and shear elastic springs among particles, so the associated continuum is characterized by three elastic constants. Born and von Kármán proved that the lattice equations converge to Navier's partial differential ones asymptotically, thus being a formulation of continuous elasticity in terms of spatial finite differences, as for Lagrange's 1D lattice. Neglecting shear springs in Born–Kármán's lattice equals to Navier's assumption of pure central forces among molecules: in the limit, the lattice behaves as a one-parameter isotropic solid ("rari-constant" theory: equal Lamé parameters, or, equivalently, Poisson's ratio $\upsilon = 1/4$). Hrennikoff and McHenry revisited the lattice approach with pure central interactions using a plane truss; the equivalent Born–Kármán's lattice in plane stress in the limit tends to a continuum with Poisson's

Communicated by Andreas Öchsner.

N. Challamel (✉)
Université Bretagne Sud, IRDL (CNRS UMR 6027), Centre de Recherche, Rue de Saint Maudé, BP92116, 56321 Lorient Cedex, France
E-mail: noel.challamel@univ-ubs.fr

Y. P. Zhang · C. M. Wang
School of Civil Engineering, University of Queensland, St Lucia, QLD 4072, Australia
E-mail: y.zhang16@uq.edu.au

C. M. Wang
E-mail: cm.wang@uq.edu.au

G. Ruta
Dipartimento d'ingegneria strutturale e geotecnica, Università "La Sapienza", and Gruppo nazionale di fisica matematica, Rome, Italy
E-mail: giuseppe.ruta@uniroma1.it

F. dell'Isola
University of L'Aquila and International Research Center for Mathematics and Mechanics of Complex Systems M&MOCS, L'Aquila, Italy
E-mail: fdellisola@gmail.com

ratio $\upsilon = 1/3$. Contrary to McHenry–Hrennikoff's truss, Born–Kármán's lattice leads to a "free" Poisson's ratio bounded by its "limit' bound ($\upsilon = 1/4$ for plane strain or 3D elasticity; $\upsilon = 1/3$ for plane stress elasticity). Unfortunately, Born–Kármán's lattice model does not comply with rotational invariance principle, for non-central forces. The consistent generalization of Lagrange's lattice in 3D was achieved only by Gazis et al. considering an elastic energy that depends on changes in both lengths and angles of the lattice. An alternative consistent three-parameter elastic lattice is the Hrennikoff's, with additional structure in the cell. We also discuss the capability of nonlocal continuous models to bridge the gap between continuum isotropic elasticity at low frequencies and lattice anisotropic elasticity at high frequencies.

Keywords Lattice/discrete elasticity · Continuum elasticity · Elastodynamics · Discrete elasticity · Difference equations · Partial differential equations · Microstructured solids · Constrained kinematics · Metamaterials

1 Introduction

Connecting worlds at different scales has been the dream of philosophers and scientists in the quest for a rational understanding of fundamental laws in natural or human sciences. Bergson's famous quote "l'intelligence ne se représente clairement que le discontinu" (1907), that is "Intelligence depicts clearly only the discontinuous" can be understood as an invitation to question the behavior of interaction laws at a finer scales, possibly ruled by discontinuous variations, for a better understanding of the world at larger scales [1]. As for economics, in 1926, Keynes said [2]: "we are faced with the problem of organic unity, of discreteness, of discontinuity, the whole is not equal to the sum of the parts, small changes produce large effects, the assumptions of a uniform and homogeneous continuum are not satisfied." Thus, continuous models with smooth variation fields may be not sufficient to represent specific phenomena. These questions are echoed in physics and mechanics as well: understanding the behavior at a macroscopic scale, mathematically represented by some continuous representative variables, may be supported by the evolution of some discontinuous microstructure at a finer scale. The present paper aims to present, in a concise way, the main contributors who succeeded in connecting discrete (or lattice) and continuous models for linear elasticity. This can be viewed also as the first bridge between discrete and continuous mechanics, since linear elasticity can be viewed as the simplest constitutive law among all complex rheological laws that were developed during the two last centuries. From a mathematical point of view, lattice elasticity is ruled by mixed differential-difference equations, with spatial difference operators and time derivatives due to supposed time continuous dependence, whereas partial differential equations both in time and in space define continuous elasticity evolutions. Bridging discrete and continuous theories equals to relating mixed differential-difference equations with partial differential equations, assuming some smoothness of the field variables [3].

Lattice elasto-dynamics was first solved through uniaxial models by Lagrange: in 1759, he presented both the mixed differential-difference equations of a 1D lattice and the related wave partial differential equation [4,5]. Lagrange studied the vibration of a discrete string composed of a finite number n of masses with fixed ends (Lagrange, 1759; 1788) and obtained the exact natural frequencies of this 1D lattice for any n, showing that its asymptotic behavior is that of a continuous string. In Lagrange [4], it is also shown that this problem is mathematically analogous to that of a 1D axial (dubbed Lagrange's) lattice, composed of a finite number of particles joined by equal linear elastic springs, the asymptotic behavior of which is that of a continuous bar (see Fig. 3). Lagrange's equation for this lattice is

$$\alpha \left(u_{i+1} - 2u_i + u_{i-1}\right) = M \ddot{u}_i \tag{1}$$

where α is the spring stiffness; M is the mass; and u_i is the axial displacement of each particle, initially at a distance a from each other (lattice spacing). Equation (1) is a mixed differential-difference equation that couples a spatial difference operator (matter is discrete in space) with some time differential operator (time is continuous) (see [3] for a general presentation of mixed differential-difference equations). Equation (1) was written explicitly by Lagrange in 1759 (see Figs. 1, 2 for this equation related to the propagation of sound and to natural vibration). Lagrange's lattice is sometimes also referred to as a 1D Born–Kármán's lattice [6]; as a particular case of their 3D lattice model. As reported by Burkhardt [7], Cannon and Dostrovsky [8] or more recently by Myshkis [3] that Bernoulli [9] had already approximated the geometrical curvature of a string by some straight segments (for up to $n = 7$ elements), thus implicitly formulating a discrete Laplacian

$$\frac{d^2 y_m}{dt^2} = \frac{2\,\mathrm{A}\,h}{\mathrm{T}^2}\,\frac{y_{m+1} - 2y_m + y_{m-1}}{r^2}.$$

Fig. 1 Mixed differential-difference equation—vibration of one dimensional lattice for a sound propagation model; from Lagrange [4], Recherche sur la nature et la propagation du son, page 55

$$\begin{aligned}
\frac{d^2 y_1}{dt^2} &= \frac{2\,\mathrm{P}\,h}{\mathrm{MT}^2}\,\frac{y_2 - 2y_1}{r},\\
\frac{d^2 y_2}{dt^2} &= \frac{2\,\mathrm{P}\,h}{\mathrm{MT}^2}\,\frac{y_3 - 2y_2 + y_1}{r},\\
\frac{d^2 y_3}{dt^2} &= \frac{2\,\mathrm{P}\,h}{\mathrm{MT}^2}\,\frac{y_4 - 2y_3 + y_2}{r},\\
&\cdots\cdots\cdots\cdots\cdots\cdots\cdots\cdots,
\end{aligned}$$

Fig. 2 Mixed differential-difference equation—vibration of one dimensional string lattice; From Lagrange [4], Recherche sur la nature et la propagation du son, page 60

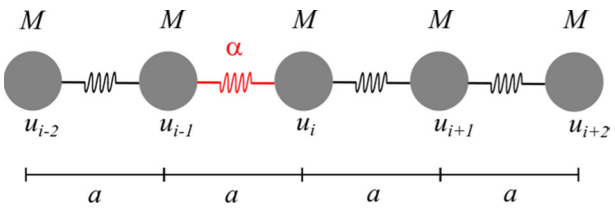

Fig. 3 One-dimensional axial lattice with mass M and longitudinal springs of stiffness σ (for Lagrange lattice or one dimensional Born – Kármán lattice)

(or discrete second-order spatial difference operator in Eq. (1)). In this sense, Lagrange's mixed differential-difference equation can also be attributed to the preliminary works of Bernoulli. Lagrange [4] derived the exact solution for Eq. (1) by a discrete summation of trigonometric functions of time (which may be reinterpreted in terms of discrete Fourier transform method) [4]. A very concise solution based on such finite trigonometric summation is presented by Filimonov et al. [10] for initial conditions based on Dirac distribution [10]. The exact solution of Eq. (1) was alternatively found elegantly during the twentieth century by Schrödinger [11] for general initial conditions in terms of Bessel functions (see more recently [12,13] or [14]) (Fig. 3).

By setting the scaling parameters:

$$\alpha = \frac{ES}{a} \text{ and } M = \rho S a \tag{2}$$

where E is the Young's modulus, S is the equivalent cross sectional area, and ρ the mass density per unit volume. Equation (1) may be expressed as:

$$ES\frac{u_{i+1} - 2u_i + u_{i-1}}{a^2} = \rho S\,\ddot{u}_i \tag{3}$$

i.e., the lattice difference equations are equivalent to a central finite difference formulation of the continuous wave equation, as Maugin [15] pointed out [15]. In the asymptotic limit, for a sufficiently smooth function $u_i\,(t) = u\,(x = ai, t)$, the long wave approximation of Eq. (3) is:

$$ES\frac{\partial^2 u\,(x,t)}{\partial x^2} = \rho S\,\frac{\partial^2 u\,(x,t)}{\partial t^2} \tag{4}$$

This continuous approximation of a discrete problem is particularly efficient in computing the low order frequencies of the finite system (see [4,16,17]). However, even in the linear elastic range, described by Eq. (1) with given elastic constant α for the lattice, the continuous approximation Eq. (4) is not able to reproduce its wave dispersive properties (see the extensive analyses of Born and von Kármán [6]—see also Born and Huang [18]; Maradudin et al. [19]; Askar [20]; Eringen [21]; Maugin [15]; Eringen [22]; Kittel [23]). Furthermore,

it was shown by Filimonov et al. [10] that the solution of the continuous problem may be asymptotically significantly different from the lattice one for large time evolution (even in the linear range). Schrödinger [11] also discussed the limits of the continuous approximation of the wave equation with respect to the lattice wave behavior (see also [12,13] or [14]).

However, this brief historical presentation will not address the strong mathematical difficulties related to the connection of nonlinear discrete lattices and nonlinear wave equations, including the soliton phenomenon [24]. The investigation of the complex behavior of nonlinear elastic lattices started with the pioneer works by Fermi et al. [25], who studied the dynamic behavior of a 1D axial lattice with a nonlinear elastic restoring force [25]. Continuous approximations have been developing since the 1960s to approximate such nonlinear dynamic models (see [26–28], for instance). The reader is directed to the seminal works of Rosenau [28], Maugin [15], Kosevich [29] or more recently to the monograph of Abramian et al. [30], for an extensive treatment of nonlinear lattices and enriched nonlinear wave equations. The present paper is, however, restricted to linear elasticity both for the lattice and its possible continuum representation.

The question about the relations of 2D or 3D elastic lattices with the relevant continua is tantamount to asking for the foundation of continuum mechanics from the lattice one. This question was first addressed by Boscovich (1763), who proposed the key idea of the molecular foundation of elasticity [31]. The link between discrete (or molecular) and continuous elasticity dates from the beginning of the nineteenth century, with the studies of French mechanists: indeed, a partial molecular theory of elasticity was first built by Navier [32], Cauchy [33] and Poisson [34], inspired by Boscovich's fundamental assumption that elastic bodies are composed of particles interacting along their joining lines. These inner forces are supposed repulsive when the distance between particles becomes smaller than a given quantity, attractive when the distance is between such a lower limit and another quantity, called radius of molecular activity (which, however, is much smaller with respect to ordinary lengths), and vanish outside such radius ([31]; see also the analysis of Boscovich's contribution in Thomson [35]; Kelvin [36]; Timoshenko [37]). These theories rely on the concept of central forces between particles, and in the asymptotic limit of an isotropic continuum lead to a unique elastic constant: this is in contradiction with the energetic formulation of linear isotropic elasticity for continua leading to two independent elastic constants [38]. Navier [32] first elaborated the molecular theory leading to a single constant for isotropic solids ("rari-constant" theory), which Cauchy and Poisson generalized to orthotropic solids. This leads to a model of constrained elasticity where Poisson's ratio equal to 1/4 for 3D bodies (i.e., what we call Lamé parameters λ and μ coincide). For anisotropic elastic solids, Cauchy [33] found 15 constants basing on the central interaction assumption, while Green's energetic approach foresaw 21 (Green continuum theory of linear elastic anisotropic solids, [39]). The controversy ended only at the end of the nineteenth century (see the historical analysis of Foce [40]; Capecchi et al. [41]; Capecchi et al. [42]). Voigt [39,43] considered molecules as small corpuscules with orientation, thus admitting that molecular interactions consist of both the usual central forces and additional moments depending on the orientation of the molecules (see also [44]). Voigt thus obtained two elastic constants for isotropic solids, succeeding in reconciling the molecular and continuum elasticity theories. Poincaré [45] derived the same results by considering a multi-potential theory that generalizes pure central interactions, with an additional potential of angle variation for the three-body interaction [45]. In other words, the theory of the French mechanists at the beginning of the nineteenth century was partial, since it included only central forces, and may be viewed as a constrained discrete elasticity theory.

The consistent 3D generalization of the 1D lattice elasticity developed by Lagrange [4] appeared much later: Born and von Kármán presented the mixed differential-difference equations of discrete isotropic elasticity in 1912 [6], based on a model that can be reduced to three parameters. Their mechanical model is a regular cubic lattice of body-points connected by longitudinal, diagonal and shear linear elastic springs. The lattice equations asymptotically converge to Navier's partial differential equations of elastodynamics for sufficiently small lattice spacing, thus coinciding with a spatial finite difference formulation of continuous elasticity, as for 1D Lagrange's lattice. When shear springs are neglected, Born–Kármán's lattice involves only central forces, in accord with Navier's molecular assumption [32], and in the limit, follows the "rari-constant" theory. As a consequence, a truss (which is a discrete system composed of nodes connected by axial springs interacting only by central forces) is generally not able to reproduce elasticity at the microscale (for general macroscopic elastic properties): a complete lattice theory needs to incorporate rotational or shear springs (see also the extensive review on general lattice models for heterogeneous structures by Ostoja-Starzewski [46]).

The full mixed differential-difference equations of discrete elasticity, valid for a monatomic cubic lattice, are given by Born and von Kármán [6] and their Eq. (10) (see Fig. 4), and include both central and non-central (shear in Born–Kármán's lattice) forces, even in the isotropic case. These maybe seen as axial springs, joining nearest particles and next-to-nearest particles), and shear springs joining nearest particles: on page 300 of

$$
\begin{aligned}
X_{lmn} = {} & \alpha\,(u_{l+1,m,n} + u_{l-1,m,n} - 2\,u_{l,m,n}) \\
& + \beta\,(u_{l,m+1,n} + u_{l,m-1,n} + u_{l,m,n+1} \\
& \quad + u_{l,m,n-1} - 4\,u_{l,m,n}) \\
& + \gamma\,(u_{l+1,m,n+1} + u_{l+1,m+1,n} \\
& \quad + u_{l+1,m,n-1} + u_{l+1,m-1,n} \\
& \quad - 4\,u_{l,m,n} + u_{l-1,m,n+1} \\
& \quad + u_{l-1,m+1,n} + u_{l-1,m,n-1} \\
& \quad + u_{l-1,m-1,n} - 4\,u_{l,m,n}) \\
& + \delta\,(u_{l,m+1,n+1} + u_{l,m-1,n+1} \\
& \quad + u_{l,m+1,n-1} + u_{l,m-1,n-1} \\
& \quad - 4\,u_{l,m,n}) \\
& + \varkappa\,(v_{l+1,m+1,n} + v_{l-1,m-1,n} \\
& \quad - v_{l+1,m-1,n} - v_{l-1,m+1,n} \\
& \quad + w_{l+1,m,n+1} + w_{l-1,m,n-1} \\
& \quad - w_{l+1,m,n-1} - w_{l-1,m,n+1}).
\end{aligned}
\qquad (10)
$$

Fig. 4 Mixed differential-difference equation—vibration of three-dimensional elastic lattice; Eq. (10) from Born and von Kármán [6]

Born and von Kármán [6], one reads: "Es stammen dabei die erste und zweite klammer von den relativen x-Verschiebungen der 6 Punkte in der Entfernung a, wobei natürlich den beiden Punkten auf der x-Achse im allgemeinen ein anderer Faktor zukommt, als den 4 Punkten senkrecht dazu." that is "The first and second brackets [of their Eq. (10)] depend on the relative x-displacements of the 6 points at distance a, where of course, the two points on the x-axis generally have a different factor than the 4 points perpendicular to it." This fundamental statement introduces non-central (shear) forces, orthogonal to the lattice lines joining nearest particles and not incorporated in Navier's molecular theory [32]. Born–Kármán's lattice is widely studied (see, e.g., the lattice model of Suiker et al. [47] and Zhang et al. [48]). For pure central forces, Born–Kármán's lattice is limited to horizontal, vertical and diagonal axial springs, with two stiffnesses, and its limit behavior implies a specific Poisson's ratio. This constrained lattice in 2D is generally dubbed square Bravais lattice in the literature, and was also widely used (see [49–55]). It was revisited during the twentieth century in a truss framework analysis by Wieghardt [56], Riedel [57], Hrennikoff [58], Hrennikoff [59], McHenry [60] and McHenry [61]. McHenry truss (re-considered by Hrennikoff, who introduced additional auxiliary bars [59]) is equivalent to the square Bravais lattice, or to Born–Kármán's limited to central forces. For plane stress, Poisson's ratio of the asymptotic continuum associated to these lattices is restricted to the value $\upsilon = 1/3$. In contrast to McHenry-Hrennikoff truss, the complete Born–Kármán's lattice model leads to a "free" Poisson's ratio, bounded by $\upsilon = 1/4$ for plane strain or 3D elasticity and $\upsilon = 1/3$ for plane stress elasticity.

However, Born–Kármán's lattice does not comply with rotational invariance, which is required, together with invariance in translation, for a consistent lattice theory [62–66]. The non-central force term associated with shear forces is responsible for the violation of the rotational invariance principle, with confusion between rigid rotation and shear modes. As in Gazis and Wallis [63], the energy of the lattice should be expressed as a function of such invariant quantities as distances between pairs of atoms or angles formed by three atoms (idea also shared by Voigt and Poincaré). Gazis et al. [67] gave a definite answer to the paradoxical properties of Born–Kármán's lattice by replacing the shear interaction with rotational springs. Gazis et al. lattice is consistent, in the sense that it fulfills both rotational and translational invariance, and asymptotically converges toward a linear isotropic elastic continuum with free equivalent Poisson's ratio. Thus, in Gazis et al. [67], there is a bridge between discrete and continuous linear isotropic elasticity from a monatomic cubic lattice with central first and second neighborhood interactions, plus additional rotationally invariant angular forces [67]. In the present paper, we do not discuss in detail other lattices with their mechanical representations; for instance, Clark et al. [26] developed a consistent lattice model with four (two central and two angular) interactions for body-centered cubic lattices, which are rotationally invariant [68]. This model is an alternative to De launay's lattice body-centered cubic lattice model [51] which relies on four mechanical interactions, but with non-rotationally invariant angular forces. However, surprisingly, the frequency dispersive equations for these two models may coincide for some parameter equivalence, as shown by Bose et al. [69], Kothari and Singhal [70], Shukla [71] and Ramamurthy [72]. Here, we show that Born–Kármán [6] and Gazis et al. lattice [67] coincide only in the long wave range limit (isotropic continuous medium), but their mixed differential-

difference equations and frequency dispersive equations differ, except in the case of central interactions. An alternative three-parameter linear elastic lattice model, also converging toward Navier's isotropic continuous equations, is the truss in Hrennikoff [59] (see also [73]), where the square Bravais lattice (central forces) foresees additional bars connected to the diagonal ones instead of the shear springs of Born and von Kármán. Triangular lattices (with unit hexagonal cell) with both central and angular interactions which also asymptotically converge toward isotropic linear elastic continuum may be also mentioned [74,75]. As for the cubic lattice with angular interactions (Gazis et al. lattice [67]), the angular interaction (non-central interaction) in the triangular regular lattice allows to calibrate the Poisson's ratio of the associated asymptotic linear elastic isotropic continuum solid. More recent lattices that also converge toward the isotropic elastic continua are those of Zhang et al. lattice with three parameters characterizing normal, secondary springs and rotational springs [48,76], and that of Nannapaneni et al. [77] with three parameters characterizing normal, diagonal and equivalent volumetric interactions. Even if these lattice models are physically and mathematically different, and also differ from their mixed differential-difference equations, it is worth noting that they all converge toward the isotropic continuum, always yielding Navier's partial differential equations of elastodynamics.

This paper also briefly presents the main contributions on discrete and continuous structural mechanics. Discrete beams (or lattice beams) were investigated by Hencky [78]; his model consists of rigid beam segments connected by frictionless hinges and elastic rotational springs, the stiffness of which is defined as the ratio of beam flexural rigidity to the segment length [78]. This system called Hencky-Bar-Chain system, asymptotically converges toward a continuous Euler-Bernoulli beam, for a sufficiently large number of segments, with a mathematical analogy between the difference equations of the lattice beam, and the finite difference formulation of the continuous Euler-Bernoulli beam (see [79] for the validity of this equivalence for various boundary conditions [79]). For all these one-dimensional problems (strings, rods or beams), discrete models may be built from repetition of simple structural elements, which asymptotically converge toward the associated one-dimensional continuum. The difference equations of the discrete elasticity problem coincide with the finite difference formulation of the continuous one. Hencky's model of discrete beam was extended to discrete plate [79–82]. Bridging discrete and continuous models (for elasticity or even more general constitutive laws) is an old and fundamental topic in the history of physics and mechanics. This brief historical study may find a resonance today, with a regained interest in bridging scales, with the active development of metamaterials based on design-oriented macroscopic properties [79,83].

Below, we present several lattice models that are not mathematically equivalent, yet all converging asymptotically toward the continuous linear isotropic elastic solid if the lattice spacing goes to zero. It is not the scope of this paper to present more complex anisotropic or inelastic lattices. However, we shall close the paper with a brief discussion on the capability of nonlocal continua to bridge the scale from anisotropic cubic lattices to isotropic continuous elasticity.

2 3D discrete elasticity: the Born–Karman model

The lattice is assumed to be monatomic and cubic, composed of particles with equal mass M and lattice spacing a. The elastic interaction consists of nearest and next-to-nearest central forces corresponding to fictitious axial springs of stiffness α, for the links between nearest particles, and β, for the links among next-to-nearest particles (notations used by Gazis et al. [67]) and non-central forces corresponding to fictitious shear springs of stiffness δ located along the lines between nearest particles. Thus, pure central forces (Navier, Poisson's or Cauchy's molecular assumption) are retrieved when $\delta = 0$ and do not tend toward a general Hooke's law at the continuum limit with prescribed values of Poisson's ratio. Pure central forces do not allow in the case of direct interactions the formulation of a general Hooke's law at the continuum limit with prescribed values of Poisson's ratio. Born–Kármán's lattice thus depends on three stiffness parameters (α, β, δ) to simulate central and shear interactions, respectively. In the case of isotropy, a constraint equation for α, β, δ holds, so that the model has two independent parameters that can then be related to those of the elastic isotropic continuum. In the paper, we will restrict our analysis to linear difference equation of the displacement in space, so that nonlinear geometrical effects will be neglected.

The mixed differential-difference equation of the 3D Born–Kármán's lattice is expressed by Eq. (10) of Born and von Kármán [6]—(see Fig. 4)—and is originally written for a non-isotropic lattice (which converges toward a non-isotropic continuum) by the five- parameters $\left(\alpha', \beta', \gamma', \delta', \chi'\right)$:

$$\begin{aligned}
&\alpha'\left(u_{i+1,j,k}-2u_{i,j,k}+u_{i-1,j,k}\right)+\beta'\left(u_{i,j+1,k}+u_{i,j-1,k}+u_{i,j,k+1}+u_{i,j,k-1}-4u_{i,j,k}\right)\\
&\quad+\gamma'\left(u_{i+1,j+1,k}+u_{i-1,j+1,k}+u_{i+1,j-1,k}+u_{i-1,j-1,k}+u_{i+1,j,k+1}\right.\\
&\quad\left.+u_{i-1,j,k+1}+u_{i+1,j,k-1}+u_{i-1,j,k-1}-8u_{i,j,k}\right)\\
&\quad+\delta'\left(u_{i,j+1,k+1}+u_{i,j-1,k+1}+u_{i,j+1,k-1}+u_{i,j-1,k-1}-4u_{i,j,k}\right)\\
&\quad+\chi'\left(v_{i+1,j+1,k}+v_{i-1,j-1,k}-v_{i-1,j+1,k}-v_{i+1,j-1,k}\right.\\
&\quad\left.+w_{i+1,j,k+1}+w_{i-1,j,k-1}-w_{i+1,j,k-1}-w_{i-1,j,k+1}\right)\\
&=M\,\ddot{u}_{i,j,k}
\end{aligned}\tag{5}$$

For isotropic solids (in the long wave limit), Born and von Kármán's model reduces to three parameters by setting:

$$\delta'=0\,\text{and}\,\chi'=\gamma'\tag{6}$$

It is more convenient to introduce the following equivalent parameters:

$$\alpha'=\alpha;\quad \beta'=\delta\quad\text{and}\quad\gamma'=\frac{\beta}{2}\tag{7}$$

so that the governing equation of the three-parameter Born–Kármán's model reduces to:

$$\begin{aligned}
&\alpha\left(u_{i+1,j,k}-2u_{i,j,k}+u_{i-1,j,k}\right)+\frac{\beta}{2}\left(u_{i+1,j+1,k}+u_{i-1,j+1,k}+u_{i+1,j-1,k}\right.\\
&\quad\left.+u_{i-1,j-1,k}+u_{i+1,j,k+1}+u_{i-1,j,k+1}+u_{i+1,j,k-1}+u_{i-1,j,k-1}-8u_{i,j,k}\right)\\
&\quad+\frac{\beta}{2}\left(v_{i+1,j+1,k}+v_{i-1,j-1,k}-v_{i-1,j+1,k}-v_{i+1,j-1,k}+w_{i+1,j,k+1}+w_{i-1,j,k-1}\right.\\
&\quad\left.-w_{i+1,j,k-1}-w_{i-1,j,k+1}\right)\\
&\quad+\delta\left(u_{i,j+1,k}+u_{i,j-1,k}+u_{i,j,k+1}+u_{i,j,k-1}-4u_{i,j,k}\right)=M\,\ddot{u}_{i,j,k}
\end{aligned}\tag{8}$$

where(α, β, δ) are the stiffnesses mentioned above, illustrated in Fig. 5.

Born and von Kármán [6] did not detail the mechanical model behind these equations, since they wished to asymptotically attain the partial differential equation of Navier's elastodynamics in the continuum limit. It is worth mentioning that at the boundary, the stiffness of the vertical and longitudinal elements is $\alpha/4$, the shear stiffness is $\delta/4$ and the stiffness of the diagonal element is $\beta/2$ (see Fig. 5). Equation (8) may be viewed as a generalization of Lagrange's mixed differential-difference equation (1) for 3D lattices, and can be derived from a direct expression of equilibrium including inertia forces. It is also possible to derive this mixed differential-difference equation by an energy approach, based on the following potential energy:

$$U=\sum_i\sum_j\sum_k\frac{\alpha}{8}\left[\begin{array}{l}
\left(u_{i+1,j,k}-u_{i,j,k}\right)^2+\left(u_{i+1,j+1,k}-u_{i,j+1,k}\right)^2\\
+\left(u_{i+1,j,k+1}-u_{i,j,k+1}\right)^2+\left(u_{i+1,j+1,k+1}-u_{i,j+1,k+1}\right)^2\\
+\left(v_{i,j+1,k}-v_{i,j,k}\right)^2+\left(v_{i+1,j+1,k}-v_{i+1,j,k}\right)^2\\
+\left(v_{i,j+1,k+1}-v_{i,j,k+1}\right)^2+\left(v_{i+1,j+1,k+1}-v_{i+1,j,k+1}\right)^2\\
+\left(w_{i,j,k+1}-w_{i,j,k}\right)^2+\left(w_{i+1,j,k+1}-w_{i+1,j,k}\right)^2\\
+\left(w_{i,j+1,k+1}-w_{i,j+1,k}\right)^2+\left(w_{i+1,j+1,k+1}-w_{i+1,j+1,k}\right)^2
\end{array}\right]$$

$$
\begin{aligned}
&+\frac{\beta}{8}\left[\begin{array}{l}
\left(u_{i+1,j+1,k}-u_{i,j,k}+v_{i+1,j+1,k}-v_{i,j,k}\right)^2\\
+\left(u_{i+1,j,k}-u_{i,j+1,k}+v_{i+1,j,k}-v_{i,j+1,k}\right)^2\\
+\left(u_{i+1,j+1,k+1}-u_{i,j,k+1}+v_{i+1,j+1,k+1}-v_{i,j,k+1}\right)^2\\
+\left(u_{i+1,j,k+1}-u_{i,j+1,k+1}+v_{i+1,j,k+1}-v_{i,j+1,k+1}\right)^2\\
+\left(u_{i+1,j,k+1}-u_{i,j,k}+w_{i+1,j,k+1}-w_{i,j,k}\right)^2\\
+\left(u_{i+1,j,k}-u_{i,j,k+1}+w_{i+1,j,k}-w_{i,j,k+1}\right)^2\\
+\left(u_{i+1,j+1,k+1}-u_{i,j+1,k}+w_{i+1,j+1,k+1}-w_{i,j+1,k}\right)^2\\
+\left(u_{i+1,j+1,k}-u_{i,j+1,k+1}+w_{i+1,j+1,k}-w_{i,j+1,k+1}\right)^2\\
+\left(v_{i,j+1,k+1}-v_{i,j,k}+w_{i,j+1,k+1}-w_{i,j,k}\right)^2\\
+\left(v_{i,j+1,k}-v_{i,j,k+1}+w_{i,j+1,k}-w_{i,j,k+1}\right)^2\\
+\left(v_{i+1,j+1,k+1}-v_{i+1,j,k}+w_{i+1,j+1,k+1}-w_{i+1,j,k}\right)^2\\
+\left(v_{i+1,j+1,k}-v_{i+1,j,k+1}+w_{i+1,j+1,k}-w_{i+1,j,k+1}\right)^2
\end{array}\right]\\
&+\frac{\delta}{8}\left[\begin{array}{l}
\left(u_{i,j+1,k}-u_{i,j,k}\right)^2+\left(u_{i+1,j+1,k}-u_{i+1,j,k}\right)^2\\
+\left(u_{i,j+1,k+1}-u_{i,j,k+1}\right)^2+\left(u_{i+1,j+1,k+1}-u_{i+1,j,k+1}\right)^2\\
+\left(w_{i,j+1,k}-w_{i,j,k}\right)^2+\left(w_{i+1,j+1,k}-w_{i+1,j,k}\right)^2\\
+\left(w_{i,j+1,k+1}-w_{i,j,k+1}\right)^2+\left(w_{i+1,j+1,k+1}-w_{i+1,j,k+1}\right)^2\\
+\left(v_{i+1,j,k}-v_{i,j,k}\right)^2+\left(v_{i+1,j+1,k}-v_{i,j+1,k}\right)^2\\
+\left(v_{i+1,j,k+1}-v_{i,j,k+1}\right)^2+\left(v_{i+1,j+1,k+1}-v_{i,j+1,k+1}\right)^2\\
+\left(w_{i+1,j,k}-w_{i,j,k}\right)^2+\left(w_{i+1,j+1,k}-w_{i,j+1,k}\right)^2\\
+\left(w_{i+1,j,k+1}-w_{i,j,k+1}\right)^2+\left(w_{i+1,j+1,k+1}-w_{i,j+1,k+1}\right)^2\\
+\left(u_{i,j,k+1}-u_{i,j,k}\right)^2+\left(u_{i+1,j,k+1}-u_{i+1,j,k}\right)^2\\
+\left(u_{i,j+1,k+1}-u_{i,j+1,k}\right)^2+\left(u_{i+1,j+1,k+1}-u_{i+1,j+1,k}\right)^2\\
+\left(v_{i,j,k+1}-v_{i,j,k}\right)^2\\
+\left(v_{i+1,j,k+1}-v_{i+1,j,k}\right)^2+\left(v_{i,j+1,k+1}-v_{i,j+1,k}\right)^2\\
+\left(v_{i+1,j+1,k+1}-v_{i+1,j+1,k}\right)^2
\end{array}\right]
\end{aligned}
\tag{9}
$$

The kinetic energy of this lattice with concentrated masses at each "node" is reduced to:

$$
T=\sum_i\sum_j\sum_k M\,\dot{u}_{i,j,k}^2+M\,\dot{v}_{i,j,k}^2++M\,\dot{w}_{i,j,k}^2 \tag{10}
$$

Hamilton's principle applied to the Lagrangian $L=T-U$ yields Eq. (8). The difference equations can be extended to an equivalent continuum via a continualization method that is valid for a sufficiently smooth deflection function. The following relation between the discrete and the equivalent continuous system $u_{i,j,k}=u\,(x=ai,y=aj,z=ak)$, $v_{i,j,k}=v\,(x=ai,y=aj,z=ak)$ and $w_{i,j,k}=w\,(x=ai,y=aj,z=ak)$holds true for sufficiently smooth displacements given by:

$$
u_{i+1,j+1,k+1}=u\,(x+a,y+a,z+a)=e^{a\left(\partial_x+\partial_y+\partial_z\right)}u\,(x,y,z) \tag{11}
$$

where ∂_x, ∂_y and ∂_z are the spatial derivatives with respect to x, y and z. Equation (11) is based on the use of a Taylor-based asymptotic expansion of the discrete displacement field of a neighbored node around the considered node. The exponential differential operator in front of the continuous displacement field belongs to the so-called pseudo-differential operator. Such an expansion of difference operators was already known at the beginning of the nineteenth century (e.g., [84,85]), see Figs. 6, 7, and was used in Piola [85] for bridging discrete and continuum elasticity (a presentation of Piola's works is in Todhunter and Pearson [86] and Dell'Isola et al. [87,88]). Piola [87] considered central force potential and made an asymptotic expansion with respect to the small quantities in the associated molecular energy. Piola also mentioned angular interactions as possible additional potential interactions. A modern treatment of this expansion method related to the numerical efficiency of finite difference schemes can be found in Shokin [89] and Godunov and Ryabenkii [90].

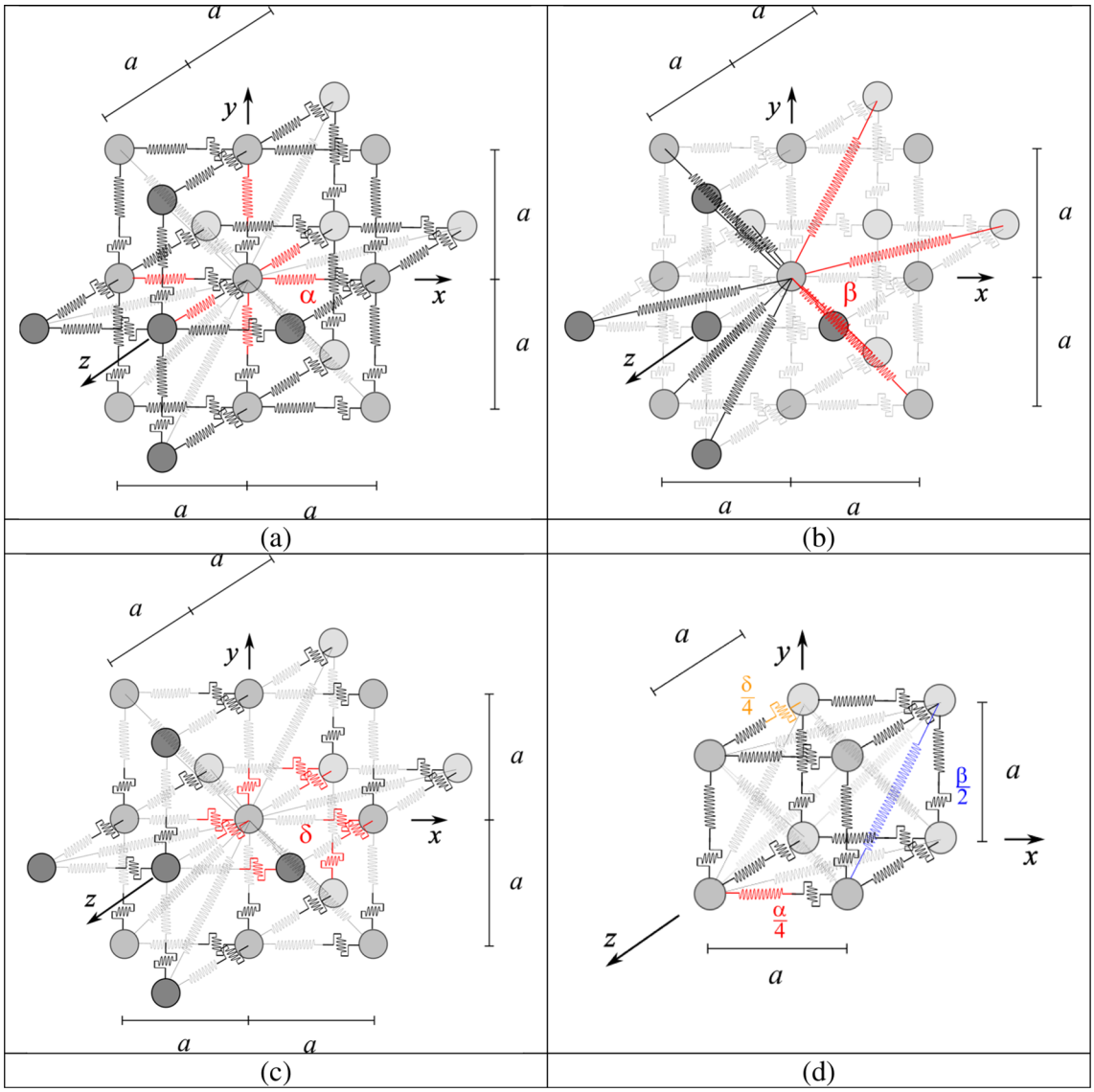

Fig. 5 Mechanical representation of Born and von Kármán [6] lattice

Dans le cas particulier où l'on suppose $m = 1$, les formules symboliques (10) et (11) se réduisent à

$$\Delta u = \left(e^{hD} - 1\right)u = e^{hD}u - u, \tag{12}$$

$$\Delta^{-1}u = \left(e^{hD} - 1\right)^{-1}u; \tag{13}$$

et l'on en conclut

$$\Delta u = hDu + \frac{h^2}{1.2}D^2u + \frac{h^3}{1.2.3}D^3u + \text{etc...}, \tag{14}$$

Fig. 6 Asymptotic expansion of difference operators through differential operators; From Cauchy, page 157, Exercices de mathématiques; Cauchy [33] – Sur les différences finies et les intégrales aux différences des fonctions entières d'une ou de plusieurs variables; page 155–159

The system of spatial difference equations in Eq. (8) leads to the continuous formulations at the long wave limit:

$$(\alpha+2\beta)\frac{\partial^2 u}{\partial x^2}+2\beta\frac{\partial^2 v}{\partial x\partial y}+2\beta\frac{\partial^2 w}{\partial x\partial z}+(\delta+\beta)\frac{\partial^2 u}{\partial y^2}+(\delta+\beta)\frac{\partial^2 u}{\partial z^2}=\rho a\frac{\partial^2 u}{\partial t^2} \tag{12}$$

where we used the mass scaling identity $M=\rho a^3$. Equation (12) can be identified with Navier's partial differential equation of linear elasticity for material with the constant (c_{11}, c_{12}, c_{44}) of cubic symmetry, using Voigt's notation [6]:

$$c_{11}\frac{\partial^2 u}{\partial x^2}+(c_{12}+c_{44})\frac{\partial^2 v}{\partial x\partial y}+(c_{12}+c_{44})\frac{\partial^2 w}{\partial x\partial z}+c_{44}\frac{\partial^2 u}{\partial y^2}+c_{44}\frac{\partial^2 u}{\partial z^2}=\rho\frac{\partial^2 u}{\partial t^2} \tag{13}$$

Navier's partial differential equation of linear isotropic elasticity can be derived as a particular case, for $c_{11}=c_{12}+2c_{44}$:

$$(\lambda+2\mu)\frac{\partial^2 u}{\partial x^2}+(\lambda+\mu)\frac{\partial^2 v}{\partial x\partial y}+(\lambda+\mu)\frac{\partial^2 w}{\partial x\partial z}+\mu\frac{\partial^2 u}{\partial y^2}+\mu\frac{\partial^2 u}{\partial z^2}=\rho\frac{\partial^2 u}{\partial t^2}\quad\text{with}$$
$$\begin{cases} c_{11}=\lambda+2\mu \\ c_{44}=\mu \\ c_{12}=\lambda \end{cases} \tag{14}$$

where λ and μ are Lamé coefficients. By comparing Eq. (12) with Eq. (14), it is clear that the lattice parameters can be identified through (see also Eq. (13) of Born and von Kármán [6]):

$$\begin{cases} \alpha=a\ (c_{11}-c_{12}-c_{44})=\mu\, a \\ \delta=\frac{a}{2}\,(c_{44}-c_{12})=\frac{a}{2}\,(\mu-\lambda) \\ \beta=\frac{a}{2}\,(c_{44}+c_{12})=\frac{a}{2}\,(\mu+\lambda) \end{cases} \tag{15}$$

Equation (15) shows that Born and von Kármán's lattice model asymptotically converges toward a continuum linear elastic material with cubic symmetry, which contains the linear elastic isotropic medium for some constrained material parameters. In fact, Eq. (15) can be inverted to furnish

$$\mu=\frac{\alpha}{a};\quad \lambda=\frac{\beta-\delta}{a}\quad\text{and}\,\delta=\alpha-\beta \tag{16}$$

which clearly shows that the three microscopic parameters can be constrained so that they can be identified from Lamé parameters of macroscopic elasticity. Keating [64] remarked that if $\beta=0$, i.e., by neglecting the next-nearest interaction, one obtains unsatisfactory macroscopic physical results, with a negative Lamé coefficient:

$$\beta=0\quad\Rightarrow\quad\mu=\frac{\alpha}{a}\geq 0\quad\text{and}\quad\lambda=\frac{-\alpha}{a}\leq 0 \tag{17}$$

A possible answer to this is that the positivity of the microscopic shear stiffness implies:

$$\delta\geq 0\quad\Rightarrow\quad\lambda\leq\mu\quad\Rightarrow\quad\upsilon\leq 1/4 \tag{18}$$

In the particular case of pure central forces, one obtains:

$$\delta=0\quad\Rightarrow\quad\mu=\lambda\quad\Rightarrow\quad\upsilon=1/4 \tag{19}$$

which is Eq. (14) of Born and von Kármán [6], equivalently written as $c_{44}=c_{12}$, and known as Cauchy-Poisson's relation. In this case, we also have:

$$\delta=0\quad\Rightarrow\quad\alpha=\beta \tag{20}$$

In the 3D McHenry-Hrennikoff truss (which is equivalent to the 3D Born–Kármán lattice with central forces), we have $\alpha=\beta$, i.e., no shear interactions ($\delta=0$). Born and von Kármán [6] noticed that central forces ($\delta=0$) in the limit lead to constrained continuum elasticity with a single constant $\lambda=\mu$, as obtained by Navier and

$$x(f,g,h) = x(a,b,c) + \frac{f-a}{\alpha}\Delta_a x + \frac{g-b}{\beta}\Delta_b x + \frac{h-c}{\gamma}\Delta_c x$$
$$+\frac{(f-a)(f-a-\alpha)}{2\alpha^2}\Delta_a^2 x + \frac{(f-a)(g-b)}{\alpha\beta}\Delta_a\Delta_b x + \frac{(f-a)(h-c)}{\alpha\gamma}\Delta_a\Delta_c x$$
$$+\frac{(g-b)(g-b-\beta)}{2\beta^2}\Delta_b^2 x + \frac{(g-b)(h-c)}{\beta\gamma}\Delta_b\Delta_c x + \frac{(h-c)(h-c-\gamma)}{2\gamma^2}\Delta_c^2 x + \text{ec.}$$

Fig. 7 Piola, p 179; asymptotic expansion of difference operators through differential operators; Nuovo analisi del moto e dell' equilibrio de' corpi omogenei considerati come ammassi di molecule, in Memorie di Matematica e di Fisica della Societa Italiana delle Scienze, Modena, 1836

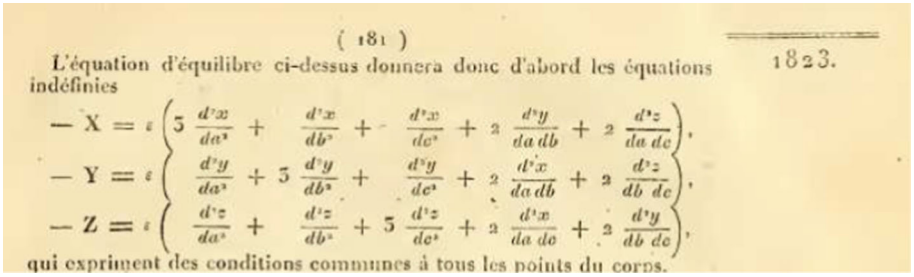
(181)

1823.

L'équation d'équilibre ci-dessus donnera donc d'abord les équations indéfinies

$$-X = \varepsilon\left(3\frac{d^2x}{da^2} + \frac{d^2x}{db^2} + \frac{d^2x}{dc^2} + 2\frac{d^2y}{da\,db} + 2\frac{d^2z}{da\,dc}\right),$$
$$-Y = \varepsilon\left(\frac{d^2y}{da^2} + 3\frac{d^2y}{db^2} + \frac{d^2y}{dc^2} + 2\frac{d^2x}{da\,db} + 2\frac{d^2z}{db\,dc}\right),$$
$$-Z = \varepsilon\left(\frac{d^2z}{da^2} + \frac{d^2z}{db^2} + 3\frac{d^2z}{dc^2} + 2\frac{d^2x}{da\,dc} + 2\frac{d^2y}{db\,dc}\right),$$

qui expriment des conditions communes à tous les points du corps.

Fig. 8 Navier [32]—Navier's elastodynamics partial differential equations for the rare-constant theory; $\lambda = \mu$

Poisson; assuming central forces, Kelvin [36] came to the same conclusion for the compressibility modulus K:

$$K = \frac{3\lambda + 2\mu}{3} = \frac{5\alpha}{3a} \quad \text{with} \quad \alpha = \beta = \mu a = \lambda a \tag{21}$$

In this last case, for $\lambda = \mu$, Navier's partial differential equation Eq. (14) reduces to:

$$3\frac{\partial^2 u}{\partial x^2} + 2\frac{\partial^2 v}{\partial x \partial y} + 2\frac{\partial^2 w}{\partial x \partial z} + \frac{\partial^2 u}{\partial y^2} + \frac{\partial^2 u}{\partial z^2} = \frac{\rho}{\mu}\frac{\partial^2 u}{\partial t^2} \tag{22}$$

and is usually labelled as given by the so-called "rari-constant" theory, Fig. 8.

Using the stiffness calibration Eq. (15), the mixed difference-differential equations of Born von Karman [6] are a spatial finite difference formulation of Navier's continuous partial differential equations, as for Lagrange's 1D lattice:

$$\begin{aligned}
&\mu\left(u_{i+1,j,k} - 2u_{i,j,k} + u_{i-1,j,k}\right) + \frac{\lambda+\mu}{4}\left(u_{i+1,j+1,k} + u_{i-1,j+1,k} + u_{i+1,j-1,k}\right.\\
&\left.+u_{i-1,j-1,k} + u_{i+1,j,k+1} + u_{i-1,j,k+1} + u_{i+1,j,k-1} + u_{i-1,j,k-1} - 8u_{i,j,k}\right)\\
&+\frac{\lambda+\mu}{4}\left(v_{i+1,j+1,k} + v_{i-1,j-1,k} - v_{i-1,j+1,k} - v_{i+1,j-1,k} + w_{i+1,j,k+1} + w_{i-1,j,k-1}\right.\\
&\left.- w_{i+1,j,k-1} - w_{i-1,j,k+1}\right)\\
&+\frac{\mu-\lambda}{2}\left(u_{i,j+1,k} + u_{i,j-1,k} + u_{i,j,k+1} + u_{i,j,k-1} - 4u_{i,j,k}\right) = \rho a^2\,\ddot{u}_{i,j,k}
\end{aligned} \tag{23}$$

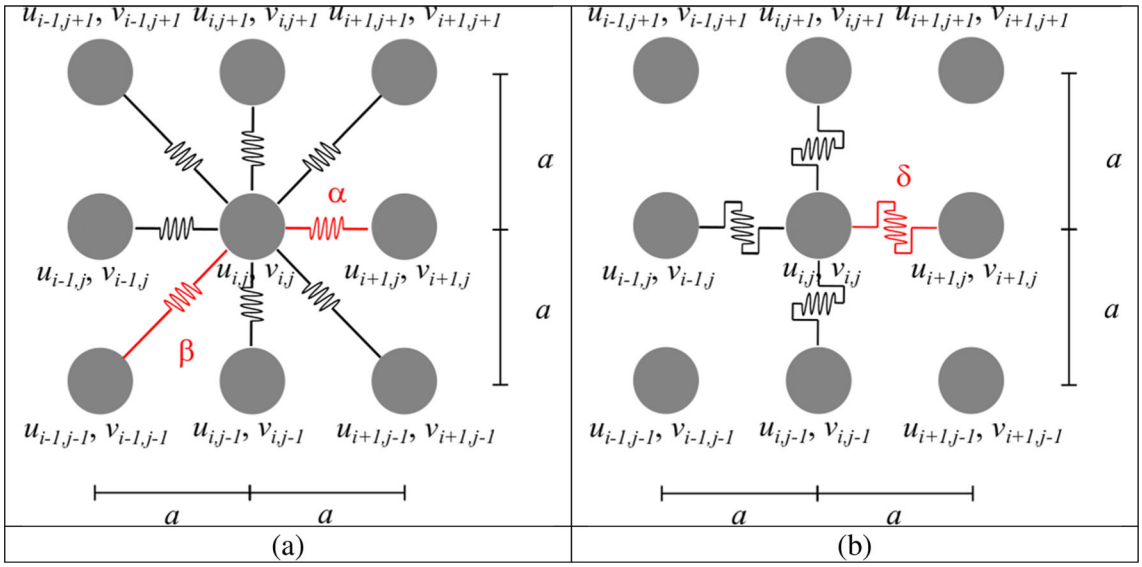

Fig. 9 Two-dimensional Born and Kármán [6] lattice with longitudinal and vertical elastic springs (of stiffness α), diagonal elastic springs (of stiffness β), and shear springs (of stiffness δ)

An asymptotic expansion of Born–Kármán's mixed differential-difference equations Eq. (23), leads to higher-order gradient elasticity partial differential equations of the lattice:

$$\begin{aligned}
&\mu\left(\frac{\partial^2 u}{\partial x^2}+\frac{a^2}{12}\frac{\partial^4 u}{\partial x^4}\right)\\
&+\left(\frac{\lambda+\mu}{4}\right)\left(4\frac{\partial^2 u}{\partial x^2}+2\frac{\partial^2 u}{\partial y^2}+a^2\frac{\partial^4 u}{\partial x^2\partial y^2}+\frac{a^2}{3}\frac{\partial^4 u}{\partial x^4}+\frac{a^2}{6}\frac{\partial^4 u}{\partial y^4}+2\frac{\partial^2 u}{\partial z^2}+a^2\frac{\partial^4 u}{\partial x^2\partial z^2}+\frac{a^2}{6}\frac{\partial^4 u}{\partial z^4}\right)\\
&+\left(\frac{\mu-\lambda}{2}\right)\left(\frac{\partial^2 u}{\partial y^2}+\frac{a^2}{12}\frac{\partial^4 u}{\partial y^4}+\frac{\partial^2 u}{\partial z^2}+\frac{a^2}{12}\frac{\partial^4 u}{\partial z^4}\right)\\
&+\left(\frac{\lambda+\mu}{4}\right)\left(4\frac{\partial^2 v}{\partial x\partial y}+\frac{2}{3}a^2\frac{\partial^4 v}{\partial x\partial y^3}+\frac{2}{3}a^2\frac{\partial^4 v}{\partial y\partial x^3}+4\frac{\partial^2 w}{\partial x\partial z}+\frac{2}{3}a^2\frac{\partial^4 w}{\partial x\partial z^3}+\frac{2}{3}a^2\frac{\partial^4 w}{\partial z\partial x^3}\right)=\rho\frac{\partial^2 u}{\partial t^2}
\end{aligned} \tag{24}$$

The zeroth order of this expansion is Navier's elastodynamic partial differential equation; the terms proportional to the square of the lattice spacing account for scale effects. Born–Kármán's model may also include long range interactions and is extensively presented in the seminal books of Born and Huang [18] and Askar [20]. Exact solutions exist for the dispersion wave propagation equation in 2D or 3D elastic lattices: Born and von Kármán [6] presented the 3D case [6].

3 Two-dimensional discrete elasticity: the Born–Karman model

A 2D version of Born–Kármán's lattice is studied in detail by Suiker et al. [47] (Fig. 9), and is governed by:

$$\begin{cases}
\alpha\left(u_{i+1,j}-2u_{i,j}+u_{i-1,j}\right)+\frac{\beta}{2}\left(u_{i+1,j+1}+u_{i-1,j-1}+u_{i-1,j+1}+u_{i+1,j-1}-4u_{i,j}\right)\\
+\frac{\beta}{2}\left(v_{i+1,j+1}-v_{i-1,j+1}-v_{i+1,j-1}+v_{i-1,j-1}\right)+\delta\left(u_{i,j+1}-2u_{i,j}+u_{i,j-1}\right)=M\,\ddot{u}_{i,j}\\
\alpha\left(v_{i,j+1}-2v_{i,j}+v_{i,j-1}\right)+\frac{\beta}{2}\left(v_{i+1,j+1}+v_{i-1,j-1}+v_{i-1,j+1}+v_{i+1,j-1}-4v_{i,j}\right)\\
+\frac{\beta}{2}\left(u_{i+1,j+1}-u_{i-1,j+1}-u_{i+1,j-1}+u_{i-1,j-1}\right)+\delta\left(v_{i+1,j}-2v_{i,j}+v_{i-1,j}\right)=M\,\ddot{v}_{i,j}
\end{cases} \tag{25}$$

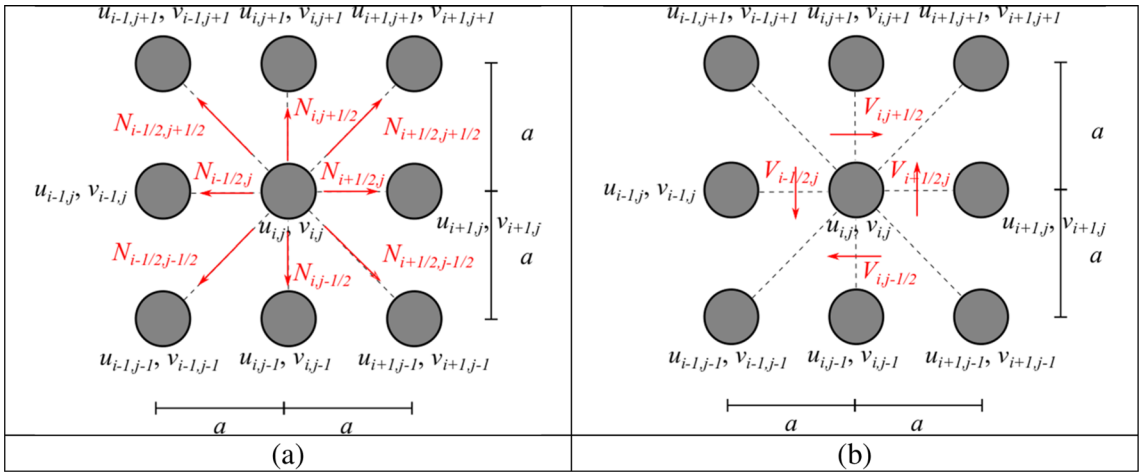

Fig. 10 Schematic diagram of the force equilibrium of two-dimensional [6] lattice

which results from a direct equilibrium of normal (N) and shear (V) forces around the node *(i,j)*:

$$\begin{cases} N_{i+1/2,j} - N_{i-1/2,j} + \frac{\sqrt{2}}{2} N_{i+1/2,j+1/2} + \frac{\sqrt{2}}{2} N_{i+1/2,j-1/2} \\ -\frac{\sqrt{2}}{2} N_{i-1/2,j+1/2} - \frac{\sqrt{2}}{2} N_{i-1/2,j-1/2} + V_{i,j+1/2} - V_{i,j-1/2} = M\ddot{u}_{i,j} \\ N_{i,j+1/2} - N_{i,j-1/2} + \frac{\sqrt{2}}{2} N_{i+1/2,j+1/2} + \frac{\sqrt{2}}{2} N_{i-1/2,j+1/2} \\ -\frac{\sqrt{2}}{2} N_{i-1/2,j-1/2} - \frac{\sqrt{2}}{2} N_{i+1/2,j-1/2} + V_{i+1/2,j} - V_{i-1/2,j} = M\ddot{v}_{i,j} \end{cases} \tag{26}$$

with

$$\begin{cases} N_{i+1/2,j} = \alpha \left(u_{i+1,j} - u_{i,j} \right) \\ N_{i-1/2,j} = \alpha \left(u_{i,j} - u_{i-1,j} \right) \\ N_{i,j+1/2} = \alpha \left(v_{i,j+1} - v_{i,j} \right) \\ N_{i,j-1/2} = \alpha \left(v_{i,j} - v_{i,j-1} \right) \\ N_{i+1/2,j+1/2} = \beta\sqrt{2}/2 \left(u_{i+1,j+1} - u_{i,j} + v_{i+1,j+1} - v_{i,j} \right) \\ N_{i+1/2,j-1/2} = \beta\sqrt{2}/2 \left(u_{i+1,j-1} - u_{i,j} - v_{i+1,j-1} + v_{i,j} \right) \\ N_{i-1/2,j+1/2} = \beta\sqrt{2}/2 \left(u_{i,j} - u_{i-1,j+1} + v_{i-1,j+1} - v_{i,j} \right) \\ N_{i-1/2,j-1/2} = \beta\sqrt{2}/2 \left(-u_{i-1,j-1} + u_{i,j} - v_{i-1,j-1} + v_{i,j} \right) \\ V_{i,j+1/2} = \delta \left(u_{i,j+1} - u_{i,j} \right) \\ V_{i,j-1/2} = \delta \left(u_{i,j} - u_{i,j-1} \right) \\ V_{i+1/2,j} = \delta \left(v_{i+1,j} - v_{i,j} \right) \\ V_{i-1/2,j} = \delta \left(v_{i,j} - v_{i-1,j} \right) \end{cases} \tag{27}$$

Figure 10 shows a scheme of forces with central (longitudinal, vertical and diagonal) and non-central (shear) forces: Eqs. (27) and (26) provide Eq. (25). The latter are obtained in an equivalent way starting from the following potential energy:

$$\begin{aligned} U = & \sum_i \sum_j \frac{\alpha}{4} \left[\left(u_{i+1,j} - u_{i,j} \right)^2 + \left(u_{i+1,j+1} - u_{i,j+1} \right)^2 + \left(v_{i,j+1} - v_{i,j} \right)^2 + \left(v_{i+1,j+1} - v_{i+1,j} \right)^2 \right] \\ & + \frac{\beta}{4} \left[\left(u_{i+1,j+1} - u_{i,j} + v_{i+1,j+1} - v_{i,j} \right)^2 + \left(u_{i+1,j} - u_{i,j+1} - v_{i+1,j} + v_{i,j+1} \right)^2 \right] \\ & + \frac{\delta}{4} \left[\left(v_{i+1,j} - v_{i,j} \right)^2 + \left(v_{i+1,j+1} - v_{i,j+1} \right)^2 + \left(u_{i,j+1} - u_{i,j} \right)^2 + \left(u_{i+1,j+1} - u_{i+1,j} \right)^2 \right] \end{aligned} \tag{28}$$

Equation (28) agrees with Eq. (5) of Montroll [50] where the shear is neglected (only longitudinal and diagonal interaction). Montroll's square lattice is purely central, and can be viewed as a particular case of Born–Kármán's one without shear interaction, i.e., $\delta = 0$, and coincides with Navier's lattice (lattice with pure

central interactions):

$$\begin{cases} \alpha\left(u_{i+1,j}-2u_{i,j}+u_{i-1,j}\right)+\frac{\beta}{2}\left(u_{i+1,j+1}+u_{i-1,j-1}+u_{i-1,j+1}+u_{i+1,j-1}-4u_{i,j}\right) \\ +\frac{\beta}{2}\left(v_{i+1,j+1}-v_{i-1,j+1}-v_{i+1,j-1}+v_{i-1,j-1}\right)=M\,\ddot{u}_{i,j} \\ \alpha\left(v_{i,j+1}-2v_{i,j}+v_{i,j-1}\right)+\frac{\beta}{2}\left(v_{i+1,j+1}+v_{i-1,j-1}+v_{i-1,j+1}+v_{i+1,j-1}-4v_{i,j}\right) \\ +\frac{\beta}{2}\left(u_{i+1,j+1}-u_{i-1,j+1}-u_{i+1,j-1}+u_{i-1,j-1}\right)=M\,\ddot{v}_{i,j} \end{cases} \tag{29}$$

These mixed differential-difference equations were also obtained by Blackman [49] from a direct approach [49]. Another particular case is the model of Rosenstock and Newell [91], which is equivalent to that of Montroll and Potts [92], who considered direct neighboring interactions only with central and non-central (shear) contributions. The model of Montroll and Potts [92] is equivalent to considering $\beta = 0$ in Eq. (25) (i.e., no diagonal springs):

$$\begin{cases} \alpha\left(u_{i+1,j}-2u_{i,j}+u_{i-1,j}\right)+\delta\left(u_{i,j+1}-2u_{i,j}+u_{i,j-1}\right)=M\,\ddot{u}_{i,j} \\ \alpha\left(v_{i,j+1}-2v_{i,j}+v_{i,j-1}\right)+\delta\left(v_{i+1,j}-2v_{i,j}+v_{i-1,j}\right)=M\,\ddot{v}_{i,j} \end{cases} \tag{30}$$

A consistent lattice theory should fulfil both translational and rotational invariance principle [62–66]. The energy of Born–Kármán's model fulfils invariance in translation: since all particles have the same displacement, it is trivial to check that Eq. (28) equals zero for any superposed translation. Lax [62], Keating [64,65] highlighted that Born–Kármán's lattice based on two central interactions and one non-central interaction (the shear interaction) does not fulfill rotational invariance (see also [66]). The same critique concerns the lattice model of Montroll and Potts [92] (equivalent to the model of Rosenstock and Newell [91]), particular cases of Born–Kármán's without central second-neighboring interactions, as analyzed by Gazis and Wallis [63]. This can be seen in the simple translation and rotation ω of one cell around a point $P_{i,j}$:

$$\begin{pmatrix} u_{i+1,j} \\ v_{i+1,j} \end{pmatrix}=\begin{pmatrix} u_{i,j} \\ v_{i,j}+\omega a \end{pmatrix};\quad \begin{pmatrix} u_{i,j+1} \\ v_{i,j+1} \end{pmatrix}=\begin{pmatrix} u_{i,j}-\omega a \\ v_{i,j} \end{pmatrix}\quad \text{and}\quad \begin{pmatrix} u_{i+1,j+1} \\ v_{i+1,j+1} \end{pmatrix}=\begin{pmatrix} u_{i,j}-\omega a \\ v_{i,j}+\omega a \end{pmatrix} \tag{31}$$

Inserting Eq. (31) in one cell of Eq. (28) furnishes

$$\begin{aligned} U_{i,j} &= \frac{\alpha}{4}\left[\left(u_{i+1,j}-u_{i,j}\right)^2+\left(u_{i+1,j+1}-u_{i,j+1}\right)^2+\left(v_{i,j+1}-v_{i,j}\right)^2+\left(v_{i+1,j+1}-v_{i+1,j}\right)^2\right] \\ &+\frac{\beta}{4}\left[\left(u_{i+1,j+1}-u_{i,j}+v_{i+1,j+1}-v_{i,j}\right)^2+\left(u_{i+1,j}-u_{i,j+1}-v_{i+1,j}+v_{i,j+1}\right)^2\right] \\ &+\frac{\delta}{4}\left[\left(v_{i+1,j}-v_{i,j}\right)^2+\left(v_{i+1,j+1}-v_{i,j+1}\right)^2+\left(u_{i,j+1}-u_{i,j}\right)^2+\left(u_{i+1,j+1}-u_{i+1,j}\right)^2\right] \\ &= \frac{\alpha}{4}\left[0^2+0^2+0^2+0^2\right]+\frac{\beta}{4}\left[(-\omega a+\omega a)^2+(\omega a-\omega a)^2\right]+\frac{\delta}{4}\left[(\omega a)^2+(\omega a)^2+(\omega a)^2+(\omega a)^2\right] \\ &= \delta\,(\omega a)^2\neq 0 \end{aligned} \tag{32}$$

which is nonzero due to non-central interactions, since $\delta \neq 0$. In conclusion, Born–Kármán's lattice does not fulfil the rotational invariance principle, in general, thus is inconsistent. The kinetic energy of this lattice with concentrated masses has the simple form:

$$T=\sum_i\sum_j M\,\dot{u}_{i,j}^2+M\,\dot{v}_{i,j}^2 \tag{33}$$

Applying Hamilton's principle to the Lagrangian $L = T - U$ gives the mixed differential-difference equation Eq. (25), which can be obtained equivalently by the direct approach, as for the 3D Born–Kármán's model. Again, its asymptotic expansion shows that it converges to Navier's partial differential equations of elastodynamics. For this 2D problem, the following relation between the discrete and the equivalent continuum $u_{i,j}=u\,(x=ai,y=aj)$and $v_{i,j}=v\,(x=ai,y=aj)$holds for sufficiently smooth functions given by:

$$u_{i+1,j+1}=u\,(x+a,y+a)=e^{a\left(\partial_x+\partial_y\right)}u\,(x,y) \tag{34}$$

By using again an asymptotic expansion, one obtains the long wave continuum limit as:

$$\begin{cases} (\alpha+\beta)\frac{\partial^2 u}{\partial x^2}+2\beta\frac{\partial^2 v}{\partial x\partial y}+(\delta+\beta)\frac{\partial^2 u}{\partial y^2}=\rho h\frac{\partial^2 u}{\partial t^2} \\ (\alpha+\beta)\frac{\partial^2 v}{\partial y^2}+2\beta\frac{\partial^2 u}{\partial x\partial y}+(\delta+\beta)\frac{\partial^2 v}{\partial x^2}=\rho h\frac{\partial^2 v}{\partial t^2} \end{cases} \tag{35}$$

where h the depth of the plane element. From Eq. (35), it is possible to identify the constant of Navier's partial differential equations in plane stress elasticity (see, e.g., Love [93]), which are:

$$\begin{cases} \frac{E}{1-\upsilon^2}\frac{\partial^2 u}{\partial x^2}+\frac{E}{2(1-\upsilon)}\frac{\partial^2 v}{\partial x\partial y}+\frac{E}{2(1+\upsilon)}\frac{\partial^2 u}{\partial y^2}=\rho\frac{\partial^2 u}{\partial t^2} \\ \frac{E}{1-\upsilon^2}\frac{\partial^2 v}{\partial y^2}+\frac{E}{2(1-\upsilon)}\frac{\partial^2 u}{\partial x\partial y}+\frac{E}{2(1+\upsilon)}\frac{\partial^2 v}{\partial x^2}=\rho\frac{\partial^2 v}{\partial t^2} \end{cases} \tag{36}$$

with E the Young's modulus, υ the Poisson's ratio. One identifies:

$$\begin{cases} \alpha+\beta=\frac{Eh}{1-\upsilon^2} \\ 2\beta=\frac{Eh}{2(1-\upsilon)} \\ \delta+\beta=\frac{Eh}{2(1+\upsilon)} \end{cases} \Rightarrow \begin{cases} \alpha=\frac{Eh(3-\upsilon)}{4\left(1-\upsilon^2\right)} \\ \beta=\frac{Eh}{4(1-\upsilon)} \\ \delta=\frac{Eh(1-3\upsilon)}{4\left(1-\upsilon^2\right)} \end{cases} \tag{37}$$

Equation (37) can be rewritten as

$$\begin{cases} \frac{\beta}{\alpha}=\frac{1+\upsilon}{3-\upsilon} \\ \frac{\delta}{\alpha}=\frac{1-3\upsilon}{3-\upsilon} \end{cases} \tag{38}$$

Note from Eq. (38) implies that if $\delta=0$ (central forces), Poisson's ratio must be $\upsilon=1/3$, as reported by Hrennikoff [58], Hrennikoff [59], McHenry [60], McHenry [61] or Hrennikoff [73] for plane stress problems.

$$\delta=0 \quad \Rightarrow \quad \upsilon=1/3 \tag{39}$$

The truss composed of horizontal, vertical and diagonal bars, equivalent to Born–Kármán's lattice with central forces (or Navier's lattice with pure central interactions, also equivalent to McHenry-Hrennikoff truss), foresees a constraint for the stiffnesses of the bars in plane stress:

$$\delta=0 \quad \Rightarrow \quad \alpha=2\beta \tag{40}$$

i.e., the stiffness of the horizontal and vertical elements is twice that of the diagonal elements for a McHenry truss. For the equivalence, the stiffness parameters must be

$$\upsilon=1/3 \quad \Rightarrow \quad \begin{cases} \alpha=\frac{3Eh}{4} \\ \beta=\frac{3Eh}{8} \end{cases} \tag{41}$$

In McHenry-Hrennikoff's truss, the cross sectional area of each horizontal or vertical bar is denoted by A_N, that of each diagonal bar is denoted by A_D, Young's modulus of each horizontal or vertical bar is denoted by E_N, and the Young's modulus of each diagonal bar is denoted by E_D:

$$A_N E_N=\alpha a=\frac{Eh\,(3-\upsilon)}{4\left(1-\upsilon^2\right)}a=\frac{3Eha}{4} \quad \text{and} \quad A_D E_D=\beta a\sqrt{2}=\frac{Eh}{4\,(1-\upsilon)}a\sqrt{2}=\frac{3Eh}{8}a\sqrt{2} \quad \text{for} \quad \upsilon=1/3 \tag{42}$$

If Young's modulus is uniform, as in Hrennikoff [59] or McHenry [61], Eq. (42) yields:

$$E_N=E_D=E \quad \Rightarrow \quad A_N=\frac{3ha}{4} \quad \text{and} \quad A_D=\frac{3\sqrt{2}ha}{8} \tag{43}$$

For finite elastic solids, McHenry [61] reported that the border springs must have stiffness $\alpha/2$ for an accurate correspondence of the lattice with its asymptotic continuum (see Fig. 11). The uniaxial compression of a square specimen composed of McHenry trusses (or central Born–Kármán's lattice, often referred to as Bravais lattices in physics) is shown in Fig. 12 for several repetitions of McHenry cells. The boundary conditions both in terms of border springs and given loads must be carefully set. Whatever the number of cells,

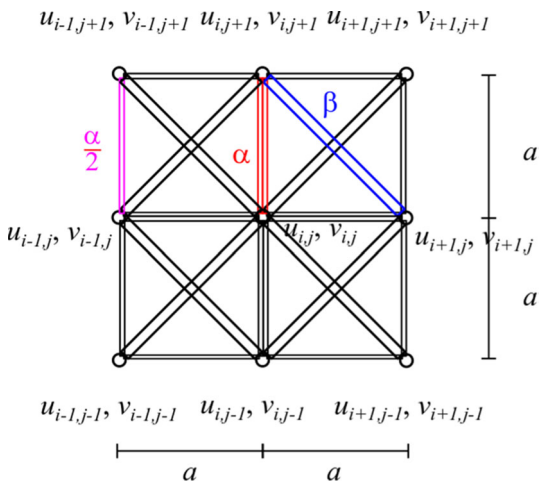

Fig. 11 Representation of McHenry truss model

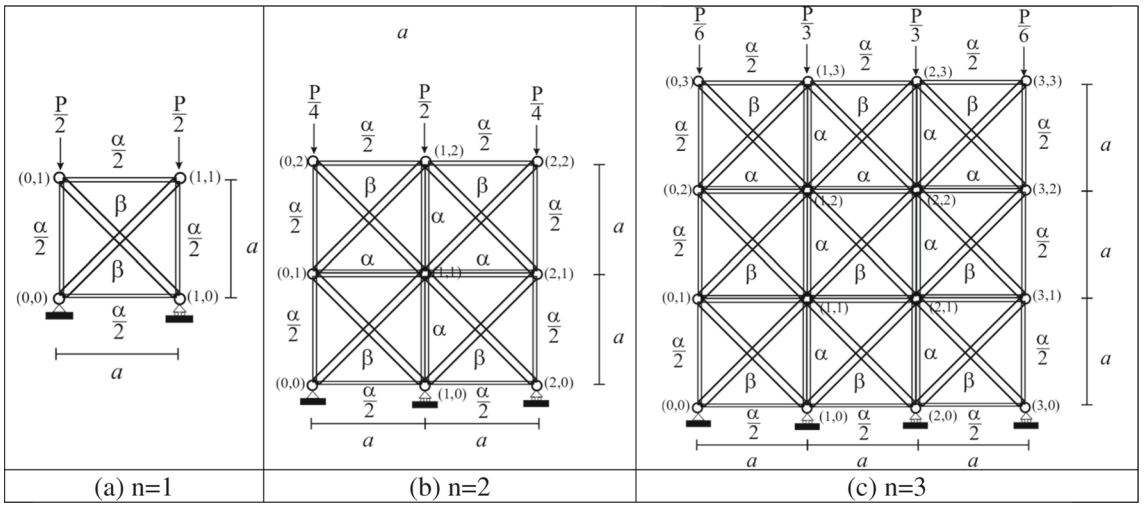

Fig. 12 McHenry truss with specific border springs under uniform compression; $\alpha = 2\beta$; $u(n,n) = -\frac{1}{3}v(n,n)$; $v = \frac{1}{3}$ for McHenry truss in plane stress

the ratio of the horizontal displacement to the vertical displacement of the specimen is *1/3*. For 3D McHenry cells (3D Born–Kármán's lattice with central interactions), the equivalent Poisson's ratio is *1/4*, as given by Eq. (19) (see Fig. 13). For 3D McHenry-Hrennikoff lattices, the stiffness of each horizontal, vertical and diagonal bar derives from Eq. (20):

$$\delta = 0 \quad \Rightarrow \quad \upsilon = 1/4 \quad \Rightarrow \quad \alpha = \beta \tag{44}$$

It is remarkable that the strict equality between stiffness parameters $\alpha = 2\beta$ for plane stress differs from that of 3D elasticity $\alpha = \beta$. From Eq. (44), using Eq. (14), one identifies easily that

$$\upsilon = 1/4 \quad \Rightarrow \quad \begin{cases} \alpha = \frac{E_N A_N}{a} = \frac{2Ea}{5} \\ \beta = \frac{E_D A_D}{a\sqrt{2}} = \frac{2Ea}{5} \end{cases} \tag{45}$$

For uniform Young's modulus, this gives the cross-section areas reported by Hrennikoff [59]:

$$E_N = E_D = E \quad \Rightarrow \quad A_N = \frac{2a^2}{5} \quad \text{and} \quad A_D = \frac{2\sqrt{2}}{5}a^2 \tag{46}$$

Figure 13 shows some 3D Hrennikoff trusses in compression, with border springs having half the stiffness of the inner ones, under the central force assumption (with truss properties $\alpha = \beta$ or equivalently with the

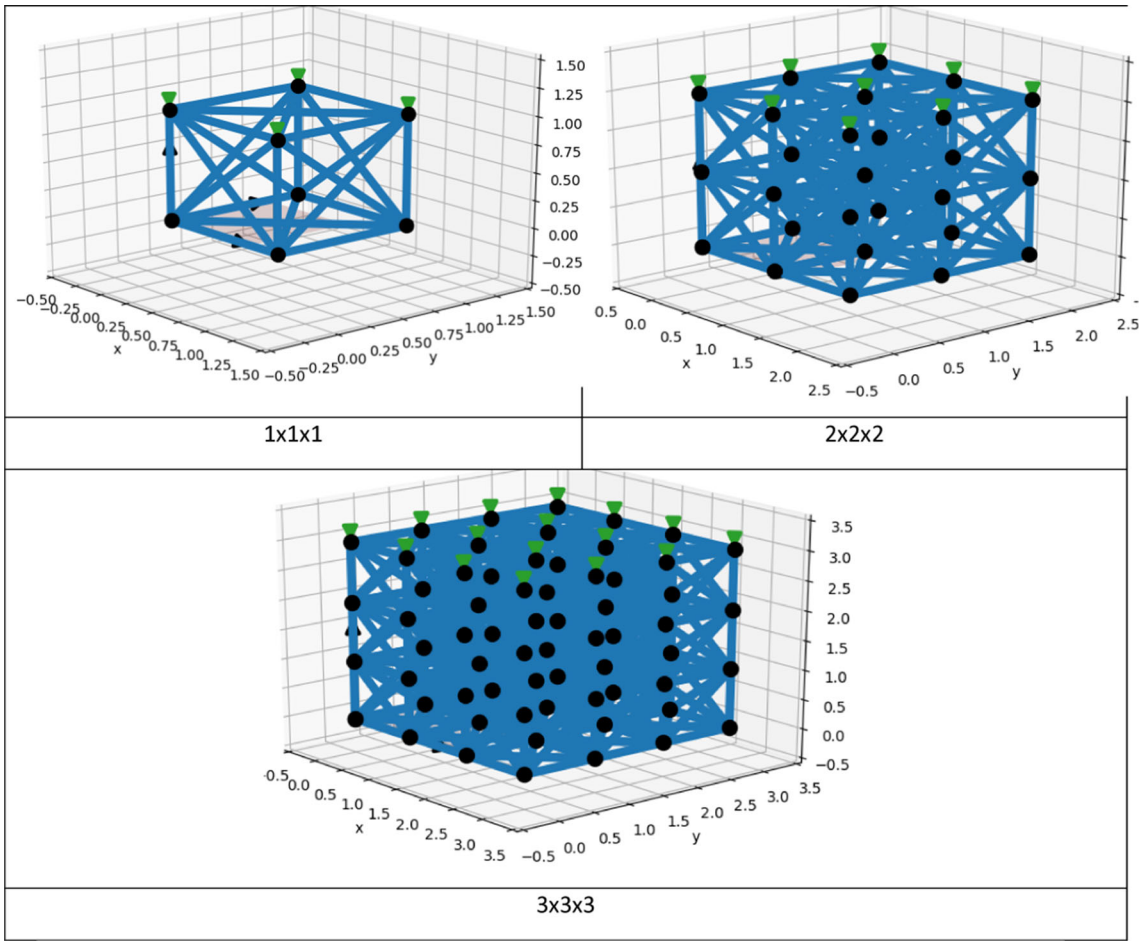

Fig. 13 Three-dimensional McHenry truss with specific border springs under uniform compression; $\alpha = \beta$; $u(n,n,n) = -\frac{1}{4}v(n,n,n) = -\frac{1}{4}w(n,n,n)$; $\upsilon = \frac{1}{4}$ for three-dimensional McHenry truss; computation for three trusses $1 \times 1 \times 1$, $2 \times 2 \times 2$ and $3 \times 3 \times 3$

cross sectional properties of Eq. (46)). The macroscopic response of the n-cell specimen to a pure compression gives a ratio of the lateral to the vertical end displacement equal in absolute value to Poisson's ratio, which is 1/4 under the considered central force assumption.

For the energy of the 2D Born–Kármán's lattice (Fig. 14) to be positive definite, Poisson's ratio must be less than its critical value in plane stress, i.e.

$$\delta \geq 0 \quad \Rightarrow \quad \upsilon \leq 1/3 \tag{47}$$

The mixed differential-difference equations of the 2D Born–Kármán's lattice in plane stress are:

$$\begin{cases} \frac{E(3-\upsilon)}{4(1-\upsilon^2)}\left(u_{i+1,j} - 2u_{i,j} + u_{i-1,j}\right) + \frac{E}{8(1-\upsilon)}\left(u_{i+1,j+1} + u_{i-1,j-1} + u_{i-1,j+1} + u_{i+1,j-1} - 4u_{i,j}\right) + \\ \frac{E}{8(1-\upsilon)}\left(v_{i+1,j+1} - v_{i-1,j+1} - v_{i+1,j-1} + v_{i-1,j-1}\right) + \frac{E(1-3\upsilon)}{4(1-\upsilon^2)}\left(u_{i,j+1} - 2u_{i,j} + u_{i,j-1}\right) = \rho a^2 \ddot{u}_{i,j} \\ \frac{E(3-\upsilon)}{4(1-\upsilon^2)}\left(v_{i,j+1} - 2v_{i,j} + v_{i,j-1}\right) + \frac{E}{8(1-\upsilon)}\left(v_{i+1,j+1} + v_{i-1,j-1} + v_{i-1,j+1} + v_{i+1,j-1} - 4v_{i,j}\right) + \\ \frac{E}{8(1-\upsilon)}\left(u_{i+1,j+1} - u_{i-1,j+1} - u_{i+1,j-1} + u_{i-1,j-1}\right) + \frac{E(1-3\upsilon)}{4(1-\upsilon^2)}\left(v_{i+1,j} - 2v_{i,j} + v_{i-1,j}\right) = \rho a^2 \ddot{v}_{i,j} \end{cases} \tag{48}$$

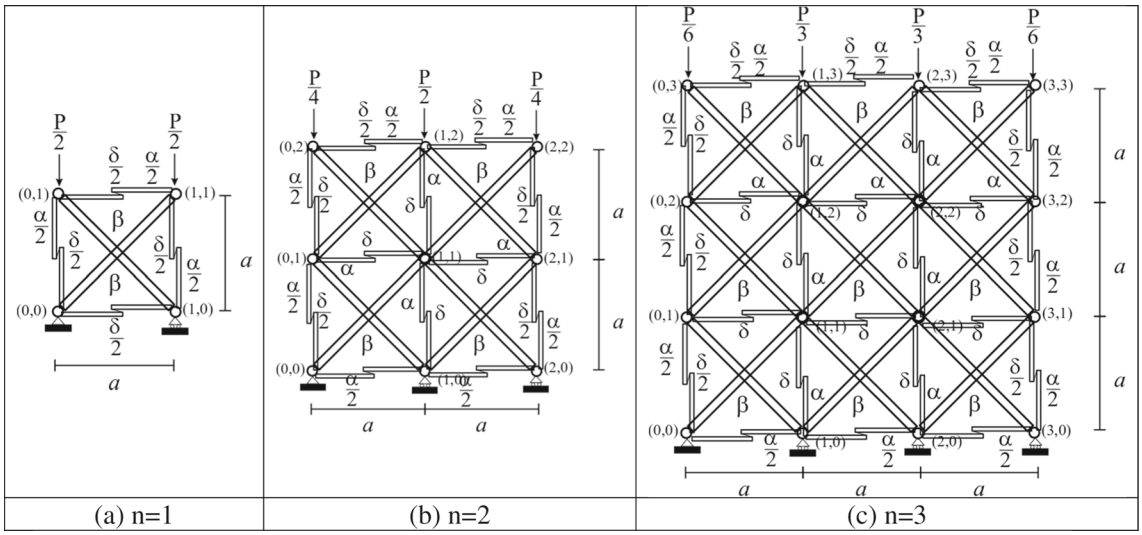

Fig. 14 Born–Kármán lattice with specific border springs under uniform compression

Equation (48) can be expanded up to some higher gradient terms, to formulate a higher-gradient continuous Born–Kármán's lattice equations in plane stress, as an approximation of discrete elasticity:

$$\begin{cases} \frac{E(3-\upsilon)}{4(1-\upsilon^2)}\left[\frac{\partial^2 u}{\partial x^2}+\frac{a^2}{12}\frac{\partial^4 u}{\partial x^4}\right]+\frac{E}{8(1-\upsilon)}\left[2\frac{\partial^2 u}{\partial x^2}+2\frac{\partial^2 u}{\partial y^2}+a^2\frac{\partial^4 u}{\partial x^2\partial y^2}+\frac{a^2}{6}\frac{\partial^4 u}{\partial x^4}+\frac{a^2}{6}\frac{\partial^4 u}{\partial y^4}\right]+ \\ \frac{E}{8(1-\upsilon)}\left[4\frac{\partial^2 v}{\partial x\partial y}+2\frac{a^2}{3}\frac{\partial^4 v}{\partial x\partial y^3}+2\frac{a^2}{3}\frac{\partial^4 v}{\partial y\partial x^3}\right]+\frac{E(1-3\upsilon)}{4(1-\upsilon^2)}\left[\frac{\partial^2 u}{\partial y^2}+\frac{a^2}{12}\frac{\partial^4 u}{\partial y^4}\right]+o\left(a^4\right)=\rho\,\ddot{u} \\ \frac{E(3-\upsilon)}{4(1-\upsilon^2)}\left[\frac{\partial^2 v}{\partial y^2}+\frac{a^2}{12}\frac{\partial^4 v}{\partial y^4}\right]+\frac{E}{8(1-\upsilon)}\left[2\frac{\partial^2 v}{\partial x^2}+2\frac{\partial^2 v}{\partial y^2}+a^2\frac{\partial^4 v}{\partial x^2\partial y^2}+\frac{a^2}{6}\frac{\partial^4 v}{\partial x^4}+\frac{a^2}{6}\frac{\partial^4 v}{\partial y^4}\right]+ \\ \frac{E}{8(1-\upsilon)}\left[4\frac{\partial^2 u}{\partial x\partial y}+2\frac{a^2}{3}\frac{\partial^4 u}{\partial x\partial y^3}+2\frac{a^2}{3}\frac{\partial^4 u}{\partial y\partial x^3}\right]+\frac{E(1-3\upsilon)}{4(1-\upsilon^2)}\left[\frac{\partial^2 v}{\partial x^2}+\frac{a^2}{12}\frac{\partial^4 v}{\partial x^4}\right]+o\left(a^4\right)=\rho\,\ddot{v} \end{cases} \tag{49}$$

For plane strain, Navier's elastodynamic continuous equations are given by:

$$\begin{cases} (\lambda+2\mu)\frac{\partial^2 u}{\partial x^2}+(\lambda+\mu)\frac{\partial^2 v}{\partial x\partial y}+\mu\frac{\partial^2 u}{\partial y^2}=\rho\frac{\partial^2 u}{\partial t^2} \\ (\lambda+2\mu)\frac{\partial^2 v}{\partial y^2}+(\lambda+\mu)\frac{\partial^2 u}{\partial x\partial y}+\mu\frac{\partial^2 v}{\partial x^2}=\rho\frac{\partial^2 v}{\partial t^2} \end{cases} \tag{50}$$

One identifies for the 2D Born–Kármán's lattice (see also Suiker et al. [47]), under plane strain:

$$\begin{cases} \alpha+\beta=(\lambda+2\mu)\,h \\ 2\beta=(\lambda+\mu)\,h \\ \delta+\beta=\mu h \end{cases} \quad\Rightarrow\quad \begin{cases} \alpha=\frac{\lambda+3\mu}{2}h \\ \beta=\frac{\lambda+\mu}{2}h \\ \delta=\frac{\mu-\lambda}{2}h \end{cases} \tag{51}$$

For central forces in plane strain from Eq. (51), we obtain:

$$\delta=0 \quad\Rightarrow\quad \lambda=\mu \quad\Rightarrow\quad \alpha=2\beta \tag{52}$$

and Poisson's ratio $\upsilon=1/4$, which is the value given by the "rari-constant" molecular theory of Poisson and Cauchy; Eq. (52) was obtained in plane strain by Suiker et al. [47]. We can summarize that the stiffness of the 2D McHenry-Hrennikoff truss (or equivalently, Born–Kármán's lattice with central forces) in plane strain or plane stress, foresees $\alpha=2\beta$, whereas 3D truss (or 3D lattice with central forces) foresees $\alpha=\beta$.

In plane strain, the positive definiteness of the energy imposes that:

$$\delta\geq 0 \quad\Rightarrow\quad \upsilon\leq 1/4 \tag{53}$$

The constraint Eq. (18) for Poisson's ratio still holds and the central forces require $\upsilon = 1/4$. The mixed differential-difference equations of 2D Born–Kármán's lattice model in plane strain are given by:

$$\begin{cases} \frac{\lambda+3\mu}{2}\left(u_{i+1,j}-2u_{i,j}+u_{i-1,j}\right)+\frac{\lambda+\mu}{4}\left(u_{i+1,j+1}+u_{i-1,j-1}+u_{i-1,j+1}+u_{i+1,j-1}-4u_{i,j}\right)+ \\ \frac{\lambda+\mu}{4}\left(v_{i+1,j+1}-v_{i-1,j+1}-v_{i+1,j-1}+v_{i-1,j-1}\right)+\frac{\mu-\lambda}{2}\left(u_{i,j+1}-2u_{i,j}+u_{i,j-1}\right)=a^2\,\ddot{u}_{i,j} \\ \frac{\lambda+3\mu}{2}\left(v_{i,j+1}-2v_{i,j}+v_{i,j-1}\right)+\frac{\lambda+\mu}{4}\left(v_{i+1,j+1}+v_{i-1,j-1}+v_{i-1,j+1}+v_{i+1,j-1}-4v_{i,j}\right)+ \\ \frac{\lambda+\mu}{4}\left(u_{i+1,j+1}-u_{i-1,j+1}-u_{i+1,j-1}+u_{i-1,j-1}\right)+\frac{\mu-\lambda}{2}\left(v_{i+1,j}-2v_{i,j}+v_{i-1,j}\right)=a^2\,\ddot{v}_{i,j} \end{cases} \tag{54}$$

The mixed differential-difference equations of the 2D Born–Kármán's lattice model (in plane strain) can be expanded using the higher-order differential operators, in the following form:

$$\begin{cases} \left(\frac{\lambda+3\mu}{2}\right)\left[\frac{\partial^2 u}{\partial x^2}+\frac{a^2}{12}\frac{\partial^4 u}{\partial x^4}\right]+\left(\frac{\lambda+\mu}{4}\right)\left[2\frac{\partial^2 u}{\partial x^2}+2\frac{\partial^2 u}{\partial y^2}+a^2\frac{\partial^4 u}{\partial x^2\partial y^2}+\frac{a^2}{6}\frac{\partial^4 u}{\partial x^4}+\frac{a^2}{6}\frac{\partial^4 u}{\partial y^4}\right]+ \\ \left(\frac{\lambda+\mu}{4}\right)\left[4\frac{\partial^2 v}{\partial x\partial y}+2\frac{a^2}{3}\frac{\partial^4 v}{\partial x\partial y^3}+2\frac{a^2}{3}\frac{\partial^4 v}{\partial y\partial x^3}\right]+\left(\frac{\mu-\lambda}{2}\right)\left[\frac{\partial^2 u}{\partial y^2}+\frac{a^2}{12}\frac{\partial^4 u}{\partial y^4}\right]+o\left(a^4\right)=\rho\,\ddot{u} \\ \\ \left(\frac{\lambda+3\mu}{2}\right)\left[\frac{\partial^2 v}{\partial y^2}+\frac{a^2}{12}\frac{\partial^4 v}{\partial y^4}\right]+\left(\frac{\lambda+\mu}{4}\right)\left[2\frac{\partial^2 v}{\partial y^2}+2\frac{\partial^2 v}{\partial x^2}+a^2\frac{\partial^4 v}{\partial x^2\partial y^2}+\frac{a^2}{6}\frac{\partial^4 v}{\partial y^4}+\frac{a^2}{6}\frac{\partial^4 v}{\partial x^4}\right]+ \\ \left(\frac{\lambda+\mu}{4}\right)\left[4\frac{\partial^2 u}{\partial x\partial y}+2\frac{a^2}{3}\frac{\partial^4 u}{\partial x\partial y^3}+2\frac{a^2}{3}\frac{\partial^4 u}{\partial y\partial x^3}\right]+\left(\frac{\mu-\lambda}{2}\right)\left[\frac{\partial^2 v}{\partial x^2}+\frac{a^2}{12}\frac{\partial^4 v}{\partial x^4}\right]+o\left(a^4\right)=\rho\,\ddot{v} \end{cases} \tag{55}$$

4 Three-dimensional discrete elasticity: Gazis et al. model

The general violation of rotational invariance of Born–Kármán's lattice, encouraged researchers to replace the non-central forces (shear forces) by angular ones. This idea was already employed by Born [94] in developing a two-constant model for diamond, with both central and angular forces among nearest neighbors, an idea that is already present in Voigt's assumption of a potential that depends also on the orientation of molecules, or in Poincaré's three-body potential that accounts for angles formed by triples of molecules. A three-constant lattice with vertical and longitudinal springs (central interaction between nearest neighbors), diagonal springs (central interaction between next-nearest neighbors) and rotational springs (angular interaction) is due to Smith [95] for the diamond structure [95]. De Launay [51] presented in detail Smith's lattice and also referred to Nagendra [96] for results [96]. To avoid theoretical inconsistencies, the lattice energy shall depend on invariant quantities, such as distances between atoms or angles among triples of atoms [63]. Gazis et al. [67] gave a final answer to the paradoxical properties of Born–Kármán's lattice by replacing the shear (non central) force therein with rotation springs. The lattice of Gazis et al. [67] is monatomic, simple cubic, composed of particles of equal mass M and lattice spacing a that interact by: nearest and next-to-nearest central forces as due to axial springs of stiffnesses α (edges) and β (diagonal) (notation as in Born–Kármán's lattice); "angular forces" as due to rotation springs of stiffness γ (the mechanical interactions of such a lattice are represented in Fig. 16 for the 3D Gazis et al. lattice, and in Fig. 17 for the 2D Gazis et al. lattice). This lattice is energetically consistent, fulfilling invariance in rotation and translation; its governing mixed differential-difference equations asymptotically converge to Navier's partial differential ones for elastodynamics. For plane stress, this system was also considered by Wu (1989) in his PhD thesis where 2D elasticity was investigated by a three-parameter lattice with one angular and two central interactions [80]. Central forces (Navier, Poisson's or Cauchy's molecular assumption) is retrieved for $\gamma = 0$, but do not lead to a general Hooke's law at the continuum limit with free Poisson's ratio. Gazis et al. lattice coincides with Born–Kármán's for central forces, i.e., $\delta = 0$ (Born–Kármán) and $\gamma = 0$ (Gazis et al.). The governing equation and the lattice of Gazis et al. are shown in Figs. 15 and 16. Exact solutions are available for the dispersive wave propagation equation in 2D or 3D for these lattices (see for instance [67] for 3D lattices [67]). Exact solutions for the in-plane shear vibration of such a lattice have been obtained by

$$
\begin{aligned}
M\ddot{u}_{l,m,n} = {} & \alpha(u_{l+1,m,n} - 2u_{l,m,n} + u_{l-1,m,n}) \\
& + \beta(u_{l+1,m+1,n} + u_{l-1,m+1,n} + u_{l+1,m-1,n} \\
& \quad + u_{l-1,m-1,n} + u_{l+1,m,n+1} + u_{l-1,m,n+1} \\
& \quad + u_{l+1,m,n-1} + u_{l-1,m,n-1} - 8u_{l,m,n}) \\
& + (\beta+\gamma)(v_{l+1,m+1,n} + v_{l-1,m-1,n} \\
& \quad - v_{l-1,m+1,n} - v_{l+1,m-1,n} + w_{l+1,m,n+1} \\
& \quad + w_{l-1,m,n-1} - w_{l+1,m,n-1} - w_{l-1,m,n+1}) \\
& + 4\gamma(u_{l,m+1,n} + u_{l,m-1,n} + u_{l,m,n+1} \\
& \quad + u_{l,m,n-1} - 4u_{l,m,n}), \quad (34)
\end{aligned}
$$

Fig. 15 Mixed differential-difference equation—vibration of three-dimensional elastic lattice; Eq. (34) from Gazis et al. [67]

Mindlin [97]. The mixed differential-difference equation is given by Gazis et al. [67] (Fig. 15):

$$
\begin{aligned}
& \alpha\left(u_{i+1,j,k} - 2u_{i,j,k} + u_{i-1,j,k}\right) \\
& + \frac{\beta}{2}\left(u_{i+1,j+1,k} + u_{i-1,j+1,k} + u_{i+1,j-1,k} + u_{i-1,j-1,k} + u_{i+1,j,k+1} + u_{i-1,j,k+1}\right. \\
& \left. + u_{i+1,j,k-1} + u_{i-1,j,k-1} - 8u_{i,j,k}\right) \\
& + \left(\frac{\beta}{2} + \gamma\right)\left(v_{i+1,j+1,k} + v_{i-1,j-1,k} - v_{i-1,j+1,k} - v_{i+1,j-1,k} + w_{i+1,j,k+1} + w_{i-1,j,k-1}\right. \\
& \left. - w_{i+1,j,k-1} - w_{i-1,j,k+1}\right) \\
& + 4\gamma\left(u_{i,j+1,k} + u_{i,j-1,k} + u_{i,j,k+1} + u_{i,j,k-1} - 4u_{i,j,k}\right) = M\,\ddot{u}_{i,j,k}
\end{aligned}
\tag{56}
$$

The potential energy of the lattice of Gazis et al. is given by (Fig. 17):

$$
\begin{aligned}
U = \sum_i \sum_j \sum_k \frac{\alpha}{8} & \left[\begin{array}{l}
\left(u_{i+1,j,k} - u_{i,j,k}\right)^2 + \left(u_{i+1,j+1,k} - u_{i,j+1,k}\right)^2 \\
+ \left(u_{i+1,j,k+1} - u_{i,j,k+1}\right)^2 + \left(u_{i+1,j+1,k+1} - u_{i,j+1,k+1}\right)^2 \\
+ \left(v_{i,j+1,k} - v_{i,j,k}\right)^2 + \left(v_{i+1,j+1,k} - v_{i+1,j,k}\right)^2 \\
+ \left(v_{i,j+1,k+1} - v_{i,j,k+1}\right)^2 + \left(v_{i+1,j+1,k+1} - v_{i+1,j,k+1}\right)^2 \\
+ \left(w_{i,j,k+1} - w_{i,j,k}\right)^2 + \left(w_{i+1,j,k+1} - w_{i+1,j,k}\right)^2 \\
+ \left(w_{i,j+1,k+1} - w_{i,j+1,k}\right)^2 + \left(w_{i+1,j+1,k+1} - w_{i+1,j+1,k}\right)^2
\end{array}\right] \\
+ \frac{\beta}{8} & \left[\begin{array}{l}
\left(u_{i+1,j+1,k} - u_{i,j,k} + v_{i+1,j+1,k} - v_{i,j,k}\right)^2 \\
+ \left(u_{i+1,j,k} - u_{i,j+1,k} + v_{i+1,j,k} - v_{i,j+1,k}\right)^2 \\
+ \left(u_{i+1,j+1,k+1} - u_{i,j,k+1} + v_{i+1,j+1,k+1} - v_{i,j,k+1}\right)^2 \\
+ \left(u_{i+1,j,k+1} - u_{i,j+1,k+1} + v_{i+1,j,k+1} - v_{i,j+1,k+1}\right)^2 \\
+ \left(u_{i+1,j,k+1} - u_{i,j,k} + w_{i+1,j,k+1} - w_{i,j,k}\right)^2 + \left(u_{i+1,j,k} - u_{i,j,k+1} + w_{i+1,j,k} - w_{i,j,k+1}\right)^2 \\
+ \left(u_{i+1,j+1,k+1} - u_{i,j+1,k} + w_{i+1,j+1,k+1} - w_{i,j+1,k}\right)^2 \\
+ \left(u_{i+1,j+1,k} - u_{i,j+1,k+1} + w_{i+1,j+1,k} - w_{i,j+1,k+1}\right)^2 \\
+ \left(v_{i,j+1,k+1} - v_{i,j,k} + w_{i,j+1,k+1} - w_{i,j,k}\right)^2 \\
+ \left(v_{i,j+1,k} - v_{i,j,k+1} + w_{i,j+1,k} - w_{i,j,k+1}\right)^2 \\
+ \left(v_{i+1,j+1,k+1} - v_{i+1,j,k} + w_{i+1,j+1,k+1} - w_{i+1,j,k}\right)^2 \\
+ \left(v_{i+1,j+1,k} - v_{i+1,j,k+1} + w_{i+1,j+1,k} - w_{i+1,j,k+1}\right)^2
\end{array}\right]
\end{aligned}
$$

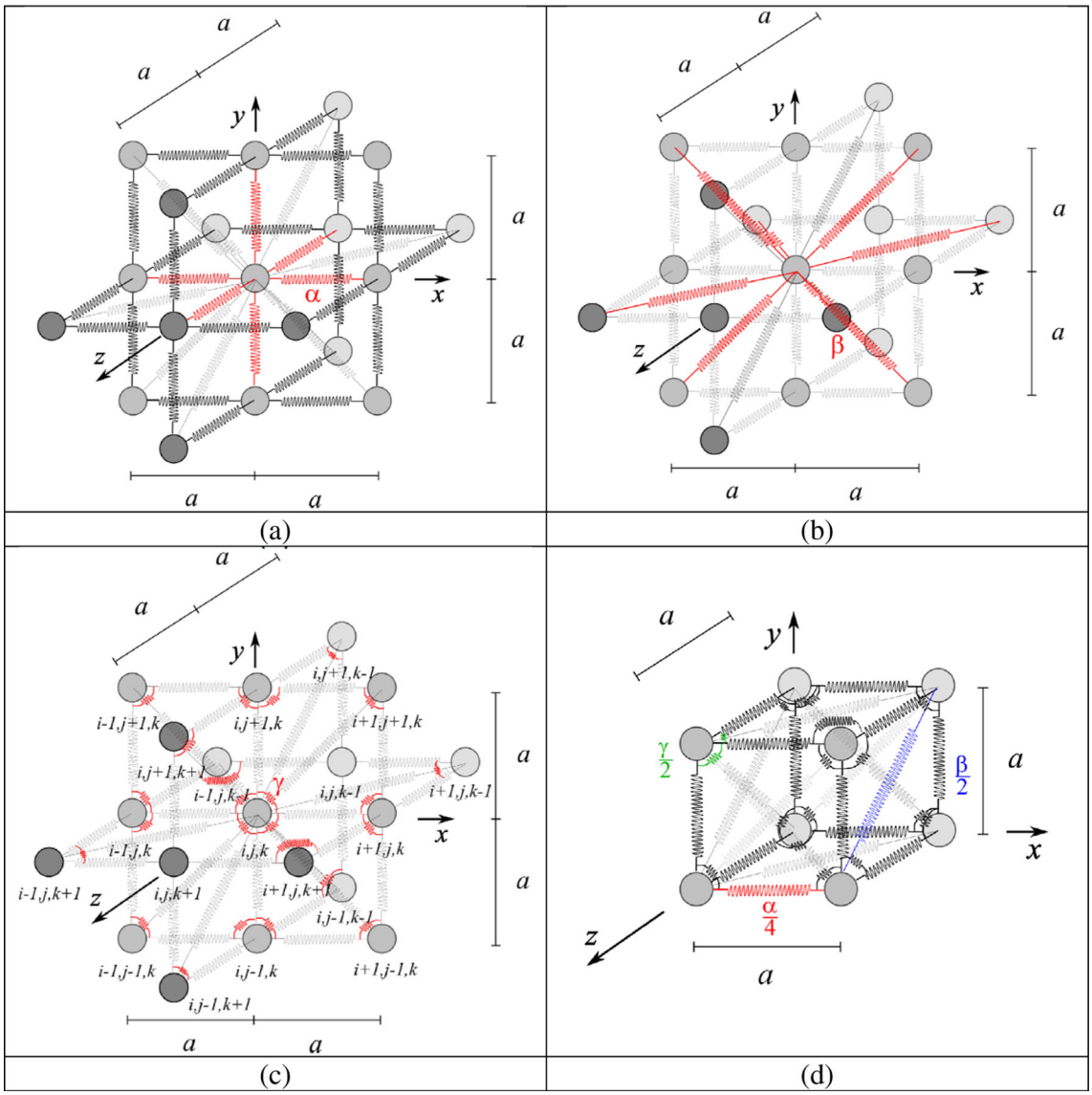

Fig. 16 Three-dimensional [67] lattice with longitudinal and vertical elastic springs (of stiffness α), diagonal elastic springs (of stiffness β), and rotational springs (of stiffness γ)

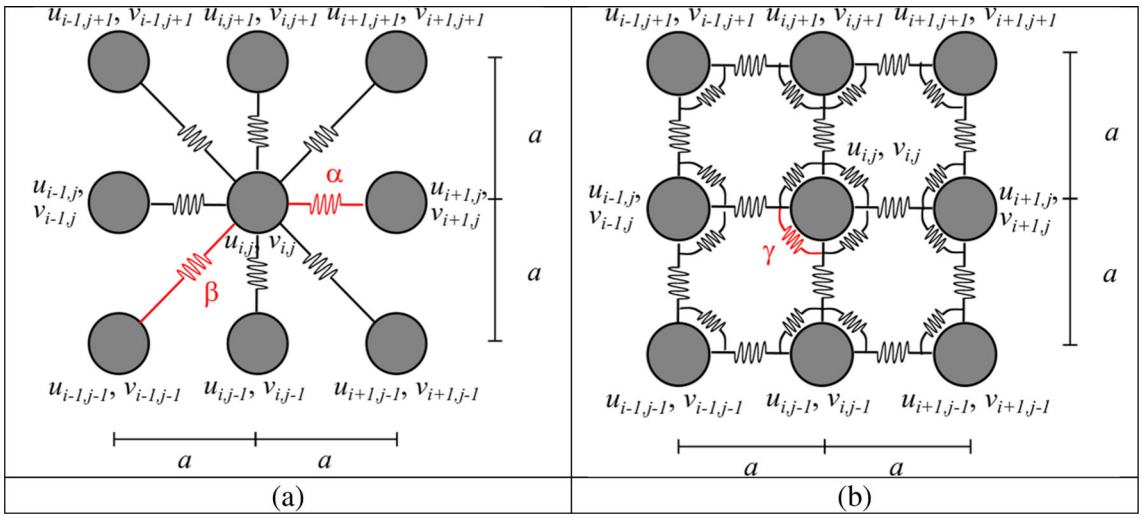

Fig. 17 Two-dimensional [67] lattice with longitudinal and vertical elastic springs (of stiffness α), diagonal elastic springs (of stiffness β), and rotational springs (of stiffness γ)

$$
+\frac{\gamma}{4}\left[\begin{array}{l}
\left(u_{i,j+1,k}-u_{i,j,k}+v_{i+1,j,k}-v_{i,j,k}\right)^2\\
+\left(u_{i+1,j+1,k}-u_{i+1,j,k}+v_{i+1,j,k}-v_{i,j,k}\right)^2\\
+\left(u_{i+1,j+1,k}-u_{i+1,j,k}+v_{i+1,j+1,k}-v_{i,j+1,k}\right)^2\\
+\left(u_{i,j+1,k}-u_{i,j,k}+v_{i+1,j+1,k}-v_{i,j+1,k}\right)^2\\
+\left(u_{i,j+1,k+1}-u_{i,j,k+1}+v_{i+1,j,k+1}-v_{i,j,k+1}\right)^2\\
+\left(u_{i+1,j+1,k+1}-u_{i+1,j,k+1}+v_{i+1,j,k+1}-v_{i,j,k+1}\right)^2\\
+\left(u_{i+1,j+1,k+1}-u_{i+1,j,k+1}+v_{i+1,j+1,k+1}-v_{i,j+1,k+1}\right)^2\\
+\left(u_{i,j+1,k+1}-u_{i,j,k+1}+v_{i+1,j+1,k+1}-v_{i,j+1,k+1}\right)^2\\
+\left(u_{i,j,k+1}-u_{i,j,k}+w_{i+1,j,k}-w_{i,j,k}\right)^2\\
+\left(u_{i+1,j,k+1}-u_{i+1,j,k}+w_{i+1,j,k}-w_{i,j,k}\right)^2\\
+\left(u_{i+1,j,k+1}-u_{i+1,j,k}+w_{i+1,j,k+1}-w_{i,j,k+1}\right)^2\\
+\left(u_{i,j,k+1}-u_{i,j,k}+w_{i+1,j,k+1}-w_{i,j,k+1}\right)^2\\
+\left(u_{i,j+1,k+1}-u_{i,j+1,k}+w_{i+1,j+1,k}-w_{i,j+1,k}\right)^2\\
+\left(u_{i+1,j+1,k+1}-u_{i+1,j+1,k}+w_{i+1,j+1,k}-w_{i,j+1,k}\right)^2\\
+\left(u_{i+1,j+1,k+1}-u_{i+1,j+1,k}+w_{i+1,j+1,k+1}-w_{i,j+1,k+1}\right)^2\\
+\left(u_{i,j+1,k+1}-u_{i,j+1,k}+w_{i+1,j+1,k+1}-w_{i,j+1,k+1}\right)^2\\
+\left(v_{i,j,k+1}-v_{i,j,k}+w_{i,j+1,k}-w_{i,j,k}\right)^2\\
+\left(v_{i,j+1,k+1}-v_{i,j+1,k}+w_{i,j+1,k}-w_{i,j,k}\right)^2\\
+\left(v_{i,j+1,k+1}-v_{i,j+1,k}+w_{i,j+1,k+1}-w_{i,j,k+1}\right)^2\\
+\left(v_{i,j,k+1}-v_{i,j,k}+w_{i,j+1,k+1}-w_{i,j,k+1}\right)^2\\
+\left(v_{i+1,j,k+1}-v_{i+1,j,k}+w_{i+1,j+1,k}-w_{i+1,j,k}\right)^2\\
+\left(v_{i+1,j+1,k+1}-v_{i+1,j+1,k}+w_{i+1,j+1,k}-w_{i+1,j,k}\right)^2\\
+\left(v_{i+1,j+1,k+1}-v_{i+1,j+1,k}+w_{i+1,j+1,k+1}-w_{i+1,j,k+1}\right)^2\\
+\left(v_{i+1,j,k+1}-v_{i+1,j,k}+w_{i+1,j+1,k+1}-w_{i+1,j,k+1}\right)^2
\end{array}\right] \tag{57}
$$

Expanding Eq. (57) yields Navier's partial differential equation and second-order terms:

$$\begin{aligned}
&\alpha a^2\left(\frac{\partial^2 u}{\partial x^2}+\frac{a^2}{12}\frac{\partial^4 u}{\partial x^4}\right)\\
&+\frac{\beta\, a^2}{2}\left(4\frac{\partial^2 u}{\partial x^2}+2\frac{\partial^2 u}{\partial y^2}+a^2\frac{\partial^4 u}{\partial x^2\partial y^2}+\frac{a^2}{3}\frac{\partial^4 u}{\partial x^4}+\frac{a^2}{6}\frac{\partial^4 u}{\partial y^4}+2\frac{\partial^2 u}{\partial z^2}+a^2\frac{\partial^4 u}{\partial x^2\partial z^2}+\frac{a^2}{6}\frac{\partial^4 u}{\partial z^4}\right)\\
&+4\,\gamma\, a^2\left(\frac{\partial^2 u}{\partial y^2}+\frac{a^2}{12}\frac{\partial^4 u}{\partial y^4}+\frac{\partial^2 u}{\partial z^2}+\frac{a^2}{12}\frac{\partial^4 u}{\partial z^4}\right)\\
&+\left(\gamma+\frac{\beta}{2}\right)a^2\left(4\frac{\partial^2 v}{\partial x\partial y}+\frac{2a^2}{3}\frac{\partial^4 v}{\partial x\partial y^3}+\frac{2a^2}{3}\frac{\partial^4 v}{\partial x^3\partial y}+4\frac{\partial^2 w}{\partial x\partial z}+\frac{2a^2}{3}\frac{\partial^4 w}{\partial x\partial z^3}+\frac{2a^2}{3}\frac{\partial^4 w}{\partial x^3\partial z}\right)=M\,\ddot{u}
\end{aligned}\tag{58}$$

Equation (58) is the lattice-based gradient elasticity model associated with Gazis et al. lattice. This equation has been exactly derived by Mindlin [98]—see "Appendix A".

Equation (56) may be approximated by the continuous formulations at the long wave limit:

$$(\alpha+2\beta)\frac{\partial^2 u}{\partial x^2}+(2\beta+4\gamma)\frac{\partial^2 v}{\partial x\partial y}+(2\beta+4\gamma)\frac{\partial^2 w}{\partial x\partial z}+(\beta+4\gamma)\frac{\partial^2 u}{\partial y^2}+(\beta+4\gamma)\frac{\partial^2 u}{\partial z^2}=\rho a\frac{\partial^2 u}{\partial t^2}\tag{59}$$

so that it is possible to identify the lattice parameters from Navier's elastodynamic equation of continuum elasticity with cubic symmetry, which contains the linear elastic isotropic medium for some constrained material parameters.:

$$\begin{cases}\alpha=a\,(c_{11}-2c_{12})=(2\mu-\lambda)\,a\\ \beta=ac_{12}=\lambda a\\ \gamma=\frac{a}{4}\,(c_{44}-c_{12})=\frac{\mu-\lambda}{4}a\end{cases}\quad\text{with}\quad\begin{cases}c_{11}=\lambda+2\mu\\ c_{44}=\mu\\ c_{12}=\lambda\end{cases}\tag{60}$$

Equation (60) can also be inverted to furnish the values reported implicitly by Gazis et al. [67]:

$$\mu=\frac{\alpha+\beta}{2a};\quad\lambda=\frac{\beta}{a}\quad\text{and}\quad\gamma=\frac{\alpha-\beta}{8}\tag{61}$$

Equation (50) of Gazis et al. [67] in 3D elasticity here reads as:

$$\begin{cases}c_{11}=\frac{\alpha+2\beta}{a}\\ c_{12}=\frac{\beta}{a}\\ c_{44}=\frac{\beta+4\gamma}{a}\end{cases}\quad\text{with}\quad\begin{cases}c_{11}=\lambda+2\mu\\ c_{44}=\mu\\ c_{12}=\lambda\end{cases}\tag{62}$$

For central forces, Gazis et al.'s lattice coincides with Born–Kármán's and one obtains:

$$\gamma=0\quad\Rightarrow\quad\mu=\lambda\quad\Rightarrow\quad\upsilon=1/4,\alpha=\beta\tag{63}$$

For the potential energy to be positive definite, γ must be positive, which is equivalent to μ larger than λ, or equivalently υ smaller than 1/4 , a constraint found also in Born–Kármán's lattice.

5 Two-dimensional discrete elasticity: Gazis et al. model

For an isotropic material in a 2D framework (isotropic in the asymptotic limit), the governing equations of Gazis et al. lattice are:

$$\begin{cases}\alpha\left(u_{i+1,j}-2u_{i,j}+u_{i-1,j}\right)+\frac{\beta}{2}\left(u_{i+1,j+1}+u_{i-1,j-1}+u_{i-1,j+1}+u_{i+1,j-1}-4u_{i,j}\right)\\ +\left(\frac{\beta}{2}+\gamma\right)\left(v_{i+1,j+1}-v_{i-1,j+1}-v_{i+1,j-1}+v_{i-1,j-1}\right)+4\gamma\left(u_{i,j+1}-2u_{i,j}+u_{i,j-1}\right)=M\,\ddot{u}_{i,j}\\ \alpha\left(v_{i,j+1}-2v_{i,j}+v_{i,j-1}\right)+\frac{\beta}{2}\left(v_{i+1,j+1}+v_{i-1,j-1}+v_{i-1,j+1}+v_{i+1,j-1}-4v_{i,j}\right)\\ +\left(\frac{\beta}{2}+\gamma\right)\left(u_{i+1,j+1}-u_{i-1,j+1}-u_{i+1,j-1}+u_{i-1,j-1}\right)+4\gamma\left(v_{i+1,j}-2v_{i,j}+v_{i-1,j}\right)=M\,\ddot{v}_{i,j}\end{cases}\tag{64}$$

where (α, β, γ) are positive stiffness parameters (see Fig. 17). Each particle has mass $M = \rho a^2 h$, where h is the depth of the plane element and ρ is its material volumetric density. Equation (64) are obtained equivalently starting from the following potential energy:

$$\begin{aligned} U = &\sum_i \sum_j \frac{\alpha}{4}\left[\left(u_{i+1,j}-u_{i,j}\right)^2+\left(u_{i+1,j+1}-u_{i,j+1}\right)^2+\left(v_{i,j+1}-v_{i,j}\right)^2+\left(v_{i+1,j+1}-v_{i+1,j}\right)^2\right] \\ &+\frac{\beta}{4}\left[\left(u_{i+1,j+1}-u_{i,j}+v_{i+1,j+1}-v_{i,j}\right)^2+\left(u_{i+1,j}-u_{i,j+1}-v_{i+1,j}+v_{i,j+1}\right)^2\right] \\ &+\frac{1}{2}\gamma\left[\begin{array}{l}\left(u_{i,j+1}-u_{i,j}+v_{i+1,j}-v_{i,j}\right)^2+\left(u_{i+1,j+1}-u_{i+1,j}+v_{i+1,j}-v_{i,j}\right)^2 \\ +\left(u_{i,j+1}-u_{i,j}+v_{i+1,j+1}-v_{i,j+1}\right)^2+\left(u_{i+1,j+1}-u_{i+1,j}+v_{i+1,j+1}-v_{i,j+1}\right)^2\end{array}\right] \end{aligned} \tag{65}$$

Gazis et al. [67] detail the last contribution, related to the angular stiffness γ, which can be expressed in terms of the rotation stiffness C_S via the scaling $C_S = \gamma a^2$. The energy in Eq. (65) is objective, as can be seen by operating translation and rotation ω of one cell around a point $P_{i,j}$:

$$\begin{pmatrix} u_{i+1,j} \\ v_{i+1,j}\end{pmatrix} = \begin{pmatrix} u_{i,j} \\ v_{i,j}+\omega a\end{pmatrix}; \quad \begin{pmatrix} u_{i,j+1} \\ v_{i,j+1}\end{pmatrix} = \begin{pmatrix} u_{i,j}-\omega a \\ v_{i,j}\end{pmatrix} \quad \text{and} \quad \begin{pmatrix} u_{i+1,j+1} \\ v_{i+1,j+1}\end{pmatrix} = \begin{pmatrix} u_{i,j}-\omega a \\ v_{i,j}+\omega a\end{pmatrix} \tag{66}$$

The energy of one cell is equal to:

$$\begin{aligned} U_{ij} = &\frac{\alpha}{4}\left[\left(u_{i+1,j}-u_{i,j}\right)^2+\left(u_{i+1,j+1}-u_{i,j+1}\right)^2+\left(v_{i,j+1}-v_{i,j}\right)^2+\left(v_{i+1,j+1}-v_{i+1,j}\right)^2\right] \\ &+\frac{\beta}{4}\left[\left(u_{i+1,j+1}-u_{i,j}+v_{i+1,j+1}-v_{i,j}\right)^2+\left(u_{i+1,j}-u_{i,j+1}-v_{i+1,j}+v_{i,j+1}\right)^2\right] \\ &+\frac{1}{2}\gamma\left[\begin{array}{l}\left(u_{i,j+1}-u_{i,j}+v_{i+1,j}-v_{i,j}\right)^2+\left(u_{i+1,j+1}-u_{i+1,j}+v_{i+1,j}-v_{i,j}\right)^2 \\ +\left(u_{i,j+1}-u_{i,j}+v_{i+1,j+1}-v_{i,j+1}\right)^2+\left(u_{i+1,j+1}-u_{i+1,j}+v_{i+1,j+1}-v_{i,j+1}\right)^2\end{array}\right] \\ = &\frac{\alpha}{4}\left[0^2+0^2+0^2+0^2\right]+\frac{\beta}{4}\left[(-\omega a+\omega a)^2+(\omega a-\omega a)^2\right] \\ &+\frac{1}{2}\gamma\left[(-\omega a+\omega a)^2+(-\omega a+\omega a)^2+(-\omega a+\omega a)^2+(-\omega a+\omega a)^2\right] \\ = &\,0 \end{aligned} \tag{67}$$

The kinetic energy of this lattice with concentrated masses at each centre has the simple form:

$$T = \sum_i \sum_j M\,\dot{u}_{i,j}^2 + M\,\dot{v}_{i,j}^2 \tag{68}$$

Applying Hamilton's principle to the Lagrangian $L = T - U$ yields Eq. (64): its asymptotic expansion shows that the difference equations of the lattice asymptotically converge toward the partial differential equations of elastodynamics of Navier, with the lattice parameters:

$$\left\{\begin{array}{l} \alpha\frac{\partial^2 u}{\partial x^2}+\beta\left(\frac{\partial^2 u}{\partial x^2}+\frac{\partial^2 u}{\partial y^2}\right)+4\left(\frac{\beta}{2}+\gamma\right)\frac{\partial^2 v}{\partial x\partial y}+4\gamma\frac{\partial^2 u}{\partial y^2}=\frac{M}{a^2}\frac{\partial^2 u}{\partial t^2} \\ \alpha\frac{\partial^2 v}{\partial y^2}+\beta\left(\frac{\partial^2 v}{\partial x^2}+\frac{\partial^2 v}{\partial y^2}\right)+4\left(\frac{\beta}{2}+\gamma\right)\frac{\partial^2 u}{\partial x\partial y}+4\gamma\frac{\partial^2 v}{\partial x^2}=\frac{M}{a^2}\frac{\partial^2 v}{\partial t^2}\end{array}\right. \tag{69}$$

This system of partial differential equations can be also rearranged in the following way:

$$\left\{\begin{array}{l} (\alpha+\beta)\frac{\partial^2 u}{\partial x^2}+4\left(\frac{\beta}{2}+\gamma\right)\frac{\partial^2 v}{\partial x\partial y}+(4\gamma+\beta)\frac{\partial^2 u}{\partial y^2}=\rho h\frac{\partial^2 u}{\partial t^2} \\ (\alpha+\beta)\frac{\partial^2 v}{\partial y^2}+4\left(\frac{\beta}{2}+\gamma\right)\frac{\partial^2 u}{\partial x\partial y}+(4\gamma+\beta)\frac{\partial^2 v}{\partial x^2}=\rho h\frac{\partial^2 v}{\partial t^2}\end{array}\right. \tag{70}$$

From Eq. (70), it is possible to identify the elastic constants of the continuous Navier's equations for plane stress (see for instance [93]) by Eq. (36). One identifies easily:

$$\left\{\begin{array}{l} \alpha+\beta=\frac{Eh}{1-\upsilon^2} \\ 2\beta+4\gamma=\frac{Eh}{2(1-\upsilon)} \\ 4\gamma+\beta=\frac{Eh}{2(1+\upsilon)}\end{array}\right. \Rightarrow \left\{\begin{array}{l} \alpha=\frac{Eh}{1+\upsilon} \\ \beta=\frac{Eh\upsilon}{1-\upsilon^2} \\ \gamma=\frac{Eh(1-3\upsilon)}{8(1-\upsilon^2)}\end{array}\right. \tag{71}$$

Equation (71) can be rewritten as

$$\begin{cases} \frac{\beta}{\alpha} = \frac{\upsilon}{1-\upsilon} \\ \frac{\gamma}{\alpha} = \frac{1-3\upsilon}{8(1-\upsilon)} \end{cases} \tag{72}$$

The difference equations of Gazis et al.'s lattice are equivalent to a finite difference formulation of the continuous Navier's partial differential equations of elastodynamics for plane stress:

$$\begin{cases} \frac{E}{1+\upsilon}\left(u_{i+1,j} - 2u_{i,j} + u_{i-1,j}\right) + \frac{E\upsilon}{2(1-\upsilon^2)}\left(u_{i+1,j+1} + u_{i-1,j-1} + u_{i-1,j+1} + u_{i+1,j-1} - 4u_{i,j}\right) \\ +\frac{E}{8(1-\upsilon)}\left(v_{i+1,j+1} - v_{i-1,j+1} - v_{i+1,j-1} + v_{i-1,j-1}\right) + \frac{E(1-3\upsilon)}{2(1-\upsilon^2)}\left(u_{i,j+1} - 2u_{i,j} + u_{i,j-1}\right) = \rho a^2\, \ddot{u}_{i,j} \\ \frac{E}{1+\upsilon}\left(v_{i,j+1} - 2v_{i,j} + v_{i,j-1}\right) + \frac{E\upsilon}{2(1-\upsilon^2)}\left(v_{i+1,j+1} + v_{i-1,j-1} + v_{i-1,j+1} + v_{i+1,j-1} - 4v_{i,j}\right) \\ +\frac{E}{8(1-\upsilon)}\left(u_{i+1,j+1} - u_{i-1,j+1} - u_{i+1,j-1} + u_{i-1,j-1}\right) + \frac{E(1-3\upsilon)}{2(1-\upsilon^2)}\left(v_{i+1,j} - 2v_{i,j} + v_{i-1,j}\right) = \rho a^2\, \ddot{v}_{i,j} \end{cases} \tag{73}$$

This mixed differential-difference equation system for plane stress can be expanded as:

$$\begin{cases} \frac{E}{(1+\upsilon)}\left[\frac{\partial^2 u}{\partial x^2} + \frac{a^2}{12}\frac{\partial^4 u}{\partial x^4}\right] + \frac{E\upsilon}{2(1-\upsilon^2)}\left[2\frac{\partial^2 u}{\partial x^2} + 2\frac{\partial^2 u}{\partial y^2} + a^2\frac{\partial^4 u}{\partial x^2 \partial y^2} + \frac{a^2}{6}\frac{\partial^4 u}{\partial x^4} + \frac{a^2}{6}\frac{\partial^4 u}{\partial y^4}\right] \\ +\frac{E}{8(1-\upsilon)}\left[4\frac{\partial^2 v}{\partial x \partial y} + 2\frac{a^2}{3}\frac{\partial^4 v}{\partial x \partial y^3} + 2\frac{a^2}{3}\frac{\partial^4 v}{\partial y \partial x^3}\right] + \frac{E(1-3\upsilon)}{2(1-\upsilon^2)}\left[\frac{\partial^2 u}{\partial y^2} + \frac{a^2}{12}\frac{\partial^4 u}{\partial y^4}\right] + o\left(a^4\right) = \rho\, \ddot{u} \\ \frac{E}{(1+\upsilon)}\left[\frac{\partial^2 v}{\partial y^2} + \frac{a^2}{12}\frac{\partial^4 v}{\partial y^4}\right] + \frac{E\upsilon}{2(1-\upsilon^2)}\left[2\frac{\partial^2 v}{\partial y^2} + 2\frac{\partial^2 v}{\partial x^2} + a^2\frac{\partial^4 v}{\partial x^2 \partial y^2} + \frac{a^2}{6}\frac{\partial^4 v}{\partial y^4} + \frac{a^2}{6}\frac{\partial^4 v}{\partial x^4}\right] \\ +\frac{E}{8(1-\upsilon)}\left[4\frac{\partial^2 u}{\partial x \partial y} + 2\frac{a^2}{3}\frac{\partial^4 u}{\partial x \partial y^3} + 2\frac{a^2}{3}\frac{\partial^4 u}{\partial y \partial x^3}\right] + \frac{E(1-3\upsilon)}{2(1-\upsilon^2)}\left[\frac{\partial^2 v}{\partial x^2} + \frac{a^2}{12}\frac{\partial^4 v}{\partial x^4}\right] + o\left(a^4\right) = \rho\, \ddot{v} \end{cases} \tag{74}$$

From Eq. (72), if $\gamma = 0$ (central forces assumption), then $\upsilon = 1/3$, as reported by McHenry [61] or Hrennikoff [73] for plane stress and obtained in Born–Kármán's lattice with central forces.

$$\gamma = 0 \quad \Rightarrow \quad \upsilon = 1/3 \tag{75}$$

The truss analog equivalent to Born–Kármán's lattice model with central forces, composed of horizontal, vertical and diagonal bars, also foresees constrained spring parameters:

$$\gamma = 0 \quad \Rightarrow \quad \alpha = 2\beta \tag{76}$$

For the relevant lattice energy to be positive definite, the model of Gazis et al. [67] is valid for a Poisson's ratio lower than its critical value in plane stress:

$$\gamma \geq 0 \quad \Rightarrow \quad \upsilon \leq 1/3 \tag{77}$$

A simulation of the compression test of Gazis et al. lattice [67] is shown in Fig. 18, where the nodal forces and the stiffness elements have been calibrated at the border.

For plane strain, Navier's continuous equations are given by Eq. (50), and one identifies:

$$\begin{cases} \alpha + \beta = (\lambda + 2\mu)\, h \\ 2\beta + 4\gamma = (\lambda + \mu)\, h \\ 4\gamma + \beta = \mu h \end{cases} \quad \Rightarrow \quad \begin{cases} \alpha = 2\mu h = \frac{Eh}{1+\upsilon} \\ \beta = \lambda h = \frac{E\upsilon h}{(1+\upsilon)(1-2\upsilon)} \\ \gamma = \frac{\mu-\lambda}{4} h = \frac{E(1-4\upsilon)}{8(1+\upsilon)(1-2\upsilon)} h \end{cases} \tag{78}$$

If $\gamma = 0$ (central forces) here, then $\upsilon = 1/4$, which is the value provided by Cauchy-Poisson's "rari-constant" molecular theory where $\lambda = \mu$. The definiteness of energy requires that:

$$\gamma \geq 0 \quad \Rightarrow \quad \upsilon \leq 1/4 \tag{79}$$

Gazis et al.'s difference equations are equivalent to a finite difference formulation of Navier's continuous partial differential equations of elastodynamics in plane strain:

$$\begin{cases} 2\mu\left(u_{i+1,j} - 2u_{i,j} + u_{i-1,j}\right) + \frac{\lambda}{2}\left(u_{i+1,j+1} + u_{i-1,j-1} + u_{i-1,j+1} + u_{i+1,j-1} - 4u_{i,j}\right) \\ +\frac{\lambda+\mu}{4}\left(v_{i+1,j+1} - v_{i-1,j+1} - v_{i+1,j-1} + v_{i-1,j-1}\right) + (\mu - \lambda)\left(u_{i,j+1} - 2u_{i,j} + u_{i,j-1}\right) = \rho a^2\, \ddot{u}_{i,j} \\ 2\mu\left(v_{i,j+1} - 2v_{i,j} + v_{i,j-1}\right) + \frac{\lambda}{2}\left(v_{i+1,j+1} + v_{i-1,j-1} + v_{i-1,j+1} + v_{i+1,j-1} - 4v_{i,j}\right) \\ +\frac{\lambda+\mu}{4}\left(u_{i+1,j+1} - u_{i-1,j+1} - u_{i+1,j-1} + u_{i-1,j-1}\right) + (\mu - \lambda)\left(v_{i+1,j} - 2v_{i,j} + v_{i-1,j}\right) = \rho a^2\, \ddot{v}_{i,j} \end{cases} \tag{80}$$

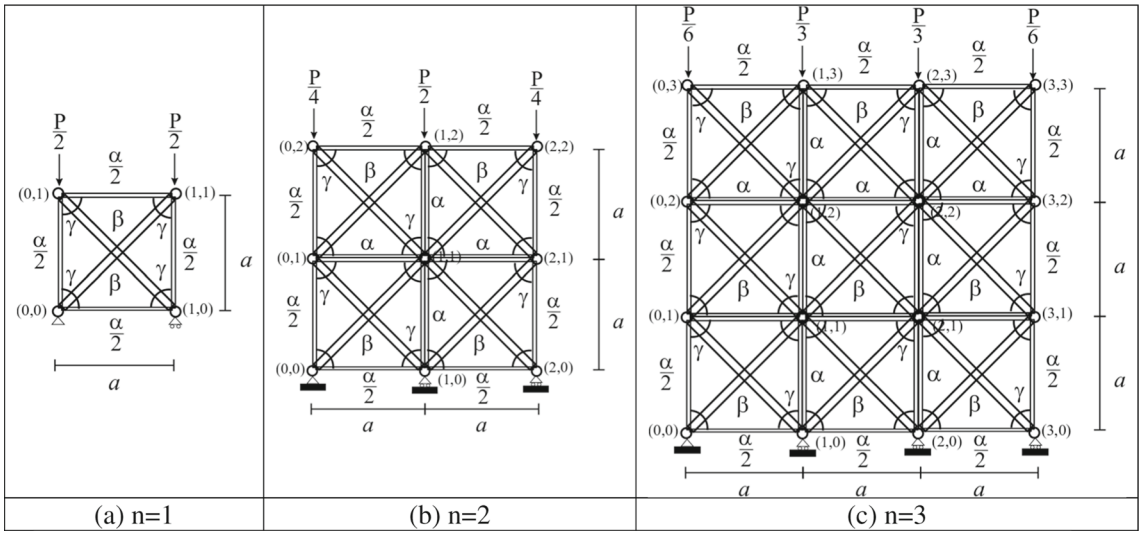

Fig. 18 Gazis et al. [67] lattice with specific border springs under uniform compression

This mixed differential-difference equations (2D Gazis et al. lattice in plane strain) can be expanded as:

$$\begin{cases} 2\mu\left[\frac{\partial^2 u}{\partial x^2}+\frac{a^2}{12}\frac{\partial^4 u}{\partial x^4}\right]+\frac{\lambda}{2}\left[2\frac{\partial^2 u}{\partial x^2}+2\frac{\partial^2 u}{\partial y^2}+a^2\frac{\partial^4 u}{\partial x^2\partial y^2}+\frac{a^2}{6}\frac{\partial^4 u}{\partial x^4}+\frac{a^2}{6}\frac{\partial^4 u}{\partial y^4}\right] \\ +\frac{\lambda+\mu}{4}\left[4\frac{\partial^2 v}{\partial x\partial y}+2\frac{a^2}{3}\frac{\partial^4 v}{\partial x\partial y^3}+2\frac{a^2}{3}\frac{\partial^4 v}{\partial y\partial x^3}\right]+(\mu-\lambda)\left[\frac{\partial^2 u}{\partial y^2}+\frac{a^2}{12}\frac{\partial^4 u}{\partial y^4}\right]+o\left(a^4\right)=\rho\,\ddot{u} \\ 2\mu\left[\frac{\partial^2 v}{\partial y^2}+\frac{a^2}{12}\frac{\partial^4 v}{\partial y^4}\right]+\frac{\lambda}{2}\left[2\frac{\partial^2 v}{\partial y^2}+2\frac{\partial^2 v}{\partial x^2}+a^2\frac{\partial^4 v}{\partial x^2\partial y^2}+\frac{a^2}{6}\frac{\partial^4 v}{\partial y^4}+\frac{a^2}{6}\frac{\partial^4 v}{\partial x^4}\right] \\ +\frac{\lambda+\mu}{4}\left[4\frac{\partial^2 u}{\partial x\partial y}+2\frac{a^2}{3}\frac{\partial^4 u}{\partial x\partial y^3}+2\frac{a^2}{3}\frac{\partial^4 u}{\partial y\partial x^3}\right]+(\mu-\lambda)\left[\frac{\partial^2 v}{\partial x^2}+\frac{a^2}{12}\frac{\partial^4 v}{\partial x^4}\right]+o\left(a^4\right)=\rho\,\ddot{v} \end{cases} \tag{81}$$

The model of Gazis [67] is valid for small values of Poisson's ratio ($\upsilon \leq 1/3$ for plane stress, $\upsilon \leq 1/4$ for 3D elasticity) in order to preserve the positive definiteness of the associated energy. This restriction is identical to that found for Born–Kármán's lattice. However, the mixed differential-difference equations of both lattices (Born–Kármán's lattice and Gazis et al.'s lattice) differ, and coincide only at the asymptotic limit. For 2D problems, the coincidence of the asymptotic continuum corresponding to the two lattices gives, from a comparison between Eqs. (35) and (70):

$$\begin{cases} \alpha_G = \alpha_{BK}+\delta_{BK} \\ \beta_G = \beta_{BK}-\delta_{BK} \\ \gamma_G = \frac{\delta_{BK}}{2} \end{cases} \tag{82}$$

where $(\alpha_G, \beta_G, \gamma_G)$ are the parameters of Gazis et al. [67], whereas $(\alpha_{BK}, \beta_{BK}, \delta_{BK})$ are the three parameters of Born–Kármán's lattice [6]. Only the asymptotic isotropic continuous media coincide (with different wave dispersive properties for the two-dimensional wave propagation). Comparing Eqs. (12) and (59) gives the correspondence between the two lattices in 3D:

$$\begin{cases} \alpha_G = \alpha_{BK}+2\delta_{BK} \\ \beta_G = \beta_{BK}-\delta_{BK} \\ \gamma_G = \frac{\delta_{BK}}{2} \end{cases} \tag{83}$$

The non-central contribution of Born–Kármán's lattice is based on shear interactions with a shear stiffness equal to δ_{BK}. It can be shown from the associated energy that this shear interaction is also equivalent to a frame-dependent angular interaction of angular stiffness $C_S^{BK}=\delta_{BK}a^2$, as opposed to Gazis et al. model [67] which is composed of objective angular interactions of angular stiffness $C_S^G=\gamma_G a^2$ (as shown in Fig. 19).

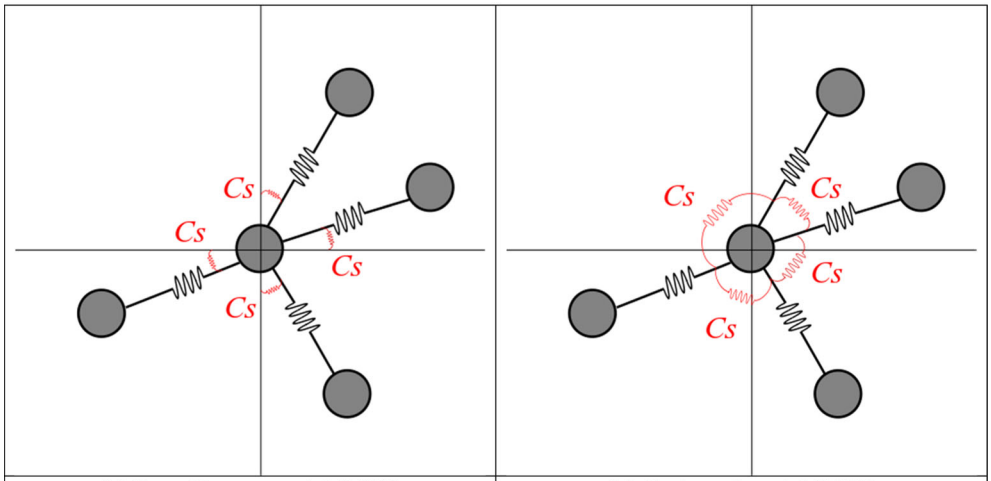

(a) Born-Karman model (1912) (b) Gazis et al model (1960)

Fig. 19 Equivalent angular interactions of Born–Kármán lattice model and Gazis et al. [67] lattice

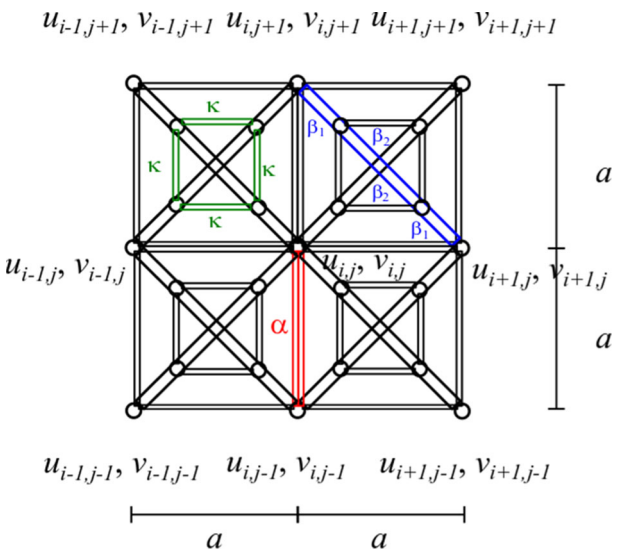

Fig. 20 Two-dimensional Hrennikoff cells

6 Two-dimensional discrete elasticity: Hrennikoff model

Gazis et al. [67] developed their three-parameter lattice model for crystal elasticity applications, and found an alternative model to Born–Kármán's non-central lattice interactions. We have shown that these two models are mathematically and physically different, even if they both converge asymptotically to Navier's partial differential equations of isotropic elastodynamics. Gazis et al.'s model [67] can be viewed as the consistent generalization of 1D Lagrange equations for 3D linear elasticity. However, before Gazis et al. [67], Hrennikoff [58,59,73] explored an other generalization of Born–Kármán's central (or Bravais) lattice, considering an enriched microstructure of central interactions. This could be seen as a meta-lattice, using modern concepts of meta-material modeling [83]. Hrennikoff's lattice method to model continuum elasticity is considered as a cornerstone of discretized methods in solid mechanics, that led to the birth of the Finite Element Method [99,100]. As shown in Figs. 20 and 21, Hrennikoff's lattice consists of edge bars-springs of stiffness α, and diagonal bars-springs of stiffness β joined at their quarter span by pinned auxiliary bars-springs of stiffness κ. All bars being hinged, Hrennikoff's lattice is a truss with central forces. The diagonal bar can be decomposed into three elements, one central of length $a\sqrt{2}/2$, and two complementary ones of length $a\sqrt{2}/4$. The equivalent

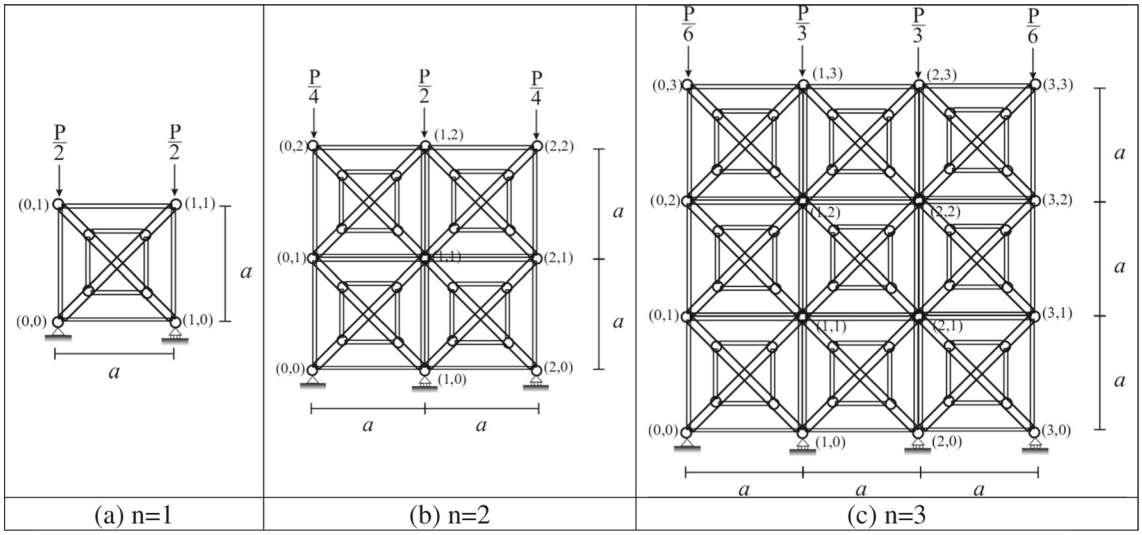

Fig. 21 Two-dimensional Hrennikoff truss [59] with specific border springs under uniform compression; Computation for three trusses 1×1, 2×2 and 3×3; $u(n, n) = -v v(n, n)$ for various values of Poisson's ratio v; Hrennikoff truss in plane stress

stiffness β of the diagonal bar results from those of its sub-elements connected in series:

$$\frac{1}{\beta} = \frac{2}{\beta_1} + \frac{1}{\beta_2} \tag{84}$$

In a uniform bar, these are related to the cross-section properties and the length of each element:

$$\beta = \frac{E_D A_D}{\sqrt{2}a}, \beta_1 = 4\frac{E_D A_D}{\sqrt{2}a} = 4\beta \quad \text{and} \quad \beta_2 = 2\frac{E_D A_D}{\sqrt{2}a} = 2\beta \tag{85}$$

The originality of Hrennikoff's approach [58,59] is to add some auxiliary bars characterized by:

$$\kappa = 2\frac{E_{aux} A_{aux}}{a} \tag{86}$$

Born and von Kármán central (or Bravais) lattice is obtained as a particular case when $\kappa = 0$, i.e., in absence of auxiliary bars, coinciding with McHenry's lattice [60,61].

The mixed differential-difference system of equations for Hrennikoff's lattice is:

$$\begin{cases} \left(\alpha + \frac{\beta\kappa}{8\beta+2\kappa}\right)\left(u_{i+1,j} - 2u_{i,j} + u_{i-1,j}\right) + \left(\frac{\beta}{2} + \frac{\beta\kappa}{16\beta+4\kappa}\right)\left(u_{i+1,j+1} + u_{i-1,j-1} + u_{i-1,j+1} + u_{i+1,j-1} - 4u_{i,j}\right) \\ + \left(\frac{\beta}{2} + \frac{\beta\kappa}{16\beta+4\kappa}\right)\left(v_{i+1,j+1} - v_{i-1,j+1} - v_{i+1,j-1} + v_{i-1,j-1}\right) - \frac{\beta\kappa}{8\beta+2\kappa}\left(u_{i,j+1} - 2u_{i,j} + u_{i,j-1}\right) = M\,\ddot{u}_{i,j} \\ \left(\alpha + \frac{\beta\kappa}{8\beta+2\kappa}\right)\left(v_{i,j+1} - 2v_{i,j} + v_{i,j-1}\right) + \left(\frac{\beta}{2} + \frac{\beta\kappa}{16\beta+4\kappa}\right)\left(v_{i+1,j+1} + v_{i-1,j-1} + v_{i-1,j+1} + v_{i+1,j-1} - 4v_{i,j}\right) \\ + \left(\frac{\beta}{2} + \frac{\beta\kappa}{16\beta+4\kappa}\right)\left(u_{i+1,j+1} - u_{i-1,j+1} - u_{i+1,j-1} + u_{i-1,j-1}\right) - \frac{\beta\kappa}{8\beta+2\kappa}\left(v_{i+1,j} - 2v_{i,j} + v_{i-1,j}\right) = M\,\ddot{v}_{i,j} \end{cases} \tag{87}$$

Hrennikoff [58,59] did not give these equations explicitly: he provided the calibration of his lattice from the static analysis, neglecting inertia, of one cell and its relevant linear isotropic elastic expected behavior at a macroscopic scale. We derived Eq. (87) assembling the stiffness matrix of each bar element around the considered node.

An expansion of Eq. (87) shows that the difference equations of the lattice converge asymptotically to Navier's partial differential ones for elastodynamics, with parameters:

$$\begin{cases} \left(\alpha + \beta + \frac{\beta\kappa}{4\beta+\kappa}\right)\frac{\partial^2 u}{\partial x^2} + \left(2\beta + \frac{\beta\kappa}{4\beta+\kappa}\right)\frac{\partial^2 v}{\partial x \partial y} + \beta\frac{\partial^2 u}{\partial y^2} = \rho h \frac{\partial^2 u}{\partial t^2} \\ \left(\alpha + \beta + \frac{\beta\kappa}{4\beta+\kappa}\right)\frac{\partial^2 v}{\partial y^2} + \left(2\beta + \frac{\beta\kappa}{4\beta+\kappa}\right)\frac{\partial^2 u}{\partial x \partial y} + \beta\frac{\partial^2 v}{\partial x^2} = \rho h \frac{\partial^2 v}{\partial t^2} \end{cases} \tag{88}$$

Equation (88) shows that Hrennikoff's lattice asymptotically converges toward a continuous elastic medium with cubic symmetry, which contains the isotropic case. By Eq. (88), we can identify the elastic constants of Navier's equations (linear isotropic elasticity) Eq. (36) for plane stress:

$$\left\{\begin{array}{l} \alpha+\beta+\frac{\beta\kappa}{4\beta+\kappa}=\frac{Eh}{1-\upsilon^2} \\ 2\beta+\frac{\beta\kappa}{4\beta+\kappa}=\frac{Eh}{2(1-\upsilon)} \\ \beta=\frac{Eh}{2(1+\upsilon)} \end{array}\right. \Rightarrow \left\{\begin{array}{l} \alpha=\frac{Eh}{1+\upsilon} \\ \beta=\frac{Eh}{2(1+\upsilon)} \\ \kappa=\frac{Eh(-1+3\upsilon)}{(1+\upsilon)(1-2\upsilon)} \end{array}\right. \tag{89}$$

The values reported by Hrennikoff are obtained from the calibration of the stiffness parameters:

$$\left\{\begin{array}{l} E_N A_N=\frac{Eha}{1+\upsilon} \\ E_D A_D=\frac{\sqrt{2}Eha}{2(1+\upsilon)} \\ E_{aux} A_{aux}=\frac{Eha(-1+3\upsilon)}{2(1+\upsilon)(1-2\upsilon)} \end{array}\right. \tag{90}$$

For uniform Young modulus, the cross-section area of each bar given by Hrennikoff [58,59] for plane stress is:

$$E_N=E_D=E_{aux}=E \quad \Rightarrow \quad \left\{\begin{array}{l} A_N=\frac{ha}{1+\upsilon} \\ A_D=\frac{\sqrt{2}ha}{2(1+\upsilon)} \\ A_{aux}=\frac{ha(-1+3\upsilon)}{2(1+\upsilon)(1-2\upsilon)} \end{array}\right. \tag{91}$$

For the potential energy to be positive definite, each stiffness parameter must be positive, thus, as mentioned by Hrennikoff [58], Hrennikoff's analysis is valid for plane stress if:

$$\kappa \geq 0 \quad \Rightarrow \quad \upsilon \geq 1/3 \tag{92}$$

Hrennikoff's model is thus valid for large values of the macroscopic Poisson's ratio for energetic consistency and can be viewed as complementary to the lattice of Gazis et al. [67], which was shown to hold for lower Poisson's ratio ($\upsilon \leq 1/3$ for plane stress). Hrennikoff [58,59] also provided the 3D lattice based on the same three interactions, including auxiliary members, and gave the identification rule in plane strain:

$$\left\{\begin{array}{l} \alpha+\beta+\frac{\beta\kappa}{4\beta+\kappa}=(\lambda+2\mu)\,h \\ 2\beta+\frac{\beta\kappa}{4\beta+\kappa}=(\lambda+\mu)\,h \\ \beta=\mu h \end{array}\right. \Rightarrow \left\{\begin{array}{l} \alpha=2\mu h=\frac{Eh}{1+\upsilon} \\ \beta=\mu h=\frac{Eh}{2(1+\upsilon)} \\ \kappa=\frac{\lambda-\mu}{2\mu-\lambda}4\mu h=\frac{Eh(-1+4\upsilon)}{(1+\upsilon)(1-3\upsilon)} \end{array}\right. \tag{93}$$

For the potential energy to be positive definite, each stiffness parameter must be positive, thus as mentioned by Hrennikoff [58], his analysis is valid for plane strain or 3D elasticity if:

$$\kappa \geq 0 \quad \Rightarrow \quad \upsilon \in \left[\frac{1}{4};\frac{1}{3}\right] \tag{94}$$

For uniform Young's modulus, we identify the cross sectional area of each bar in plane strain:

$$E_N=E_D=E_{aux}=E \quad \Rightarrow \quad \left\{\begin{array}{l} A_N=\frac{ha}{1+\upsilon} \\ A_D=\frac{\sqrt{2}ha}{2(1+\upsilon)} \\ A_{aux}=\frac{ha(-1+4\upsilon)}{2(1+\upsilon)(1-3\upsilon)} \end{array}\right. \tag{95}$$

The only difference with plane stress is the calibration of the auxiliary cross-section areas. The equations for Hrennikoff's lattice in plane stress after the previous calibration are:

$$\left\{\begin{array}{l} \frac{E(3-\upsilon)}{4(1-\upsilon^2)}\left(u_{i+1,j}-2u_{i,j}+u_{i-1,j}\right)+\frac{E}{8(1-\upsilon)}\left(u_{i+1,j+1}+u_{i-1,j-1}+u_{i-1,j+1}+u_{i+1,j-1}-4u_{i,j}\right) \\ +\frac{E}{8(1-\upsilon)}\left(v_{i+1,j+1}-v_{i-1,j+1}-v_{i+1,j-1}+v_{i-1,j-1}\right)+\frac{E(1-3\upsilon)}{4(1-\upsilon^2)}\left(u_{i,j+1}-2u_{i,j}+u_{i,j-1}\right)=\rho a^2\,\ddot{u}_{i,j} \\ \frac{E(3-\upsilon)}{4(1-\upsilon^2)}\left(v_{i,j+1}-2v_{i,j}+v_{i,j-1}\right)+\frac{E}{8(1-\upsilon)}\left(v_{i+1,j+1}+v_{i-1,j-1}+v_{i-1,j+1}+v_{i+1,j-1}-4v_{i,j}\right) \\ +\frac{E}{8(1-\upsilon)}\left(u_{i+1,j+1}-u_{i-1,j+1}-u_{i+1,j-1}+u_{i-1,j-1}\right)+\frac{E(1-3\upsilon)}{4(1-\upsilon^2)}\left(v_{i+1,j}-2v_{i,j}+v_{i-1,j}\right)=\rho a^2\,\ddot{v}_{i,j} \end{array}\right. \tag{96}$$

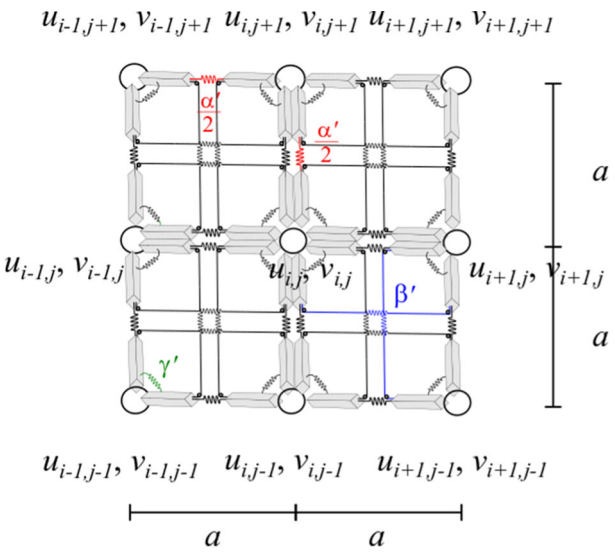

Fig. 22 Two-dimensional Zhang et al. [76] Hencky bar grid model with longitudinal and vertical elastic springs (of stiffness α'), secondary axial springs (of stiffness β'), and rotational springs (of stiffness γ')

which is exactly the mixed differential-difference system of Born–Kármán's lattice. We draw the same conclusion in plane strain, hence we see a strict mathematical equivalence of the equations of Born–Kármán and Hrennikoff lattices, which holds by the following identification:

$$\begin{cases} \alpha_{BK} = \alpha_H + \frac{\beta_H \kappa_H}{8\beta_H + 2\kappa_H} \\ \beta_{BK} = \beta_H + \frac{\beta_H \kappa_H}{8\beta_H + 2\kappa_H} \\ \delta_{BK} = -\frac{\beta_H \kappa_H}{8\beta_H + 2\kappa_H} \end{cases} \tag{97}$$

where $(\alpha_H, \beta_H, \kappa_H)$ pertain to Hrennikoff's truss, whereas $(\alpha_{BK}, \beta_{BK}, \delta_{BK})$ characterize Born–Kármán's lattice. Note that this is a strict equivalence, valid for the full lattice, not only for its asymptotic continuous limit: on the opposite, the correspondence between the lattices of Born and von Kármán and Gazis et al. was shown to hold only at the asymptotic limit. Figure 21 shows the compression of a Hrennikoff specimen with few cells. The adaptation of equivalent forces and springs at the border was repeated, as for a McHenry truss without auxiliary bars: the border springs have half the stiffness of the inner ones. Whatever the number of repetitions, the ratio of the horizontal to the vertical displacement of the specimen equals Poisson's ratio.

It is not the scope of this paper to review all kinds of lattices at various scales, with sometimes surprising macroscopic properties when so-called metamaterial or metalattices are considered. Specific lattices were extensively studied such as auxetic lattices with negative equivalent Poisson's ratio, strongly anisotropic lattices or specific lattices that do not converge asymptotically to Navier's elastodynamics partial differential equations (see [83] for alternative discrete elasticity models with complex microstructures). Recent lattices that also converge toward the isotropic elastic continuum are those of Zhang et al. [48,76], a three-parameter lattice with normal, secondary and rotational springs (see Figs. 22, 23), and that of Nannapaneni et al. [77], a three-parameter lattice with normal, diagonal and equivalent volumetric interactions (see also the paper of Chen et al. [101] or the one of Yin, 2022 about volumetric interactions [102]). A numerical compression test of several cells was performed on the model of Zhang et al. [48] to find Poisson's coefficient as the ratio of the lateral to the longitudinal displacement (see Fig. 23). Even if the lattice models presented here are physically different, and so are their mixed differential-difference equations, it is worth noting that they all converge toward the linear isotropic continuum, in that their asymptotic continuum limits are Navier's elastodynamics partial differential equations.

This paper is concerned with the change of scale from 2D and 3D discrete elasticity to 2D and 3D continuous elasticity models. The same methodology can be applied as well for bridging the scale between discrete structural mechanics in terms of discrete beams, plates or shells and in terms of continuous beams, plates or shells (see [79,103] or [104]). As already discussed, discrete (or lattice) beams were introduced by Hencky [78], see Fig. 23. The Hencky model comprises rigid beam segments connected by frictionless hinges with

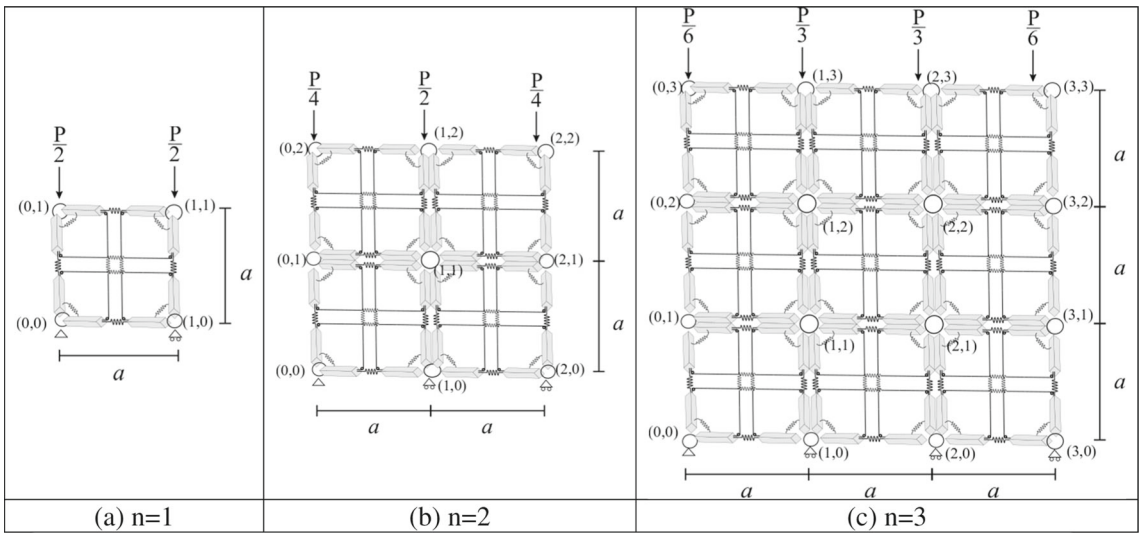

Fig. 23 Two-dimensional Zhang et al. [76] Hencky bar grid model with specific border springs under uniform compression; Computation for three trusses 1×1, 2×2 and 3×3; $u(n, n) = -v\, v(n, n)$ for various values of Poisson's ratio v in plane stress

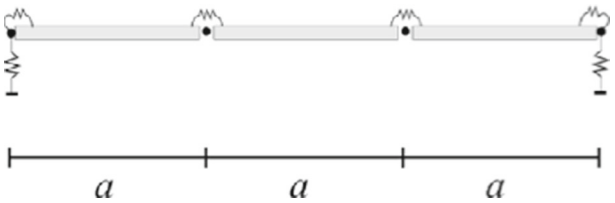

Fig. 24 Hencky bar chain: a lattice beam with concentrated bending rigidity

elastic rotational springs having stiffness equal to the flexural rigidity divided by the segment length (Fig. 24). The idea of approximating a continuous curvature by a discrete one defined by the relative angle formed by two adjacent segments was already formulated by Piola in 1825 [105]. The Hencky-Bar-Chain system (or lattice beam) asymptotically converges toward a continuous Euler-Bernoulli beam when the number of segments is sufficiently large. As for axial (Lagrange-type) lattices, there is also a mathematical analogy between the difference equations of the lattice beam problem, and the finite difference formulation of the continuous Euler-Bernoulli beams (see Wang et al. [79] for the validity of this equivalence for various boundary conditions). For both problems (strings, rods or beams), discrete elasticity mechanical problems may be built from simple repetitive structural elements, which asymptotically converge toward continuous elasticity. The difference equations of the discrete elasticity problem coincide with the finite difference formulation of the continuous one. Generalized Hencky beams were built by Kocsis and Challamel [106] to account for the possible axial and shear coupling phenomena in the discrete beam model. Hencky's discrete beam was also extended to discrete plate mechanics by Wu [80]; Wifi et al. [81]; El Naschie [82] and Wang et al. [79] (Fig. 25). The so-called Hencky-plate type model was shown again to be equivalent to the spatial finite difference formulation of the continuous Kirchhoff-Love plate model [79]. Hencky-type models may be also used to develop micro-structures with interesting macroscopic properties of 2D or 3D elastic media. The so-called Hencky-type model of pantographic sheet considered by Dell'Isola et al. [107] is a kind of generalization of Gazis et al. [67] model [67] (with central interaction with the first neighbors and angular interactions) plus additional rotational springs at the connection of each node. Discrete Hencky-type and continuous elasticity may be also related asymptotically, in presence of conservative and non-conservative loading [108].

7 Discrete, local and nonlocal elasticity

We show here the limits of the so-called local asymptotic continuous models in capturing wave dispersion phenomena of the lattice systems, both for 1D and multi-dimensional lattices. Starting from the elementary

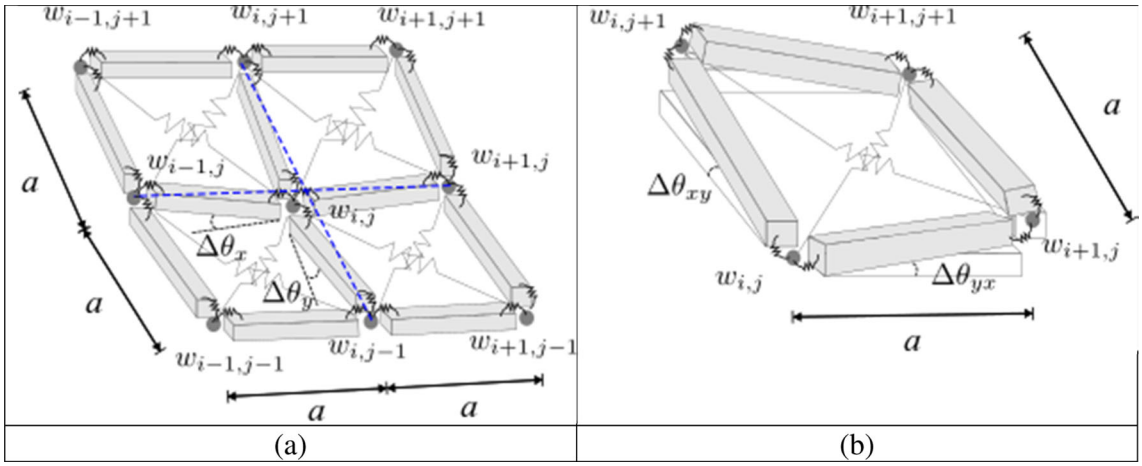

Fig. 25 Figure of Hencky bar net plate

one-dimensional Lagrange lattice, the wave dispersion equation can be obtained from the following harmonic wave formulation for the discrete displacement field:

$$u_i\,(t) = U \exp\left[J\,(\omega\, t - k\, x_i)\right] \quad \text{with} \quad x_i = a\, i \tag{98}$$

where ω is the propagating frequency, U is the amplitude, $J = \sqrt{-1}$ is the imaginary unit and k is the wave number. Introducing Eq. (98) in the mixed differential-difference equation of Lagrange Eq. (1) gives the well known dispersion equation in Born and von Kármán [6]:

$$\Omega = 2 \sin\left(\frac{ka}{2}\right) \quad \text{with} \quad \Omega = \omega\sqrt{\frac{M}{\alpha}} \tag{99}$$

One may also consider lattices with additional interactions of both short- and long-range (e.g., [109,110] or [111] for instance). Small values of $k\,a$ provide the long wave approximation, related to the wave equation of local elasticity given by Eq. (4).

$$k\,a << 1 \quad \Rightarrow \quad \Omega = k\,a - \frac{1}{24}\,(k\,a)^3 + \cdots \tag{100}$$

A shown by Fig. 26, for asymptotic local elasticity, one has $\Omega = k\,a$, which is not able to reproduce the dispersion phenomena due to the discreteness of Lagrange's lattice. Nonlocal elasticity models were developed (in particular) to capture these specific nonlinear responses in the dispersion curve of lattice theories. One of the simplest models, calibrated with respect to Lagrange lattice, is due to Eringen [21], who postulated the following constitutive relation for 1D media:

$$\sigma\,(x,t) - l_c^2 \frac{\partial^2 \sigma\,(x,t)}{\partial x^2} = E\varepsilon\,(x,t) \quad \text{and} \quad \varepsilon\,(x,t) = \frac{\partial u\,(x,t)}{\partial x} \tag{101}$$

where $\varepsilon\,(x,t), \sigma\,(x,t)$ the uniaxial strain and stress, and l_c the characteristic length related to the lattice spacing a, which is introduced to fit the wave dispersive properties of the lattice. Coupling the one-dimensional balance of a homogeneous rod of cross-section area S:

$$\frac{\partial N\,(x,t)}{\partial x} = \rho S \frac{\partial^2 u\,(x,t)}{\partial t^2} \quad \text{and} \quad N\,(x,t) = S\sigma\,(x,t) \tag{102}$$

with the nonlocal elastic constitutive law Eq. (101), one obtains the nonlocal wave elastic equation, which is a correction of the local wave equation Eq. (4):

$$ES\frac{\partial^2 u\,(x,t)}{\partial x^2} + l_c^2 \rho S \frac{\partial^4 u\,(x,t)}{\partial x^2 \partial t^2} = \rho S\,\frac{\partial^2 u\,(x,t)}{\partial t^2} \tag{103}$$

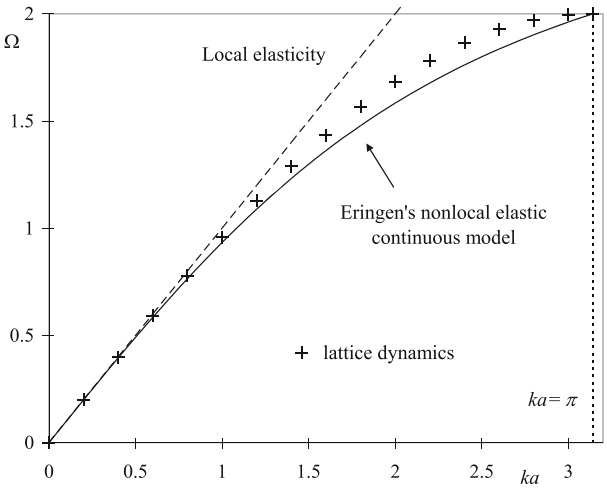

Fig. 26 Wave dispersive properties of Lagrange lattice—linear approximation of local elasticity and nonlocal continuous approximation of Eringen's model

This wave equation can be classified as a Boussinesq-type wave equation with coupled spatial and temporal derivatives (see [112,113] or the analysis of Maugin [15]). This nonlocal wave equation has been derived by Jaberolanssar and Peddieson [114] and Rosenau [28] from a continualization process of Lagrange lattice equations (and also derived by Eringen, 1983 from a nonlocal phenomenological approach [21]). The wave dispersion equation of this one-dimensional nonlocal medium can be obtained from the following harmonic wave formulation for the continuous displacement field:

$$u\,(x,t) = U\exp\left[J\,(\omega\,t - k\,x)\right] \tag{104}$$

leading to the characteristic dispersion equation of Eringen's nonlocal medium:

$$\frac{\omega^2}{c_0^2} = \frac{k^2}{1 + l_c^2 k^2} \quad \text{with} \quad c_0 = \sqrt{\frac{E}{\rho}} \tag{105}$$

c_0 is the axial wave celerity. Equation (105) can be equivalently written in dimensionless form:

$$\Omega = \frac{ka}{\sqrt{1 + e_0^2\,(ka)^2}} \quad \text{with} \quad \Omega = \frac{\omega\,a}{c_0} \quad \text{and} \quad e_0 = \frac{l_c}{a} \tag{106}$$

where e_0 is a dimensionless parameter used to calibrate the nonlocal model with respect to the lattice one. Clearly, Eqs. (99) and (106) differ, which means that this nonlocal model differs from the original lattice. However, the nonlocal model can be considered as an efficient mathematical tool to capture the dispersive properties of the lattice. In the long wave approximation, the dimensionless parameter e_0 can be calibrated by comparing Eq. (100) with Eq. (107):

$$ka << 1 \quad \Rightarrow \quad \Omega = ka - \frac{e_0^2}{2}\,(ka)^3 + \cdots \quad \Rightarrow \quad e_0 = \sqrt{\frac{1}{12}} \approx 0.289 \tag{107}$$

Eringen [21] suggested to calibrate his nonlocal model at the end of the Brillouin zone of Lagrange's lattice:

$$\Omega\,(ka = \pi) = 2 \quad \Rightarrow \quad e_0 = \sqrt{\frac{\pi^2 - 4}{4\pi^2}} \approx 0.386 \tag{108}$$

Figure 26 shows that this last approximation gives satisfactory results, as also highlighted by Eringen [21], who in a certain sense closed the chasm between Lagrange's lattice and 1D continua by a one-length scale nonlocal continuum behaving like a lattice (sometimes referred to as a *quasicontinuum*—see Collins [27]). The nonlocal model can be alternatively calibrated with respect to the long wave approximation based on Eq.

(107), as suggested by Jaberolanssar and Peddieson [114], Rosenau [28], Andrianov and Awrejcewicz [115] and Andrianov et al. [116]. This latter calibration is satisfactory for the long wavelength approximation, but it gives inadequate results at the end of the Brillouin zone. The one length-scale nonlocal model of Eringen [21] can be enriched by additional stress- or strain- gradient terms, for better calibrating the nonlocal model with the lattice. Two length-scale models, generalizing Eringen's, show satisfactory results (see e.g., [22,117–120]). However, Eringen's nonlocal model still remains very simple and efficient, and reveals the essential dispersive properties of the discrete medium.

The use of a nonlocal elastic model to analyze the wave dispersion phenomena in 2D or 3D lattice appears more complex. The wave dispersion equation of a 2D elastic lattice (we will consider both the Born–Kármán's lattice and that of Gazis et al.) can be obtained from the following harmonic wave formulation for the discrete displacement field:

$$\begin{aligned} u_{i,j}(t) &= U \exp\left\lfloor J\left(\omega t - k_x x_i - k_y y_j\right)\right\rfloor \quad \text{and} \\ v_{i,j}(t) &= V \exp\left\lfloor J\left(\omega t - k_x x_i - k_y y_j\right)\right\rfloor \quad \text{with} \quad x_i = a\,i \quad \text{and} \quad y_j = a\,j \end{aligned} \tag{109}$$

with ω is the propagating frequency, U,V the wave amplitudes, and k_x, k_y the wave numbers in the x, y directions respectively. Introducing Eq. (109) in the equation of the 2D Born–Kármán's lattice, Eq. (25), gives the 2D wave dispersion equation [6]:

$$\begin{vmatrix} 2\alpha(1-c_1)+2\beta(1-c_1c_2)+2\delta(1-c_2)-\rho a^2h\omega^2 & 2\beta s_1s_2 \\ 2\beta s_1s_2 & 2\alpha(1-c_2)+2\beta(1-c_1c_2)+2\delta(1-c_1)-\rho a^2h\omega^2 \end{vmatrix} = 0 \tag{110}$$

with the dimensionless parameters c_i and s_i for $i \in \{1;2\}$ defined from:

$$c_1 = \cos(k_x a)\,; \quad c_2 = \cos\left(k_y a\right)\,; \quad s_1 = \sin(k_x a) \quad \text{and} \quad s_2 = \sin\left(k_y a\right) \tag{111}$$

Equation (110) was obtained equivalently by Suiker et al. [47] for 2D Born–Kármán's lattices. Note that the 3D wave dispersion equation of this lattice model with non-central forces is available in the original paper of Born and von Kármán [6]. Introducing Eq. (109) in the equation of the 2D Gazis et al. lattice [67], Eq. (64), gives the two-dimensional wave dispersion equation:

$$\begin{vmatrix} 2\alpha(1-c_1)+2\beta(1-c_1c_2)+8\gamma(1-c_2)-\rho a^2h\omega^2 & (2\beta+4\gamma)s_1s_2 \\ (2\beta+4\gamma)s_1s_2 & 2\alpha(1-c_2)+2\beta(1-c_1c_2)+8\gamma(1-c_1)-\rho a^2h\omega^2 \end{vmatrix} = 0 \tag{112}$$

The 3D wave dispersion equation of this lattice with angular forces is in Gazis et al. [67]. Equation (110) would be equivalent to Eq. (112) only for central interactions:

$$\alpha_G = \alpha_{BK}, \beta_G = \beta_{BK}, \gamma_G = \frac{1}{4}\delta_{BK} \quad \text{and} \quad \beta_G + 2\gamma_G = \beta_{BK} \quad \Rightarrow \quad \gamma_G = \delta_{BK} = 0 \tag{113}$$

This confirms that both lattices are indeed mathematically and physically different. In the following, we will focus on the 2D lattice with central forces (particular case of Born–Kármán's lattice with $\delta_{BK} = 0$, or of that Gazis et al. with $\gamma_G = 0$):

$$\begin{vmatrix} 2\alpha(1-c_1)+2\beta(1-c_1c_2)-\rho a^2h\omega^2 & 2\beta\, s_1s_2 \\ 2\beta\, s_1s_2 & 2\alpha(1-c_2)+2\beta(1-c_1c_2)-\rho a^2h\omega^2 \end{vmatrix} = 0 \tag{114}$$

Equation (114) was found by Blackman [49], Montroll [50] or De Launay [51] for 2D lattices with central force (edge and diagonal) interactions among first and second neighbors. It is further necessary that $\alpha = 2\beta$, for asymptotical convergence to an isotropic medium (as seen above):

$$\begin{vmatrix} 2\alpha(1-c_1)+\alpha(1-c_1c_2)-\rho a^2h\omega^2 & \alpha s_1s_2 \\ \alpha s_1s_2 & 2\alpha(1-c_2)+\alpha(1-c_1c_2)-\rho a^2h\omega^2 \end{vmatrix} = 0 \tag{115}$$

Equation (115) covers the case $\upsilon = 1/4$ in plane strain ($\lambda = \mu$), and $\upsilon = 1/3$ in plane stress, and can be rewritten in dimensionless form:

$$\begin{vmatrix} 2(1-c_1)+1-c_1c_2-\Omega^2 & s_1s_2 \\ s_1s_2 & 2(1-c_2)+1-c_1c_2-\Omega^2 \end{vmatrix} = 0 \quad \text{with} \quad \Omega^2 = \frac{\rho a^2 h}{\alpha}\omega^2 \tag{116}$$

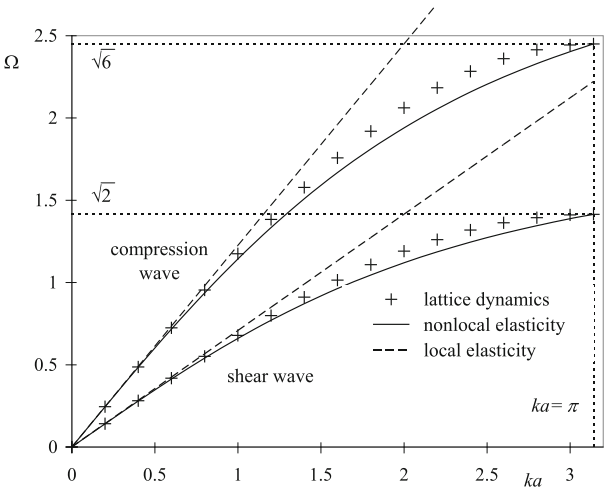

Fig. 27 Wave dispersive properties of two-dimensional Born–Karman lattice with pure central interactions—linear approximation of local elasticity and nonlocal continuous approximation of Eringen's model

Equation (116) is a quartic equation of the frequency, which in full reads:

$$\Omega^4 - \Omega^2 (6 - 2c_1 - 2c_2 - 2c_1c_2) + 9 - 6c_1 - 6c_2 - 2c_1c_2 + 2c_1^2c_2 + 2c_1c_2^2 + c_1^2c_2^2 - s_1^2s_2^2 = 0 \quad (117)$$

and admits two branches of solutions

$$\Omega_-^2 = 2 - c_1 - c_2 \quad \text{and} \quad \Omega_+^2 = 4 - c_1 - c_2 - 2c_1c_2 \quad (118)$$

as obtained by Montroll [50]. In the particular case of propagation along one direction, i.e., $k_y = 0$ (which is equivalent to $c_2 = 1$ and $s_2 = 0$), the two frequency solutions are written as:

$$\Omega_-^2 = 1 - c_1 \quad \text{and} \quad \Omega_+^2 = 3\,(1 - c_1) \quad (119)$$

These two branches, associated with shear (or transverse) and the compression (or longitudinal) waves, respectively, are shown in Fig. 27. The long wave approximation yields:

$$\Omega_- = \frac{\sqrt{2}}{2} k_x a \quad \text{and} \quad \Omega_+ = \frac{\sqrt{6}}{2} k_x a \quad (120)$$

which is also equivalent, assuming plane strain with central interactions, i.e., $\alpha = 2\mu h = 2\lambda h$:

$$\omega_- = k_x c_{shear} \quad \text{and} \quad \omega_+ = k_x c_{long} \quad \text{with} \quad c_{shear} = \sqrt{\frac{\mu}{\rho}} \quad \text{and} \quad c_{long} = \sqrt{\frac{\lambda + 2\mu}{\rho}} = \sqrt{\frac{3\mu}{\rho}} \quad (121)$$

The response is very similar to that of 1D Lagrange's lattice, with a wave dispersion phenomenon highlighted by two branches associated with the shear (or transverse) wave and the compression (or longitudinal) wave respectively. Equation (118) is the wave dispersion equation of this square lattice with central interactions, and in the long wave limit provides:

$$\Omega_-^2 = \frac{1}{2}\left[(k_x a)^2 + \left(k_y a\right)^2\right] + \cdots \quad \text{and} \quad \Omega_+^2 = \frac{3}{2}\left[(k_x a)^2 + \left(k_y a\right)^2\right] + \cdots \quad (122)$$

A 3D representation of the dimensionless frequency Ω versus the dimensionless wave numbers in both directions, $k_x a$ and $k_y a$, is a conic surface that confirms the lattice isotropic response in the low-frequency regime for both shear and compression waves, see Fig. 28, and agrees with the asymptotic expansion Eq. (122). In other words, Born–Kármán square lattice with central forces (or cubic lattice in 3D) has isotropic behavior at low frequencies. Figures 29 and 30 show that this isotropy is lost in the high-frequency regime, where the special symmetry of the lattice is revealed. This phenomenon is evidenced in Blackman [49], Montroll [50], De Launay [51] for 2D square lattices with central forces (and more recently numerically highlighted in

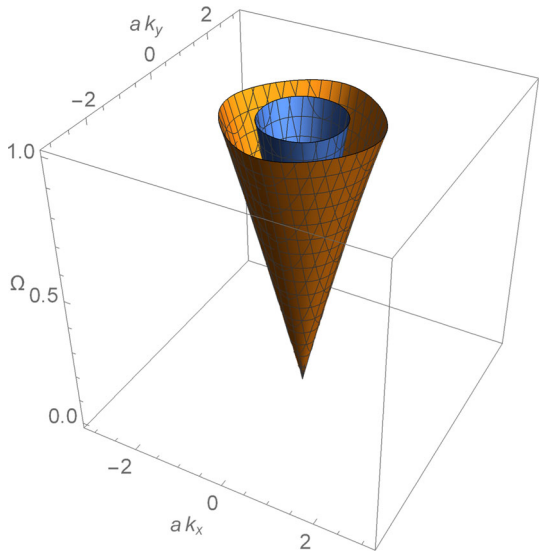

Fig. 28 $\Omega \in [0; 1]$; conic surface for low frequency range of both shear (orange surface) and compression (blue surface) waves; isotropic behavior for low frequency range

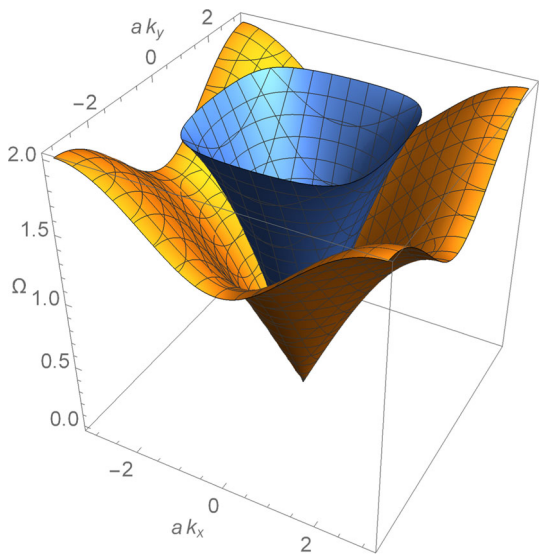

Fig. 29 $\Omega \in [0; 2]$; distorsion of the shear wave surface; loose of the isotropic nature of the frequency response for high-range frequencies

Nannapaneni et al. [77]); it resembles for triangular or hexagonal lattices (that may behave as isotropic bodies in the low-frequency regimes), showing some microstructure anisotropy in the high-frequency regimes (see [121] or more recently [122] or [123]). Indeed, there is a strong coupling between lattice anisotropy (preserving lattice symmetry) and nonlocal effects, far from the isotropic continuous long wave approximation.

An efficient approximation of the nonlocality causing the dispersion phenomena at the lattice scale can rely on the 3D nonlocal (differential) isotropic constitutive law by Eringen [21]:

$$\underline{\underline{\sigma}} - l_c^2 \Delta \underline{\underline{\sigma}} = \lambda \left(tr \underline{\underline{\varepsilon}} \right) \underline{\underline{1}} + 2\mu \underline{\underline{\varepsilon}} \tag{123}$$

where l_c being as in the uniaxial law Eq. (101), which Eq. (123) generalizes. We now investigate the capability of this 3D (or 2D) nonlocal law to capture the dispersion in the Born and von Kármán square lattice with central forces in plane strain. In view of Eq. (123) and balance, including inertia, Navier's nonlocal elastodynamic

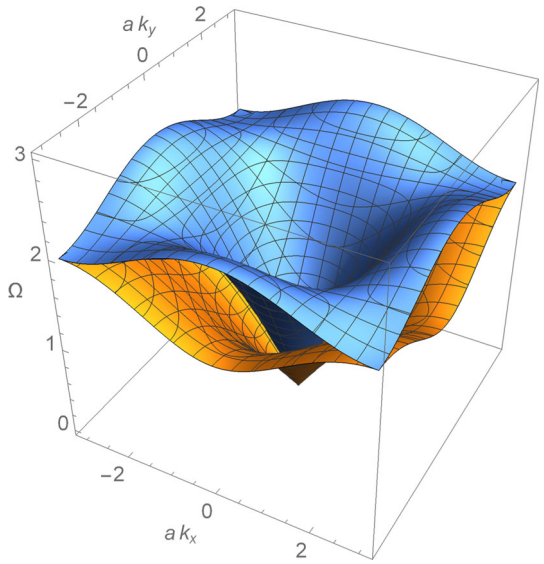

Fig. 30 $\Omega \in [0;\, 3]$; strong distorsion of both the shear wave and the compression wave surfaces; loose of the isotropic nature of the frequency response for high-range frequencies (cubic symmetry)

equations are:

$$\begin{cases} (\lambda+2\mu)\,\frac{\partial^2 u}{\partial x^2}+(\lambda+\mu)\,\frac{\partial^2 v}{\partial x\partial y}+\mu\,\frac{\partial^2 u}{\partial y^2}=\rho\left[1-l_c^2\left(\frac{\partial^2}{\partial x^2}+\frac{\partial^2}{\partial y^2}\right)\right]\frac{\partial^2 u}{\partial t^2} \\ (\lambda+2\mu)\,\frac{\partial^2 v}{\partial y^2}+(\lambda+\mu)\,\frac{\partial^2 u}{\partial x\partial y}+\mu\,\frac{\partial^2 v}{\partial x^2}=\rho\left[1-l_c^2\left(\frac{\partial^2}{\partial x^2}+\frac{\partial^2}{\partial y^2}\right)\right]\frac{\partial^2 v}{\partial t^2} \end{cases} \tag{124}$$

The wave dispersion equation of this nonlocal elastic continuum can be obtained from the following harmonic wave continuous displacement fields:

$$u\,(x,\,y,\,t)=U\exp\left[J\left(\omega\,t-k_x\,x-k_y\,y\right)\right]\quad\text{and}\quad v\,(x,\,y,\,t)=V\exp\left[J\left(\omega\,t-k_x\,x-k_y\,y\right)\right] \tag{125}$$

In view of Eqs. (125) and (124), the wave dispersion equation of the isotropic nonlocal model (in the sense of Eringen [21]) is given by

$$\begin{vmatrix} (\lambda+2\mu)\,k_x^2+\mu k_y^2-\rho\omega^2-\rho l_c^2\left(k_x^2+k_y^2\right)\omega^2 & (\lambda+\mu)\,k_x k_y \\ (\lambda+\mu)\,k_x k_y & (\lambda+2\mu)\,k_y^2+\mu k_x^2-\rho\omega^2-\rho l_c^2\left(k_x^2+k_y^2\right)\omega^2 \end{vmatrix}=0 \tag{126}$$

The frequency equation of both branches can be extracted from the determinant Eq. (126):

$$\rho\omega^2=\frac{k_x^2+k_y^2}{1+l_c^2\left(k_x^2+k_y^2\right)}\,\frac{\lambda+3\mu\pm(\lambda+\mu)}{2} \tag{127}$$

which may be written equivalently as

$$\frac{\omega_- a}{c_{shear}}=\frac{\sqrt{(k_x a)^2+\left(k_y a\right)^2}}{\sqrt{1+e_0^2\left[(k_x a)^2+\left(k_y a\right)^2\right]}}\quad\text{and}\quad\frac{\omega_+ a}{c_{long}}=\frac{\sqrt{(k_x a)^2+\left(k_y a\right)^2}}{\sqrt{1+e_0^2\left[(k_x a)^2+\left(k_y a\right)^2\right]}}\quad\text{with}$$

$$c_{shear}=\sqrt{\frac{\mu}{\rho}}\quad\text{and}\quad c_{long}=\sqrt{\frac{\lambda+2\mu}{\rho}} \tag{128}$$

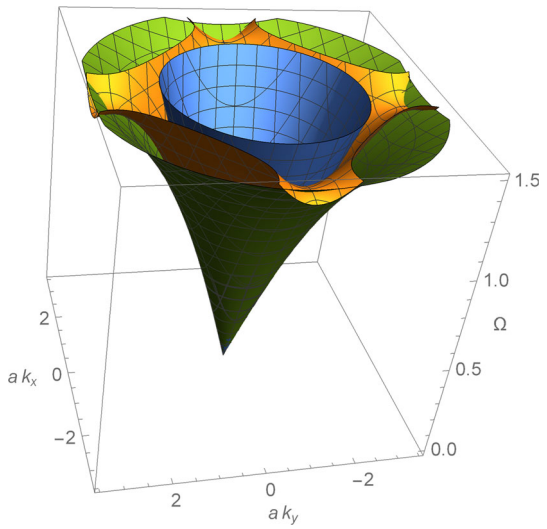

Fig. 31 $\Omega \in [0; 1.5]$; shear wave dispersive surface; comparison between the local (isotropic) (blue right circular cone), the lattice (orange surface with cubic symmetry) and the isotropic nonlocal model (green surface of revolution)

Referring to the 2D lattice with central interactions following the "rari-constant" theory $\lambda = \mu$, the nonlocal elasticity of Eringen [21] predicts the two dimensionless frequency equations:

$$\Omega_- = \frac{\sqrt{2}}{2} \frac{\sqrt{(k_x a)^2 + (k_y a)^2}}{\sqrt{1 + e_0^2 \left[(k_x a)^2 + (k_y a)^2\right]}} \quad \text{and}$$

$$\Omega_+ = \frac{\sqrt{6}}{2} \frac{\sqrt{(k_x a)^2 + (k_y a)^2}}{\sqrt{1 + e_0^2 \left[(k_x a)^2 + (k_y a)^2\right]}} \quad \text{with} \quad \Omega = \sqrt{\frac{\rho h}{\alpha}} a\omega = \sqrt{\frac{\rho}{2\mu}} a\omega = \frac{\sqrt{2}}{2} \frac{a\omega}{c_{shear}} \tag{129}$$

Figures 31 and 32 show the capability of the isotropic nonlocal model to predict the anisotropic lattice response, both for low- and high-frequency regimes. The length scale of the nonlocal model, depending on the lattice spacing, is calibrated as for 1D Lagrange's according to Eq. (108) (as also used for Fig. 27). Both local and nonlocal elastic models are isotropic. The nonlocal isotropic elastic model gives satisfactory results when compared to the cubic lattice, up to the end of the Brillouin zone, but is, as expected, unable to capture the anisotropic dispersive phenomena of the 2D lattice at high frequencies. There is definitely a need to develop anisotropic nonlocal elastic models in the high-frequency regime, even with this very elementary cubic cell. It is also possible to consider more lattice interactions in order to reduce this anisotropic effect at high frequencies, as considered for instance by Askes and Metrikine [124]: they studied an extended hexagonal lattice with additional interactions in order to make the discrete model isotropic in a second-order approximation, with hexagonal lattices asymptotically converging to the local "rari-constant" theory ($\upsilon = 1/4$ at the continuous limit).

8 Conclusions

The history of searching a bridge between discrete and continuum elasticity starts in the eighteenth century with the pioneering works of Lagrange, who first gave the mixed differential-difference equation of wave propagation in a discrete 1D lattice and its continuum limit. During the nineteenth century, scholars investigated the possibility to build 3D elasticity from molecular assumptions, which equals to connect discrete and continuum elastic models. Born and von Kármán [6] generalized Lagrange's mixed differential-difference equation to 3D elasticity, also establishing the link between a 3D monatomic cubic lattice and its continuum limit, governed by Navier's elastodynamics partial differential equation. The connection between discrete and continuum is

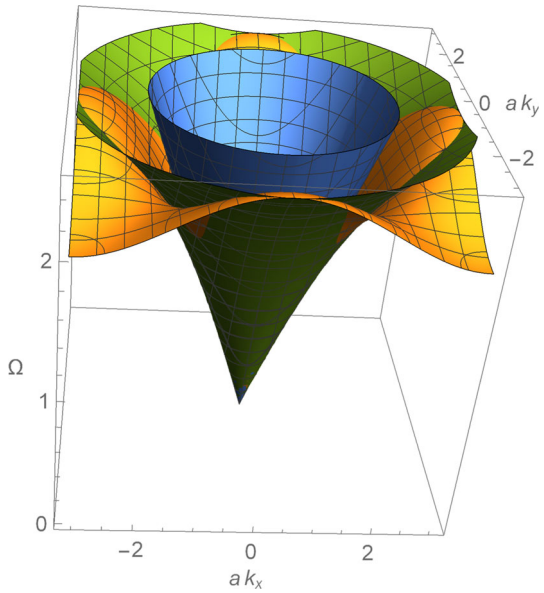

Fig. 32 $\Omega \in [0; 2.5]$; compression wave dispersive surface; comparison between the local (isotropic) (blue right circular cone), the lattice (orange surface with cubic symmetry) and the isotropic nonlocal model (green surface of revolution)

consistent only if central interactions among the first and the second neighbors are considered, which equals to model the lattice as a truss (dubbed McHenry's or Hrennikoff's) with bars transmitting axial loads that connect each node-particle. With this assumption ("rari-constant" theory, equivalent to the molecular one of Navier, Cauchy and Poisson), the macroscopic Poisson's ratio appears to be restricted to 1/4 for 3D elasticity, and 1/3 for plane stress. Born and von Kármán [6] introduced additional non-central (shear) interactions to capture general elastic properties at the macroscopic scale, including general values of Poisson's ratio. However, this was shown to be inconsistent, in the sense that the potential energy associated to these additional shear forces is not invariant under superposed rigid body rotations, confusing them with shear modes. Hrennikoff [58] gave a first consistent answer to this problem, generalizing Born–Kármán cubic lattice with central forces by adding auxiliary springs inside the cell: in this sense, his model is a meta-lattice, in that discrete cells exhibit a microstructure. Hrennikoff's lattice is energetically consistent, exhibiting only central interactions also among the auxiliary bars inside each cell. We provided the mixed differential-difference equation of Hrennikoff's truss (absent in Hrennikoff [58,59,73]) and showed that it converges to Navier's partial differential equations; it coincides with that of Born–Kármán's cubic lattice. Hrennikoff's model is valid for large values of macroscopic Poisson's ratio ($\upsilon \geq 1/3$ for plane stress) in order to preserve the definite positiveness of the associated discrete energy.

The resolution of this problematic passage from discrete to continuum elasticity problem is probably due to Gazis et al. [67] who generalized Born–Kármán cubic lattice with central forces by adding rotation interactions (as suggested earlier by Voigt and Poincaré). Indeed, Gazis and Wallis [63] have shown the necessity to build a potential energy of the lattice which is invariant under rigid motion, by formulating this energy as a function of the discrete invariant quantities such as distance between atoms and angles formed by triples of atoms. The model of Gazis et al. [67] converges toward Navier's partial differential equations in the continuum limit, and is valid for small values of Poisson's ratio ($\upsilon \leq 1/3$ for plane stress, or $\upsilon \leq 1/4$ for 3D elasticity) in order to preserve the definite positiveness of the associated discrete energy: thus, it can be viewed as complementary to Hrennikoff's truss valid for large values of Poisson's ratio. This would mean that the gap between molecular elasticity and continuum elasticity has only been closed in the 60's of the previous century, two hundred years after the initial work of Lagrange [4]. However, Gazis et al. [67] did not explore the capability of nonlocal continua to capture the full wave dispersive properties of the cubic lattice. Eringen [21] satisfactory solved this question for 1D Lagrange's lattice by fitting its frequency dispersive response with that of a one-parameter nonlocal continuum. Eringen [21,22,118] also explored the possibility to capture the 3D lattice response with an isotropic nonlocal continuous medium. We show in this paper that the isotropic nature of the cubic lattice is lost in the high frequency regime, which highlights the need of an anisotropic nonlocal medium (consistent with the symmetry properties of the considered lattice) in this regime. The full exploration of the lattice properties

with some enriched nonlocal continuous media still merits some sophisticated research with the development of anisotropic nonlocal modeling (which can be eventually explored within fractional nonlocal elasticity—see [125]). The analysis presented herein is restricted to connecting linear lattices and continuum linear elasticity. The connection between lattices and continuum nonlinear elasticity, especially in terms of wave propagation, was not treated herein, and would deserve a complete analysis, basing on the pioneer works of Fermi et al. [25] devoted to 1D nonlinear Lagrange lattices.

Appendix A: Equivalence of the lattice-based gradient elasticity model and Mindlin equation for Gazis et al. model

The continualized lattice-based gradient elasticity equations derived for Gazis et al. lattice [67] are given by Eq. (58) which is here reformulated:

$$\begin{aligned}
&\alpha\left(\frac{\partial^2 u}{\partial x^2}+\frac{a^2}{12}\frac{\partial^4 u}{\partial x^4}\right)\\
&+\frac{\beta}{2}\left(4\frac{\partial^2 u}{\partial x^2}+2\frac{\partial^2 u}{\partial y^2}+a^2\frac{\partial^4 u}{\partial x^2\partial y^2}+\frac{a^2}{3}\frac{\partial^4 u}{\partial x^4}+\frac{a^2}{6}\frac{\partial^4 u}{\partial y^4}+2\frac{\partial^2 u}{\partial z^2}+a^2\frac{\partial^4 u}{\partial x^2\partial z^2}+\frac{a^2}{6}\frac{\partial^4 u}{\partial z^4}\right)\\
&+4\gamma\left(\frac{\partial^2 u}{\partial y^2}+\frac{a^2}{12}\frac{\partial^4 u}{\partial y^4}+\frac{\partial^2 u}{\partial z^2}+\frac{a^2}{12}\frac{\partial^4 u}{\partial z^4}\right)\\
&+\left(\gamma+\frac{\beta}{2}\right)\left(4\frac{\partial^2 v}{\partial x\partial y}+\frac{2a^2}{3}\frac{\partial^4 v}{\partial x\partial y^3}+\frac{2a^2}{3}\frac{\partial^4 v}{\partial x^3\partial y}+4\frac{\partial^2 w}{\partial x\partial z}+\frac{2a^2}{3}\frac{\partial^4 w}{\partial x\partial z^3}+\frac{2a^2}{3}\frac{\partial^4 w}{\partial x^3\partial z}\right)=\rho a\,\ddot{u}
\end{aligned}\tag{A.1}$$

Equation (A.1) can be reformulated in two terms with the zero-th order and the second-order strain gradient expression:

$$\begin{aligned}
&(\alpha+2\beta)\frac{\partial^2 u}{\partial x^2}+(2\beta+4\gamma)\left(\frac{\partial^2 v}{\partial x\partial y}+\frac{\partial^2 w}{\partial x\partial z}\right)+(\beta+4\gamma)\left(\frac{\partial^2 u}{\partial y^2}+\frac{\partial^2 u}{\partial z^2}\right)\\
&+\frac{a^2}{12}\left[(\alpha+2\beta)\frac{\partial^4 u}{\partial x^4}+(\beta+4\gamma)\left(\frac{\partial^4 u}{\partial y^4}+\frac{\partial^4 u}{\partial z^4}\right)+6\beta\left(\frac{\partial^4 u}{\partial x^2\partial y^2}+\frac{\partial^4 u}{\partial x^2\partial z^2}\right)\right]\\
&+\frac{a^2}{3}(\beta+2\gamma)\left(\frac{\partial^4 v}{\partial x\partial y^3}+\frac{\partial^4 v}{\partial x^3\partial y}+\frac{\partial^4 w}{\partial x\partial z^3}+\frac{\partial^4 w}{\partial x^3\partial z}\right)=\rho a\,\ddot{u}
\end{aligned}\tag{A.2}$$

Equation (A.2) can be compared to Navier's partial differential equation Eq. (13) with cubic symmetry, for the zero-th order medium.

$$\begin{cases}\alpha = a\,(c_{11}-2c_{12})\\ \beta = ac_{12}\\ \gamma = \frac{a}{4}\,(c_{44}-c_{12})\end{cases}\tag{A.3}$$

Injecting the stiffness calibration Eq. (A.3) into the second-order expansion Eq. (A.2) of Gazis et al. lattice equations gives the gradient elasticity cubic model:

$$\begin{aligned}
&c_{11}\frac{\partial^2 u}{\partial x^2}+(c_{12}+c_{44})\left(\frac{\partial^2 v}{\partial x\partial y}+\frac{\partial^2 w}{\partial x\partial z}\right)+c_{44}\left(\frac{\partial^2 u}{\partial y^2}+\frac{\partial^2 u}{\partial z^2}\right)\\
&+\frac{a^2}{12}\left[c_{11}\frac{\partial^4 u}{\partial x^4}+c_{44}\left(\frac{\partial^4 u}{\partial y^4}+\frac{\partial^4 u}{\partial z^4}\right)+6\,c_{12}\left(\frac{\partial^4 u}{\partial x^2\partial y^2}+\frac{\partial^4 u}{\partial x^2\partial z^2}\right)\right]\\
&+\frac{a^2}{6}(c_{12}+c_{44})\left(\frac{\partial^4 v}{\partial x\partial y^3}+\frac{\partial^4 v}{\partial x^3\partial y}+\frac{\partial^4 w}{\partial x\partial z^3}+\frac{\partial^4 w}{\partial x^3\partial z}\right)=\rho\,\ddot{u}
\end{aligned}\tag{A.4}$$

This partial differential lattice-based equation exactly coincides with Eq. (10) page 315, of Mindlin [98].
In case of asymptotic linear elastic isotropy, the micro elastic parameters are related to the macro elastic parameters for Gazis et al. lattice by:

$$\begin{cases} \alpha = a\ (c_{11} - 2c_{12}) = (2\mu - \lambda)\ a \\ \beta = ac_{12} = \lambda a \\ \gamma = \frac{a}{4}\ (c_{44} - c_{12}) = \frac{\mu - \lambda}{4} a \end{cases} \quad \text{with} \quad \begin{cases} c_{11} = \lambda + 2\mu \\ c_{44} = \mu \\ c_{12} = \lambda \end{cases} \tag{A.5}$$

The gradient elasticity lattice-based equations are rewritten using Lamé parameters:

$$\begin{aligned} &(\lambda + 2\mu) \frac{\partial^2 u}{\partial x^2} + (\lambda + \mu) \left(\frac{\partial^2 v}{\partial x \partial y} + \frac{\partial^2 w}{\partial x \partial z} \right) + \mu \left(\frac{\partial^2 u}{\partial y^2} + \frac{\partial^2 u}{\partial z^2} \right) \\ &+ \frac{a^2}{12} \left[(\lambda + 2\mu) \frac{\partial^4 u}{\partial x^4} + \mu \left(\frac{\partial^4 u}{\partial y^4} + \frac{\partial^4 u}{\partial z^4} \right) + 6\lambda \left(\frac{\partial^4 u}{\partial x^2 \partial y^2} + \frac{\partial^4 u}{\partial x^2 \partial z^2} \right) \right] \\ &+ \frac{a^2}{6} (\lambda + \mu) \left(\frac{\partial^4 v}{\partial x \partial y^3} + \frac{\partial^4 v}{\partial x^3 \partial y} + \frac{\partial^4 w}{\partial x \partial z^3} + \frac{\partial^4 w}{\partial x^3 \partial z} \right) = \rho \ddot{u} \end{aligned} \tag{A.6}$$

It is worth mentioning that the gradient elasticity lattice-based equation cannot be cast in the linear isotropic strain gradient form which depends on 7 parameters, two classical Lamé parameters and 5 additional non-classical material parameters of the strain gradient form [126–128]. In fact, the generalized wave equation of the linear isotropic strain gradient medium can be shown to depend on two macroscopic additional length scales that depend on the 5 additional parameters [126,127,129,130]:

$$\left(1 - l_1^2 \Delta\right) \mu \Delta u + \left(1 - l_2^2 \Delta\right) (\lambda + \mu) \left(\partial_x^2 u + \partial_x \partial_y v + \partial_x \partial_z w\right) = \rho \ddot{u} \quad \text{with} \quad \Delta = \partial_x^2 + \partial_y^2 + \partial_z^2 \tag{A.7}$$

where l_1 and l_2 are the two additional length scales that depend on the 5 additional length scales of the linear isotropic strain gradient medium. Equation (A.7) can be equivalently rewritten using Mindlin's notations [126]:

$$\begin{aligned} &(\lambda + 2\mu) \left(1 - \tilde{l}_1^2 \Delta\right) \left(\partial_x^2 u + \partial_x \partial_y v + \partial_x \partial_z w\right) \\ &-\mu \left(1 - \tilde{l}_2^2 \Delta\right) \left(\partial_x \partial_y v + \partial_x \partial_z w - \partial_y^2 u - \partial_z^2 u\right) = \rho \ddot{u} \quad \text{with} \\ &\begin{cases} \tilde{l}_1^2 = \frac{l_1^2 \mu + l_2^2 (\lambda + \mu)}{\lambda + 2\mu} \\ \tilde{l}_2^2 = l_1^2 \end{cases} \end{aligned} \tag{A.8}$$

Equation (A.7) can be also rewritten, with the full expression of the differential operators:

$$\begin{aligned} &(\lambda + 2\mu)\, \partial_x^2 u + \mu \left(\partial_y^2 u + \partial_z^2 u\right) + (\lambda + \mu) \left(\partial_x \partial_y v + \partial_x \partial_z w\right) \\ &- \left[l_1^2 \mu + l_2^2\, (\lambda + \mu)\right] \partial_x^4 u - \left[2 l_1^2 \mu + l_2^2\, (\lambda + \mu)\right] \left(\partial_x^2 \partial_y^2 u + \partial_x^2 \partial_z^2 u\right) \\ &- l_1^2 \mu \left(\partial_y^4 u + \partial_z^4 u\right) - 2 l_1^2 \mu \partial_y^2 \partial_z^2 u \\ &- l_2^2\, (\lambda + \mu) \left[\partial_x \partial_y^3 v + \partial_y \partial_x^3 v + \partial_x \partial_z^3 w + \partial_z \partial_x^3 w + \partial_x \partial_y^2 \partial_z w + \partial_x \partial_y \partial_z^2 v\right] = \rho \ddot{u} \end{aligned} \tag{A.9}$$

It is not possible to express the lattice-based gradient elasticity model Eq. (A.6) with the isotropic gradient elasticity equation Eq. (A.9). The zero-th order continuous medium asymptotically derived from Gazis et al. lattice can be enforced to be linear isotropic, but the second-order gradient elasticity medium cannot be isotropic (cubic gradient elasticity medium, as already characterized by Mindlin, 1968 for strain gradient elasticity models of the crystal class m3m). This also explains the loss of isotropy in the high frequency regime, even if the cubic lattice may behave isotropically in the low frequency regime.

References

1. Bergson, H.: L'évolution créatrice. Librairie Félix Alcan, Paris (1907)
2. Keynes, J.M.: Essays in Biography, reprinted in Johnson, E., Moggridge, D.E. (eds.), The Collected Writings of John Maynard Keynes, vol. 10, London, Macmillan, for the Royal Economic Society (1972) (initially 1926)
3. Myshkis, A.D.: Mixed functional differential equations. J. Math. Sci. **129**(5), 4111–4226 (2005)
4. Lagrange, J.L.: Recherches sur la nature et la propagation du son, Miscellanea Philosophico-Mathematica Societatis Privatae Taurinensis I, 2rd Pagination, i-112 (1759) (see also Œuvres, Tome 1, 39–148)
5. Lagrange, J.L.: Mécanique analytique, Paris, 1788—3rd edn, Mallet-Bachelier, Gendre et successeur de Bachelier, Imprimeur-Libraire du bureau des longitudes, de l'école Polytechnique, de l'école centrale des arts et manufactures, Paris (1853)
6. Born, M., von Kármán, T.: On fluctuations in spatial grids. Physikalishe Zeitschrift **13**, 297–309 (1912)
7. Burkhardt, H.: Entwicklungen nach oscillirenden Funktionen und Integration der Differentialgleichungen der mathematischen Physik. Jahresber. Deutsch. Math.-Verein. **10**, 1–1804 (1908)
8. Cannon, J.T., Dostrovsky, S.: The Evolution of Dynamics: Vibration Theory from 1687 to 1742, Volume 6—Johann Bernoulli (1728), Studies in the History of Mathematics and Physical Sciences. Springer (1981)
9. Bernoulli, J.: Dechordis vibrantibls. Commentarii Academiae Scientiarum Imperialis Petropolitanae **3**, 13–28 (1728)
10. Filimonov, A.M., Kurchanov, P.F., Myshkis, A.D.: Some expected results in the classical problem of vibrations of the string with n beards when n is large. C. R. Acad. Sci. **313**, 961–965 (1991)
11. Schrödinger, E.: Zur Dynamik elastisch gekoppelter Punktsysteme. Ann. Phys. **349**(14), 916–934 (1914)
12. Seeger, A.: Historical note: on the simulation of dispersive wave propagation by elasticity models. Philos. Mag. **90**(09), 1101–1104 (2010)
13. Andrianov, I., Koblik, S., Starushenko, G.: Transition from discrete to continuous media: the impact of symmetry changes on asymptotic behavior of waves. Symmetry **13**(1008), 1–15 (2021)
14. Mühlich, U., Abali, B.E., Dell'Isola, F.: Commented translation of Erwin Schrödinger's paper On the dynamics of elastically coupled point systems (Zur Dynamik elastisch gekoppelter Punktsysteme). Math. Mech. Solids **26**(1), 133–147 (2021)
15. Maugin, G.A.: Nonlinear Waves in Elastic Crystals. Oxford University Press (1999)
16. Rayleigh Lord: The Theory of Sound, 2 edn. London (1894)
17. Challamel, N., Picandet, V., Collet, B., Michelitsch, T., Elishakoff, I., Wang, C.M.: Revisiting finite difference and finite element methods applied to structural mechanics within enriched continua. Eur. J. Mech. A Solids **53**, 107–120 (2015)
18. Born, M., Huang, K.: Dynamical theory of crystal lattices. Oxford University Press (1956)
19. Maradudin, A.A., Montroll, E.W., Weiss, G.H., Ipatova, I.P.: Theory of Lattice Dynamics in the Harmonic Approximation, 2nd edn. Academic Press (1971)
20. Askar, A.: Lattice Dynamical Foundations of Continuum Theories: Elasticity, Piezoelectricity, Viscoelasticity, Plasticity. World Scientific, Singapore (1986)
21. Eringen, A.C.: On differential equations of nonlocal elasticity and solutions of screw dislocation and surface waves. J. Appl. Phys. **54**, 4703–4710 (1983)
22. Eringen, A.C.: Nonlocal Continuum Field Theories. Springer, New-York (2002)
23. Kittel, C.: Introduction to Solid State Physics, 8th edn. Wiley (2005)
24. Maugin, G.A.: Solitons in elastic solids (1938–2010). Mech. Res. Commun. **38**, 341–349 (2011)
25. Fermi, E., Pasta, J., Ulam, S.: Studies of nonlinear problems. Los Alamos Rep. **1940**, 978 (1955)
26. Kruskal, M.D., Zabusky, N.J.: Stroboscopic-perturbation procedure for treating a class of nonlinear wave equations. J. Math. Phys. **5**, 231 (1964)
27. Collins, M.A.: A quasicontinuum approximation for solitons in an atomic chain. Chem. Phys. Lett. **77**, 342–347 (1981)
28. Rosenau, P.: Dynamics of nonlinear mass-spring chains near the continuum limit. Phys. Lett. A **118**(5), 222–227 (1986)
29. Kosevich, A.M.: The Crystal Lattice—Phonons, Solitons, Dislocations, Superlattices. Wiley (2005)
30. Abramian, A.K., Andrianov, I.V., Gaiko, V.A.: Nonlinear Dynamics of Discrete and Continuous Systems, Advanced Structural Materials, vol. 139. Springer (2021)
31. Boscovich, R.J.: Theoria Philosophiae Naturalis, 1st edn, Venice, 1763, English edition with a short life of Boscovich, Chicago and London (1922)
32. Navier, L.: Sur les lois de l'équilibre et du mouvement des corps solides élastiques. Bulletin des sciences par la Société Philomatique de Paris, pp. 177–181 (1823) **(in French)**
33. Cauchy, A.: Sur l'équilibre et le mouvement d'un système de points matériels sollicités par des forces d'attraction ou de répulsion mutuelle. Exercices de Mathématiques **3**, 188–212 (1828). **(in French)**
34. Poisson, S.D.: Mémoire sur l'équilibre et le mouvement des corps élastiques. Mémoire de l'Académie des Sciences de l'Institut de France **8**, 357–570 (1829). **(in French)**
35. Thomson, W., Kelvin, L.: On Boscovich's theory. Nature **40**, 545–547 (1889)
36. Kelvin, L.: On the elasticity of a crystal according to Boscovich. Proc. R. Soc. Lond. **54**, 59–75 (1893)
37. Timoshenko, S.: History of Strength of Materials with a Brief Account of the History of Theory of Elasticity and Theory of Structures. McGraw-Hill (1953)
38. Green, G.: On the reflection and refraction of light at the common surface of two non-crystallized media. In: Ferrrers, N.M. (ed.) Mathematical Papers, pp. 245–269. MacMillan, London (1971)
39. Voigt, V.: Lehrbuch der Krystallphysik. B.G. Teubner, Leipzig (1910)
40. Foce, F.: The theory of elasticity between molecular and continuum approach in the XIXth century. In: Radelet-de-Grave, P., Benvenuto, E. (eds.) Between Mechanics and Architecture. Birkhaüser (1995)
41. Capecchi, D., Ruta, G., Trovalusci, P.: From classical to Voigt's molecular models in elasticity. Arch. Hist. Exact Sci. **64**, 525–559 (2010)
42. Capecchi, D., Ruta, G., Trovalusci, P.: Voigt and Poincaré's mechanistic-energetic approaches to linear elasticity and suggestions for multiscale modelling. Arch. Appl. Mech. **81**, 1573–1584 (2011)

43. Voigt, V.: L'état actuel de nos connaissances sur l'élasticité des cristaux. In: Rapport présenté au Congrès International de Physique, Rassemblés et publiés par Ch. Guillaume, L. Poincaré (ed.), pp. 277–347. Gauthier-Villars, Paris (1900)
44. Voigt, V.: Theoretische Studien über die Elasticitätsverhältnisse der Kristalle. Abhandlungen der Gesellschaft der Wissenschaften, Zu Göttingen-Mathematische Classe **34**, 1–100 (1887)
45. Poincaré, H.: Leçons sur la théorie de l'élasticité. Carré, Paris (1892)
46. Ostoja-Sarzewski, M.: Lattice models in micromechanics. Appl. Mech. Rev. **55**(1), 35–60 (2002)
47. Suiker, A.S.J., Metrikine, A.V., de Borst, R.: Dynamic behaviour of a layer of discrete particles, part 1: analysis of body waves and eigenmodes. J. Sound Vib. **240**(1), 1–18 (2001)
48. Zhang, Y.P., Challamel, N., Wang, C.M.: Modelling nano-plane structures with body force using Hencky bar-grid model, continualised nonlocal model and Eringen nonlocal model. Contin. Mech. Thermodyn. **33**, 2453–2480 (2021)
49. Blackman, M.: Contributions to the theory of the specific heat of crystals. II. On the vibrational spectrum of cubical lattices and its application to the specific heat of crystals. Proc. R. Soc. Lond. A **148**, 384–406 (1935)
50. Montroll, E.W.: Dynamics of a square lattice. J. Chem. Phys. **15**(8), 575–591 (1947)
51. De Launay, J.D.: Solid State Physics, vol. 2, F. Seitz and D. Turnbull (eds.), pp. 219–303. Academic Press (1956)
52. Friesecke, G., Theil, F.: Validity and failure of the Cauchy–Born hypothesis in a two-dimensional mass-spring lattice. J. Nonlinear Sci. **12**, 445–478 (2002)
53. Friesecke, G., Matthies, K.: Geometric solitary waves in a 2D mass-spring lattice. Discrete Contin. Dyn. Syst. **1**, 105–114 (2003)
54. Patra, A.K., Gopalakrishnan, S., Ganguli, R.: A spectral multiscale method for wave propagation analysis: atomistic–continuum coupled simulation. Comput. Methods Appl. Mech. Eng. **278**, 744–764 (2014)
55. Mikes, K., Jirasek, M.: Quasicontinuum method extended to irregular lattices. Comput. Struct. **192**, 50–70 (2017)
56. Wieghardt, K.: Über einen Grenzübergang der Elastizitätslehre und seine Anwendung auf die Statik hochgradig statisch unbestimmter Fachwerke. In: Verhandtlungen des Vereinz z. Beförderung des Gewerbefleisses Abhandlungen, vol. 85, pp. 139-176 (1906)
57. Riedel, W.: Beiträge zur Lösung des ebenen Problems eines elastischen Körpers mittels der Ayrischen Spannungsfunktion. Zeitschrift futr angewandte Mathematik und Mechanik **7**(3), 169–188 (1927) **(in German)**
58. Hrennikoff, A.: Plane stress and bending of plates by method of articulated framework. PhD Memory, Massachusetts Institute of Technology, MIT (1940)
59. Hrennikoff, A.: Solutions of problems of elasticity by the framework method. J. Appl. Mech. **8**, A169–A175 (1941)
60. McHenry, D.: Discussion: Solution of problems of elasticity by the framework method, Hrennikoff A., ASME. J. Appl. Mech. **8**, A169–A175 (1941), **9**(3), A144–A145 (1942)
61. McHenry, D.: A lattice analogy for the solution of stress problems. J. Inst. Civ. Eng. Lond. **2**(5350), 59–82 (1943)
62. Lax, M.: E1. The relation between microscopic and macroscopic theories of elasticity. In: Wallis, R.F. (ed.) Lattice Dynamics, pp. 583–596. Pergamon Press, New-York (1965)
63. Gazis, D.C., Wallis, R.F.: Conditions for rotational invariance of a harmonic lattice. Phys. Rev. **151**(2), 578–580 (1966)—see also Gazis and Wallis R.F., Erratum, Phys. Rev. **156**, 1038 (1967)
64. Keating, P.N.: Effect of invariance requirements on the elastic strain energy of crystals with application to the diamond structure. Phys. Rev. **145**(2), 637–645 (1966)
65. Keating, P.N.: Relationship between the macroscopic and microscopic theory of crystal elasticity. I. Primitive crystals. Phys. Rev. **152**(2), 774–779 (1966)
66. Alexander, S.: Amorphous solids: their structure, lattice dynamics and elasticity. Phys. Rep. **296**, 65–236 (1998)
67. Gazis, D.C., Herman, R., Wallis, R.F.: Surface elastic waves in cubic crystals. Phys. Rev. **119**, 533–544 (1960)
68. Clark, B.C., Gazis, D.C., Wallis, R.F.: Frequency spectra of body-centered cubic lattices. Phys. Rev. **134**(6A), 1486–1491 (1964); erratum, Phys. Rev. B **2**(8), 3443 (1970)
69. Bose, G., Gupta, H.C., Tripathi, B.B.: Noncentral forces in the study of lattice dynamics of metals. J. Phys. F Met. Phys. **2**, 426–432 (1972)
70. Kothari, L.S., Singhal, U.: Lattice dynamics of sodium—comparison of de Launay and CGW models. J. Phys. C Solid State Phys. **5**, 293–299 (1972), Corrigendum. J. Phys. C Solid State Phys. **5**, 791 (1972)
71. Shukla, M.M.: The non equivalence of angular force models of de Launay and Clark, Gazis and Wallis for FCC metals. J. Phys. F Met. Phys. **8**(6), 131–133 (1978)
72. Ramamurthy, V.: Nonequivalence of general tensor force and Clark, Gazis, and Wallis angular force models. Phys. Rev. B **57**(21), 554–563 (1998)
73. Hrennikoff, A.: Framework method and its technique for solving plane stress problems. IABSE Publ. **9**, 217–248 (1949)
74. Raoult, A., Caillerie, D., Mourad, A.: Elastic lattices: equilibrium, invariant laws and homogenization. Ann. Univ. Ferrara **54**, 297–318 (2008)
75. Ostoja-Starzewski, M.: Microstructural Randomness and Scaling in Mechanics of Materials. CRC Series. Taylor and Francis Group (2008)
76. Zhang, Y.P., Wang, C.M., Pedroso, D.M., Zhang, H.: Hencky bar-grid model for plane stress elasticity problems. J. Eng. Mech. **147**(5), 04021021 (2021)
77. Nannapaneni, R.G., Nakshatrala, K.B., Stefaniuk, D., Krakowiak, K.J.: Discrete lattice modeling of wave propagation in materials with heterogeneous microstructures. J. Eng. Mech. **147**(10), 04021075 (2021)
78. Hencky, H.: Über die angenäherte Lösung von Stabilitätsproblemen im Raummittels der elastischen Gelenkkette. Der Eisenbau **11**, 437–452 (1920)
79. Wang, C.M., Zhang, H., Challamel, N., Pan, W.: Hencky-Bar-Chain/Net for Structural Analysis. World Scientific (2020)
80. Wu, C.W.: A discrete element method for linear and nonlinear stress and bifurcation problems of elastic structures. Doctoral dissertation, New Mexico State University (1985)
81. Wifi, A.S., Obeid, K.A., Wu, C.W.: A simple discrete element mechanical model for the stability analysis of elastic structures. In: Current Advances in Mechanical Design & Production IV, pp. 149–156. Pergamon, Oxford (1989)

82. El Naschie, M.S.: Stress, Stability and Chaos in Structural Engineering: An Energy Approach. McGraw-Hill, New York (1990)
83. Dell'Isola, F., Steigmann, D.J. (eds.): Discrete and Continuum Models for Complex Metamaterials. Cambridge University Press (2020)
84. Cauchy, A.: Sur les différences finies et les intégrales aux différences des fonctions entières d'une on de plusieurs variables. Exercices de mathématiques, pp. 155–159 (1828)
85. Piola, G.: Nuova analisi per tutte le questioni della meccanica molecolare. Memorie di matematica e fisica della Societá italiana delle scienze **21**, 155–163 (1836) **(in Italian)**
86. Todhunter, I., Pearson, K.: A History of the Theory of Elasticity and of the Strength of Materials, from Galileo to the Present Time. Cambridge University Press 1886, vol. I, art. 769–772, pp. 422–425 (1886)
87. Dell'Isola, F., Maier, G., Perego, U., Andreaus, U., Esposito, R., Forest, S.: The complete works of Gabrio Piola: volume I commented English translation. In: Advanced Structured Materials, Vol. 38. Springer (2014)
88. Dell'Isola, F., Andreaus, U., Placidi, L.: At the origins and in the vanguard of peridynamics, nonlocal and higher-gradient continuum mechanics: an underestimated and still topical contribution of Gabrio Piola. Math. Mech. Solids **20**(5), 887–928 (2015)
89. Shokin, Yu.: The Method of Differential Approximation. Springer (1983)
90. Godunov, S.K., Ryabenkii, V.S.: Difference Schemes—An Introduction to the Underlying Theory. North-Holland, Amsterdam (1987)
91. Rosenstock, H.B., Newell, G.F.: Vibrations of a simple cubic lattice. I. J. Chem. Phys. **21**, 1607–1608 (1953)
92. Montroll, E.W., Potts, R.B.: Effect of defects on lattice vibrations. Phys. Rev. **100**(2), 525–543 (1955)
93. Love, A.E.H.: A Treatise on the Mathematical Theory of Elasticity, 4th edn. Dover Publications, New-York (1944)
94. Born, M.: Zur Raumgittertheorie des Diamanten. Ann. Phys. **44**, 605–642 (1914)
95. Smith, H.M.J.: The theory of the vibrations and the Raman spectrum of the diamond lattice. Trans. R. Soc. **A241**, 105–145 (1948)
96. Nagendra Nath, N.S.: The dynamical theory of the diamond lattice I. Proc. Indian Acad. Sci. **1**, 333–345 (1934)
97. Mindlin, R.D.: Lattice theory of shear modes of vibration and torsional equilibrium of simple-cubic crystal plates and bars. Int. J. Solids Struct. **6**(6), 725–738 (1970)
98. Mindlin, R.D.: Theories of elastic continua and crystal lattice theories. In: Kröner, E (ed.), Mechanics of Generalized Continua, Proceedings of the IUTAM-Symposium on the Generalized Cosserat Continuum and the Continuum Theory of Dislocations with Applications, Freudenstadt and Stuttgart, Germany, pp. 312–320, 1967. Springer (1968)
99. Zienkiewicz, O.C., Taylor, R.L.: The Finite Element Method—Volume 1: The Basis, 5th edn. Butterworth-Heineman, Oxford (2000)
100. Liu, W.K., Li, S., Park, H.S.: Eighty years of the finite element method: birth, evolution, and future. Arch. Comput. Meth. Eng. **29**, 4431–4453 (2022)
101. Chen, H., Lin, E., Liu, Y.: A novel volume-compensated particle method for 2D elasticity and plasticity analysis. Int. J. Solids Struct. **51**, 1819–1833 (2014)
102. Yin, H.: A simplified continuum particle model bridging interatomic potentials and elasticity of solids. J. Eng. Mech. 04022017, **148**(5), 1–12 (2022)
103. Challamel, N., Wang, C.M., Elishakoff, I.: Discrete systems behave as nonlocal structural elements: bending, buckling and vibration analysis. Eur. J. Mech. A Solids **44**, 125–135 (2014)
104. Challamel, N., Wang, C.M., Zhang, H., Elishakoff, I.: Lattice-based nonlocal elastic structural models. In: Ghavanloo, E., Fazelzadeh, S.A., Marotti de Sciarra, F. (eds.) Size-Dependent Continuum Mechanics Approaches: Theory & Applications. Springer (2021)
105. Dell'Isola, F., Eremeyev, V.A.: Some introductory and historical remarks on mechanics of microstructured materials. In: Dell'Isola, F., Eremeyev, V.A., Porubov, A. (eds.) Advances in Mechanics of Microstructured Media and Structures, vol. 87. Springer (2018)
106. Kocsis, A., Challamel, N.: On the foundation of a generalized nonlocal extensible shear beam model from discrete interactions. Special Issue in honour of Prof. Maugin, Ed. H. Altenbach, J. Pouget, M. Rousseau, B. Collet and T. Michelitsch, Generalized Models and Non-classical Approaches in Complex Materials, Advanced Structured Materials. Springer (2018)
107. Dell'Isola, F., Giorgio, I., Pawlikowski, M., Rizzi, N.: Large deformations of planar extensible beams and pantographic lattices: heuristic homogenization, experimental and numerical examples of equilibrium. Proc. R. Soc. A **472**(2185), 20150790 (2016)
108. Lerbet, J., Challamel, N., Nicot, F., Darve, F.: Stability of Discrete Non-conservative Systems. ISTE Press, Elsevier (2020)
109. Brillouin, L.: Wave Propagation in Periodic Structures: Electric Filters and Crystal Lattices. McGraw-Hill, New York (1946)
110. Eringen, A.C., Kim, B.S.: Relation between non-local elasticity and lattice dynamics. Cryst. Lattice Defects **7**, 51–57 (1977)
111. Challamel, N., Wang, C.M., Zhang, H., Kitipornchai, S.: Exact and nonlocal solutions for vibration of axial lattices with direct and indirect neighbouring interactions. J. Eng. Mech. **144**(5), 04018025, 1–9 (2018)
112. Boussinesq, J.: Théorie de l'intumescence liquide appelée onde solitaire ou de translation, se propageant dans un canal rectangulaire. Comptes Rendus Hebdomadaires de l'Académie des Sciences de Paris **72**, 755–759 (1871)
113. Boussinesq, J.: Théorie des ondes et des remous qui se propagent le long d'un canal rectangulaire horizontal, en communiquant au liquide contenu dans ce canal des vitesses sensiblement pareilles de la surface au fond. Journal de Mathématiques Pures et Appliquées **17**, 55–108 (1872)
114. Jaberolanssar, H., Peddieson, J., Jr.: On continuum representation of mechanical behaviour of discrete lattices. Mech. Res. Commun. **8**(4), 251–257 (1981)
115. Andrianov, I.V., Awrejcewicz, J.: On the average continuous representation of an elastic discrete medium. J. Sound Vib. **264**, 1187–1194 (2003)
116. Andrianov, I.V., Awrejcewicz, J., Weichert, D.: Improved continuous models for discrete media. Math. Probl. Eng. **986242**, 1–35 (2010)
117. Kunin, I.A.: Elastic Media with Microstructure. Springer (1983)

118. Eringen, A.C.: Nonlocal continuum description of lattice dynamics and applications. Technical Report, Princeton University, 22 pp (1986)
119. Challamel, N., Rakotomanana, L., Le Marrec, L.: A dispersive wave equation using non-local elasticity. C. R. Mécanique **337**, 591–595 (2009)
120. Bacigalupo, A., Gambarotta, L.: Identification of non-local continua for lattice-like materials. Int. J. Eng. Sc. **159**, 103430 (2021)
121. Dean, P.: The vibrations of three two-dimensional lattices. Math. Proc. Camb. Philos. Soc. **59**, 383–396 (1963)
122. Phani, A.S.J., Woodhouse, J., Fleck, N.A.: Wave propagation in two-dimensional periodic lattices. J. Acoust. Soc. Am. **119**(4), 1995–2005 (2006)
123. Rosi, G., Auffray, N.: Continuum modelling of frequency dependent acoustic beam focussing and steering in hexagonal lattices. Eur. J. Mech. A Solids **77**, 103803 (2019)
124. Askes, H., Metrikine, A.V.: Higher-order continua derived from discrete media: continualisation aspects and boundary conditions. Int. J. Solids Struct. **42**, 187–202 (2005)
125. Challamel, N., Atanackovic, T., Zhang, Y.P., Wang, C.M.: A fractional nonlocal elastic model for lattice wave analysis. Mech. Res. Commun. **126**(103999), 1–9 (2022)
126. Mindlin, R.D.: Micro-structure in linear elasticity. Arch. Ration. Mech. Anal. **16**, 51–78 (1964)
127. Mindlin, R.D.: Second gradient of strain and surface-tension in linear elasticity. Int. J. Solids Struct. **1**, 417–438 (1965)
128. Dell'Isola, F., Sciarra, G., Vidoli, S.: Generalized Hooke's law for isotropic second gradient materials. Proc. R. Soc. Lond. A **465**, 2877–2196 (2009)
129. Askes, H., Aifantis, E.C.: Gradient elasticity in statics and dynamics: an overview of formulations, length scale identification procedures, finite element implementations and new results. Int. J. Solids Struct. **48**, 1962–1990 (2011)
130. Pollizzotto, C.: A hierarchy of simplified constitutive models within isotropic strain gradient elasticity. Eur. J. Mech. A Solids **61**, 92–109 (2017)